

PIERGIORGIO TOZZI

Sutureless Anastomoses

Secrets for Success

STEINKOPFF
DARMSTADT



Springer

PIERGIORGIO TOZZI

Sutureless Anastomoses

Secrets for Success

WITH 201 FIGURES IN 393 SEPARATE ILLUSTRATIONS,
MOST IN COLOR AND 16 TABLES

STEINKOPFF
DARMSTADT

 Springer

PIERGIORGIO TOZZI, MD
Department of Cardiovascular Surgery
Centre Hospitalier Universitaire Vaudois (CHUV)
46, rue du Bugnon
CH-1011 Lausanne, Switzerland

ISBN-10 3-7985-1714-2 Steinkopff Verlag, Darmstadt
ISBN-13 978-3-7985-1714-1 Steinkopff Verlag, Darmstadt

Bibliographic information published by Die Deutsche Nationalbibliothek
Die Deutsche Nationalbibliothek lists this publication in the Deutsche Nationalbibliografie;
detailed bibliographic data is available in the Internet at <http://dnb.d-nb.de>.

This work is subject to copyright. All rights are reserved, whether the whole or part of the material is concerned, specifically the rights of translation, reprinting, reuse of illustrations, recitation, broadcasting, reproduction on microfilm or in any other way, and storage in data banks. Duplication of this publication or parts thereof is permitted only under the provisions of the German Copyright Law of September 9, 1965, in its current version, and permission for use must always be obtained from Springer-Verlag. Violations are liable for prosecution under the German Copyright Law.

Steinkopff Verlag, Darmstadt
a member of Springer Science+Business Media
www.steinkopff.springer.de

© Steinkopff Verlag Darmstadt 2007
Printed in Germany

The use of general descriptive names, registered names, trademarks, etc. in this publication does not imply, even in the absence of a specific statement, that such names are exempt from the relevant protective laws and regulations and therefore free for general use.

Product liability: The publishers cannot guarantee the accuracy of any information about the application of operative techniques and medications contained in this book. In every individual case the user must check such information by consulting the relevant literature.

Medical Editor: Dr. Annette Gasser Production: Klemens Schwind
Cover Design: WMX Design GmbH, Heidelberg
Typesetting: K + V Fotosatz GmbH, Beerfelden

SPIN 11861553 85/7231-5 4 3 2 1 0 – Printed on acid-free paper

TO RAFFAELE AND JOLANDA



Preface

When doctors first look at sutureless anastomosis devices created by new technologies, the most frequent comment is how amazingly easy it is to create a vascular anastomosis and, as a direct consequence, they believe anybody could play the role of the cardiovascular surgeon. Pessimistic cardiovascular surgeons, on their side, think that creating a machine capable of perfectly reproducing their core activity, which consists in making anastomosis, will kill their profession. Actually, no medical specialty's demise has been more often predicted and, at the same time, more greatly exaggerated than that of cardiovascular surgery. According to its detractors, beginning in the late 1980s with the angioplasty boom, continuing in the mid-1990s with the introduction of bare metal stents, and then more recently with the introduction of drug-eluting stents, cardiovascular surgery has been on life support for nearly 15 years.

This specialty's claimed collapse has generally been attributed to recent advantages in percutaneous procedures and devices that give the opportunity to non-surgeon doctors to accomplish the surgeon's work.

The reality is different. Data suggest that cardiac surgery continues to survive and has not suffered the precipitous decline that was predicted. From the economical standpoint, CABG is much more of a mature market and the size of the opportunity remains impressive and relatively stable, with around 1,500,000 procedures performed annually worldwide, at a total cost approaching 2.5 billion US\$.

The introduction of sutureless anastomosis technology should not alarm cardiac and vascular surgeons. First of all, new anastomotic technologies are not as new as they seem to be, because the sutureless anastomosis technique was born few years before the suture one. Second, the technological progress only gives us more powerful tools to accomplish our everyday mission and it will never replace our spirit or our job.

Surgeons should get rid of the fear of changing their rituals, slowing down the adoption of new techniques. Being more open to progress will attract more investors and this will speed up the research development eventually leading to less technically demanding procedures and, last but not least, more and more patient friendly treatments. Indeed, patients are the real recipient of technical progress.

However, new technologies should not develop faster than the profession's ability to provide evidence-based data to support their application and, at the end of this review, the reader should be aware of the need to create standards and guidelines for a consistent evaluation of all devices for facilitated anastomosis in coronary and vascular surgery. We have a dual and somehow ambiguous role of assisting industry in bringing new devices to market and trimming down the risk of harming patients that is always relate to new therapies.

Since the beginning of cardiac surgery, proximal and distal anastomosis for coronary artery bypass grafts (CABGs) have been done with hand-held sutures based on the principles of the suture technique described by Alexis Carrel in 1902 [1]. The reason why we have been performing the suture technique for the last 100 years and we now consider it the gold standard, is because it is reliable and provides excellent long-term results. Reliability and excellence of long-term results are the two key elements for any medical device or drug to be widely accepted.

One of the basic principles of cardiovascular surgery is the precise placement of sutures between the two edges of severed vessel, keeping an intima-to-intima contact and avoiding flaps and purse-string effect. Any imprecision may lead to anastomosis occlusion or flow impairment and eventually compromises the vascular anastomosis durability with catastrophic clinical consequences. The future of Coronary Artery Bypass Grafting and all vascular surgery depends on the refinement of the anastomosis technique to produce more consistent graft patency in a surgical environment that is becoming more and more challenging for the cardiovascular surgeon since minimally invasive approach and beating heart surgery have been introduced. For example, manual suturing of the anastomosis in video-assisted port access surgery on the beating heart, even with the aid of a master-slave robotic surgery system, has proved to be prohibitively difficult [2, 3]. Besides, target vessels are increasingly smaller and diseased and surgeons have to deal with vascular reconstructions that are very complex due to the aging of the population and the increasing number of patient's comorbidity. In coronary surgery, the hand-sewn proximal anastomosis still requires the aortic cross-clamp or side clamp increasing the risk of neurological and neurocognitive complications [4] and aortic dissection [5]. Moreover, it's a matter of fact that surgical dexterity is still a determinant factor for anastomosis outcome.

The suture technique for vascular anastomosis construction is becoming inadequate to meet new surgeon's demands and surgeons need an alternative way to construct a bypass in order to reduce the technical demand and standardise the quality of the surgical procedure.

New anastomotic technologies should facilitate consistency in graft quality while expediting the anastomosis procedure. Moreover, any automated vascular suturing device should provide a standard quality of anastomosis, reducing the individual surgical dexterity as a prognostic factor for vascular anastomosis outcome.

This book is dedicated to surgeons, students, biomedical engineers and researchers with a special interest in vascular anastomosis and bypass techniques that want to update their knowledge concerning the major determinants of anastomosis outcome and all the existing alternatives to the suture technique. In this book, we review the principles of rheology applied to vascular anastomoses and the most recent anastomotic technologies. It would be virtually impossible to describe every anastomosis device that is the object of intellectual property protection, because the majority of them do not even reach the phase of prototype development. Therefore, only devices that have showed excellent experimental and clinical results are presented and discussed. We disclose the secrets and pitfalls of new sutureless anastomotic devices demonstrating that the “*new anastomotic technologies*” are based on concepts expressed in the XIXth century.

We also outline the criteria to safely evaluate sutureless anastomotic devices hoping to reduce as much as possible the risks for patients and doctors that blindly trust new technologies.

■ **Acknowledgement:** I would like to thank Prof. Ludwig K. von Segesser who encouraged me to undertake this project, and Alessandra, Iker and Marco who helped me move the book to completion.

■ References

1. Carrel A (1902) La technique operatoire des anastomoses vasculaires et la transplantation des visceres. Lyon Med 98:859–863
2. Mack MJ, Acuff TE, Casimir-Ahn H, Lönn UJ, Jansen EWL (1997) Video-assisted coronary bypass grafting on the beating heart. Ann Thorac Surg 63:S100–103
3. Falk V, Diegeler A, Walther T, Banush J, Brucerus J, Raumans J et al. (2000) Total endoscopic computer enhanced coronary artery bypass grafting. Eur J Cardiothorac Surg 17:38–45
4. Zamvar V, Williams D, Hall J, Payne N, Cann C, Young K, Karthikeyan S, Dunne J (2002) Assessment of neurocognitive impairment after off-pump and on-pump techniques for coronary artery bypass graft surgery: prospective randomised controlled trial. BMJ 30, 325(7375):1268
5. Stanger O, Oberwalder P, Dacar D, Knez I, Rigler B (2002) Late dissection of the ascending aorta after previous cardiac surgery: risk, presentation and outcome. Eur J Cardio Thor Surg 21(3):435–582

Table of contents

1	Historical overview of vascular anastomoses	1
2	The physiology of blood flow and artery wall	12
2.1	The physical nature of blood flow	12
2.2	Mechanical properties of artery wall	16
3	Mathematical modelling of vascular anastomoses	25
3.1	Realistic mathematical model	27
3.2	Symplified mathematical model	33
4	Determinants of anastomosis long term patency	39
4.1	Surgical element	40
4.2	Flow element	46
4.3	Biological element	49
5	Key issues in sutureless vascular anastomoses	53
5.1	Criteria of sutureless device evaluation	54
5.2	Anastomotic assit devices	66
6	Coronary surgery: devices for proximal anastomosis	70
6.1	Symmetry aortic connector, first generation system	70
6.2	Symmetry aortic connector, second generation system	78
6.3	The CorLink	79
6.4	The PAS-Port TM proximal anastomosis system	82
6.5	The Spyder	84
7	Coronary surgery: devices for distal anastomosis	87
7.1	St. Jude Medical Coronary Connector	87
7.2	The Graft Connector	91
7.3	Magnetic Vascular Positioner TM	95
7.4	The Heartflo Anastomosis Device	99

7.5	Converge Coronary Anastomosis Coupler	103
7.6	Cardica C-Port	105
7.7	The S2 Anastomotic System	107
7.8	Distal Anastomotic Device	110
8	Sutureless anastomotic devices for vascular surgery	114
8.1	Vessel closure system	114
8.2	The one-shot system	119
8.3	The Vascular Join	121
9	Human body and metal alloys: the never ending fight	130
10	Criteria for vascular anastomosis devices assessment	135
	Subject index	139

1

Historical overview of vascular anastomoses

The first non-scientific report of vascular anastomoses goes back to 300 A.D. when Cosma and Damiano first tried to re-implant a limb using ivory needles and a row flax stitches to suture vessels. Unfortunately, results were not reported, but it is fair to assume the results were very poor since the technique never spread out [1].

The first pseudo-scientific report goes back to 1774, when LeConte, a French medical student, replaced an injured femoral artery with a quillpen using a sutureless technique. However, infection made it an unsuccessful attempt [1]. All these attempts to restore the continuity of a severed vessel failed, as reported by Alexis Carrel, the father of vascular anastomosis, in his Nobel lecture in 1912: *“Many surgeons had previously to myself performed vascular anastomosis, but the results were far from satisfactory”* [2] and this document is now considered vascular surgery’s birth certificate. As a matter of fact, the first scientific attempt to restore vessel wall continuity goes back to January 13, 1894, 8 years before the description of the suture technique by Carrel. In the New York Medical Journal, Robert Abbe reported the possibility to replace an animal arterial conduit with hourglass shaped glass prosthesis. Glass prostheses with diameters from *“dog femoral artery”* to *“sheep aorta”*, were boiled and filled of water before the insertion into the artery and the connection with the native vessel was provided by a *“fine silk suture tied each end over the tube”* as shown in Figure 1 [3]. Results were encouraging only when large tubes were used. For dog femoral artery size graft, early occlusion was bound to happen.

In the last years of the 19th century, ivory cuffs [4], paraffined silver tubes [5] and ox shin bones [6] were inserted into vascular conduits or positioned around them, trying to replace or repair vessels, but clinical results did not encourage the pioneers of vascular surgery to continue their works. A step forward in the development of suturless technique for vascular reconstruction was done by Payr [7] in 1900 when he published the description of his absorbable extraluminal magnesium ring design (Fig. 2). The proximal end of the severed vessel was threaded through the ring, everted over its edge, and held in place by a circumferential ligature. The distal end was dilated for insertion of the rigid cuff with its everted vessel. The anastomosis was completed by another circumferential ligature, thereby achieving intima-to-intima apposition.

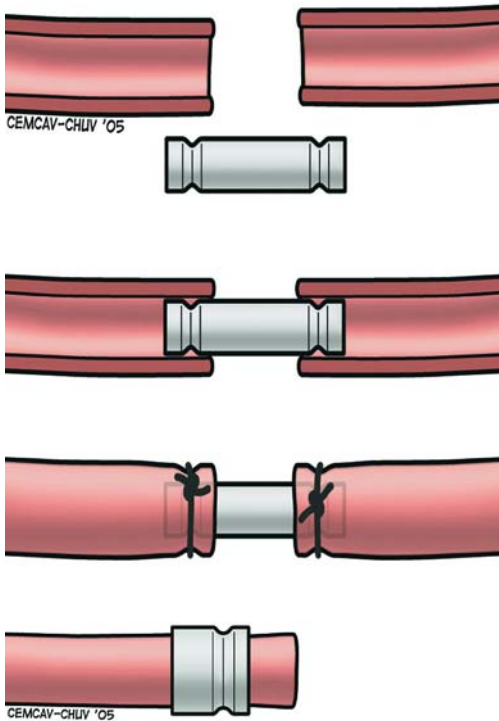


Fig. 1. Abbe's glass prostheses reminded a double sand-glass where each groove facilitate the vessel-device connection. The prostheses were boiled and filled of water before the insertion into the artery and the connection with the native vessel was provided by silk suture tied each end over the tube.

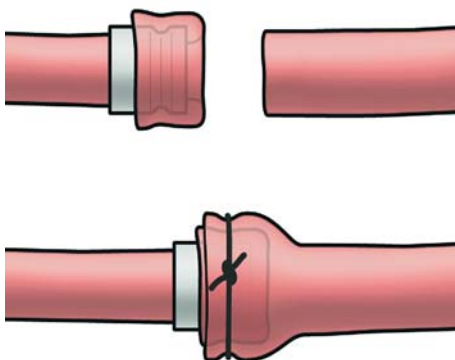


Fig. 2. Payr's absorbable extraluminal magnesium ring design. The proximal end of the severed vessel (1) was threaded through the ring (2), everted over its edge (3), and held in place by a circumferential ligature (4). The distal end was dilated for insertion of the rigid cuff with its everted vessel. The anastomosis was completed by another circumferential ligature, thereby achieving intima-to-intima apposition.

In 1904 Payr [8] presented a new device made of two interlocking magnesium rings (Fig. 3). Small pins on one side kept the vessel ends everted. The pins passed full-thickness through both vessel walls and the holes in the matching ring before being bent to secure the anastomosis.

This device showed close resemblance to the system designed by Henroz [9] in 1826 for bowel anastomosis. Payr's device results were not even comparable to those obtained with Carrel's suture technique, but his work in-

Fig. 3. The interlocking magnesium rings Payr presented in 1904 were similar to the Henroz's device for bowel anastomosis. Small pins on one side kept the vessel ends everted. The pins passed full-thickness through both vessel walls and the holes in the matching ring before being bent to secure the anastomosis.

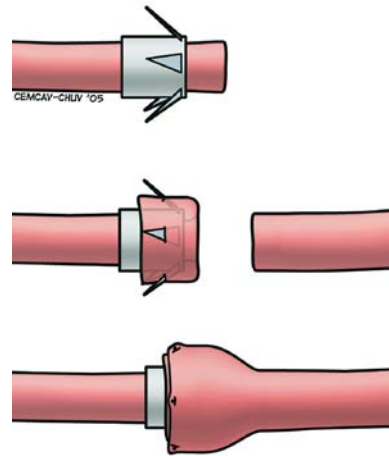
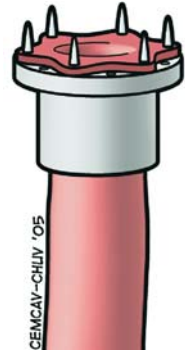


Fig. 4. Landon's metal ring was smooth on one end and contained five slightly everted teeth on the other. The everted vessel wall was connected to the anvil element by means of these five pins avoiding the need of a ligature and speeding up the anastomosis construction.

spired many surgeons that have elaborated his basic concepts over 100 years. As a modification of Payr's original design, in 1913 Landon [10] developed a metal ring that was smooth on one end and contained five slightly everted teeth on the other. The everted vessel wall was connected to the anvil element by means of these five pins avoiding the need of a ligature and speeding up the anastomosis construction (Fig. 4).

To find new consistent proposals as alternative to suture technique, we must wait until 1942. Blakemore [11] advanced Payr's technique using vein-graft-lined rigid vitallium tubes to bridge arterial defects and World War II allowed clinical trials of both suture and non-suture techniques (Fig. 5). Initially designed to bridge arterial defects, the technique was also used to facilitate end-to-end anastomoses such as in porta-cava anastomoses.

In an extensive review of vascular trauma during that war, De Bakey and Simeone stated that there was a slight increase in the number of amputation required following Blakemore's technique, although it was not sta-

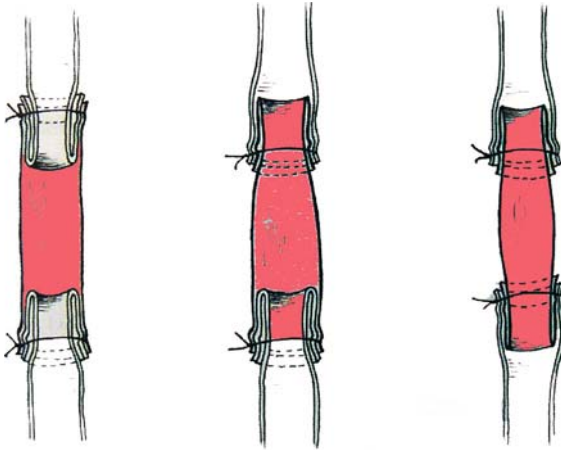


Fig. 5. Different methods of using a single vitallium tube for vascular end-to-end anastomoses as described by Blakemore et al.

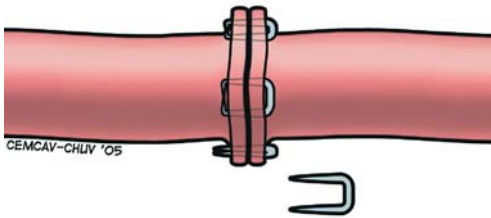


Fig. 6. Androsov developed a staple device that joined vessels by inserting multiple staples simultaneously and bending them into a B shape, thereby securing the anastomosis.

tistically significant [12]. Moreover, the sutureless technique was used in cases in which suture repair was not feasible and in which the proportion of critical vessels involved was higher. Interest in non suture technique waned as reconstructive peripheral vascular surgery began to gain acceptance using suture techniques for vein grafts in atherosclerotic vessels.

Stapling for vascular reconstruction was promoted in the USSR as a result of shortage of surgeons and the exigencies of war, because staples theoretically provided greater speed, safety and accuracy. In 1941, BF Gudov, a soviet engineer designed and constructed a vessel anastomosis stapler that was utilized successfully both in the surgical laboratory and operating room.

In 1956, Androsov's vascular anastomotic stapler [13] renovated the interest for sutureless technique. Stapling is a new concept, for that time. A stapler consists of a pusher that forces the two ends of a U-shaped wire through the objects to be joined, coupled with an anvil that bends the ends of the staple to grip the objects. The metallic staple device joined vessels by inserting multiple staples simultaneously and bending them into a B shape, thereby securing the anastomosis (Fig. 6). Androsov used this device for experimental and clinical end-to-end arterial repairs and vein grafts. Inokuchi modified this technique for end-to-side anastomoses [14].

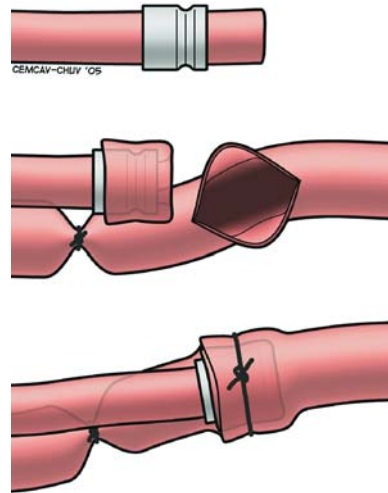


Fig. 7. Internal mammary-coronary artery end-to-end anastomosis published in 1961 by Goetz. The device was similar to Payr's rings, with tantalum instead of magnesium.

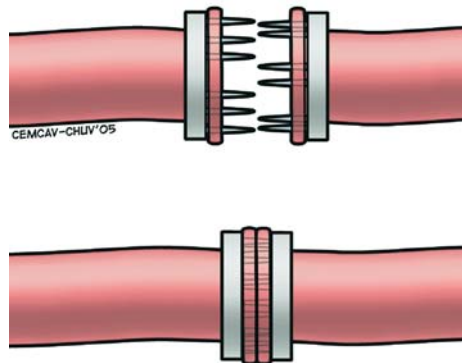


Fig. 8. Nakayama's rings. Vessel edge is everted onto a flange having 6 pins to pierce the vessel wall and 6 holes to receive the pins of the opposite flange.

The first internal mammary-coronary artery anastomosis constructed with a mechanical device in dogs was published in 1961 by Goetz [15]. The device used was similar to Payr's rings, with tantalum instead of magnesium. Goetz performed end-to-end IMA on LAD and IMA on Circumflex artery anastomoses in 12 dogs and long-term results (4 animals were still alive 20 months later) were superior to direct suture methods on beating heart (Fig. 7).

In 1962, Nakayama [16] developed two identical metallic rings with 6 spaced holes and pins to repair vessels 1.5 to 4.0 mm in diameter with virtually 100% patency in an experimental model (Fig. 8). The apparatus was also for end-to-side anastomoses, although it resulted in inclusion of a great part of the vessel wall, with subsequent stenosis at the anastomotic site.

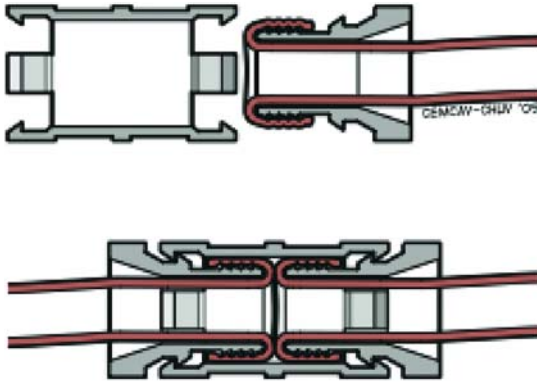


Fig. 9. This sutureless anastomotic device consists of 2 symmetric anvil elements each of which is positioned at the end of the severed vessel, with the distal part of the vessel everted onto the anvil. A 3rd element is used to connect the vessel's ends in an end-to-end fashion. The device is totally absorbed in few weeks.

Haller [17] introduced in 1965 a modernization of Payr's original cuff ring method, using a perforated tantalium ring to potentially decrease vessel wall necrosis and demonstrated a 92% early patency rate in canine vessels less than 4 mm in diameter.

A very promising absorbable anastomotic coupler device for microanastomoses (vessel diameter from 1 to 2 mm) was presented in 1984 (Fig. 9). It consists of 2 symmetric anvil elements each of which is positioned at the end of the severed vessel, with the distal part of the vessel everted onto the anvil. A 3rd element is used to connect the vessel's ends in an end-to-end fashion. This device has several potential advantages: it is made of polymer absorbable over a 3 month period, the blood exposed non-intimal surface is zero because there isn't any foreign material in the vessel lumen, and it provides a perfect intima-to-intima apposition. In an animal model, the 12-month patency rate was as high as 96%. Unfortunately, there is a mean vessel consumption of 4 mm in length due to the vessel eversion over the anvil that affected its diffusion [18].

In 1978 Obora published an original method of sutureless microvascular anastomosis (up to 2 mm in diameter) based on magnet rings and hollow cogwheel-shaped metal devices held together by magnetic energy. This is the first time in the history of sutureless anastomosis devices that magnetic force is used to restore the continuity of a severed vessel. This device allows the construction of end-to-end anastomosis and its reliability has been validated in an animal study in which it was possible to construct microanastomoses in about 8 min, dramatically reducing the technical demand of the procedure. Moreover, using this very simple and reliable technique, authors obtained excellent early graft patency rates [21].

Based on the Nakayama apparatus, Ostrup and Berggren introduced the Unilink system in 1986 [20]. This system that is still in use, consists of two polyethylene rings with alternating stainless steel pins and holes. After insertion of the vessel ends, the rings are approximated with a dedicate de-

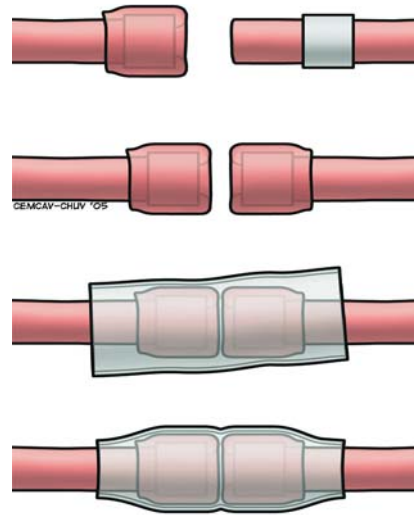


Fig. 10. In the heat-shrink tubing presented in 1991 the concept of vessel wall eversion is revisited and coupled with a heat-shrinkable tube to ensure the connection between the edges of the severed vessel. The conduit's ends are everted on an extra-vascular anvil and inserted in the 3rd polymeric element for a few millimetres. This element is then heated to 45–50 °C to make it shrink around the vessels ends, and the end-to-end anastomosis is completed.

vice. Currently four sizes of ring are available, ranging from 1.0 to 2.5 mm in diameter. Reports continue to appear on the use of the Unilink system, providing the device to be simple, efficacious and significantly faster than conventional suturing. The system seems to be best suitable for end-to-end anastomoses of soft, pliable minimally size-discrepant vessels. Although most report concern venous anastomoses, the device can be also used for arteries, but severely atherosclerotic arteries are a contradiction to its application. One potential drawback is that the rings are permanently placed with subsequent detrimental physiologic effects at the anastomotic site, inducing atrophy of the media both at the level of the ring and proximal to it [20].

In the heat-shrink tubing presented in 1991 the concept of vessel wall eversion was revisited and coupled with a heat-shrinkable tubing to ensure the connection between the edges of the severed vessel [19]. Once again, the conduit's ends are everted on an extra-vascular anvil and inserted in the 3rd polymeric element for a few millimetres. This element is then heated to 45–50 °C to make it shrink around the vessels ends, and the end-to-end anastomosis is completed (Fig. 10).

A year later, in 1992, Kirsch first published a new method to create microvascular anastomoses based on the principle of flanged, extra vascular, intimal approximation by arcuate-legged stainless steel clips [22]. Vessel ends undergo 90° eversion and are then held together with extravascular staples. This technique was considered biologically and technically superior to the penetrating microsuture. This concept has been extensively investigated for several years giving rise to different devices, the most famous being the “one-shot device”. This connector can deliver 10 to 12 titanium

clips simultaneously, allowing the construction of end-to-side and end-to-end vascular anastomosis in virtually all vessels. The graft, vein or artery, is preloaded onto the delivery system, inserted into the target vessel through standard arteriotomy, the clips are then fired and the anastomosis is completed. Clinical results, mostly based on the construction of A-V fistulas for dialysis, were very encouraging and this attracted many important investors [23]. Even with a takeoff angle for end-to-side of 45° , no foreign material in the vessel lumen and simplicity of use are without any doubt, successful elements, this device has never been widely accepted.

Lasers have been used to repair arteries since 1979 [24]. Jain and Gorisch were the first to report on vascular anastomosis using a neodymium yttrium-aluminium-garnet laser. They described a hybrid technique using few stay stitches and welding the rest of the anastomosis with laser light. This procedure requires less time than conventional technique and the patency rate are at least equal. There is an ongoing debate regarding which type of laser has the greatest potential. The laser power measured in watts, and the amount of energy and time required vary for the type of laser and for the size of the vessels. Whenever the CO_2 laser is used, the tissue temperature is reported to rise to 80° to 120°C and adhesion occurs through melting of collagen and coagulation of cells in the media and adventitia. In the process of wound healing, this coagulum is gradually replaced by fi-

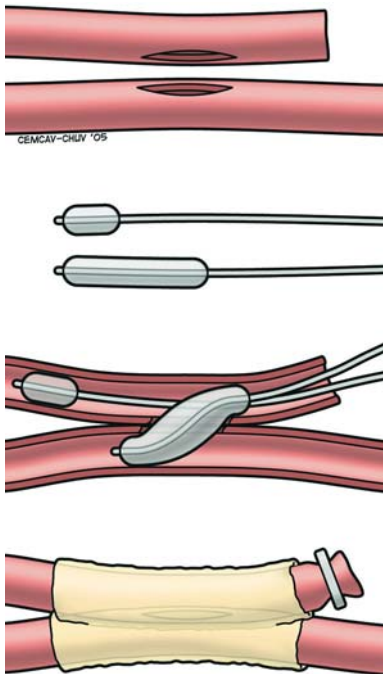


Fig. 11. Biological glue coupled with a catheter system that stabilise the anastomosis during glue injection to perform a side-to-side anastomosis.

brous and muscular tissues. Argon lasers used for vascular anastomoses generate a surface temperature of 43° to 48°C which is below the temperature at which collagen degenerates. The largely accepted theory explaining the mechanism by which the Argon laser fuses tissues is that protein bonds are degraded thermally, allowing proteins to rebind to adjacent proteins resulting in a smooth tissue-tissue connection. However, even if the anastomosis strength has been improved with the use of albumin solder [25], this technique has some important limitations: thermal injury to the vessel wall can lead to pseudoaneurysm formation and anastomotic failure [26]. Moreover, the acute histology suggests entry of albumin into the arterial lumen [23] and the role this has on long-term patency has not been determined yet.

Recently, biological glue coupled with a catheter system that stabilise the anastomosis during glue injection has been developed to perform a coronary anastomosis in 3 goats, demonstrating the feasibility of the technique (Fig. 11), but the development of this technique seems to be stuck in the experimental phase [25].

A chronological resume of sutureless anastomosis devices is reported in Figure 12.

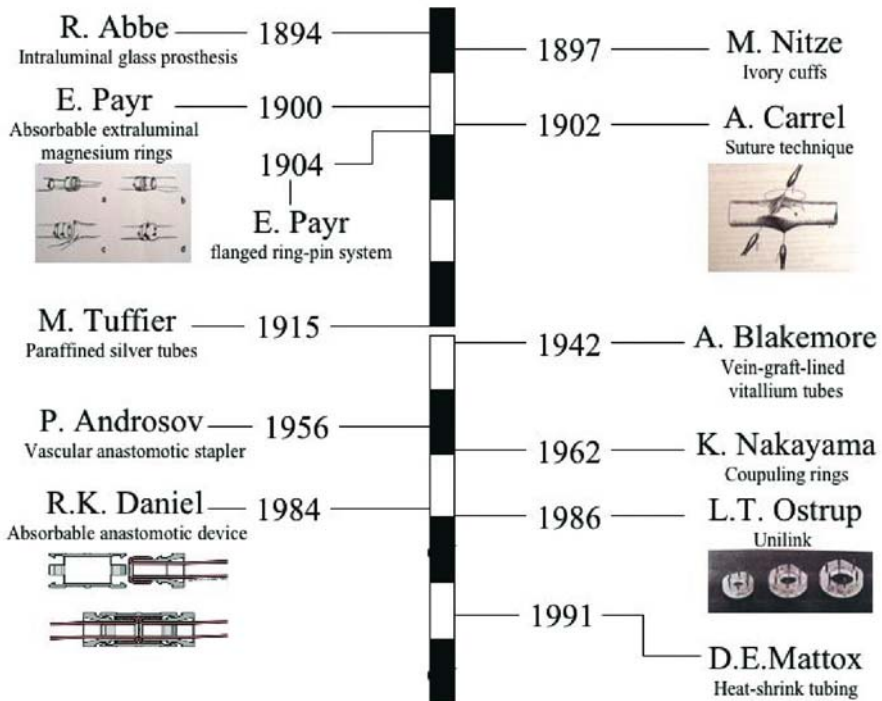


Fig. 12. Chronological summary of the sutureless anastomoses history.

Virtually all the presented devices have more than one limitation that have prevented their wide acceptance and we can summarize the fundamental drawbacks of the historical sutureless devices as follows:

- complex and cumbersome instrumentation
- rigid foreign body enclosing a dynamic dilating structure
- nonflexible technique inapplicable for significant vessel size discrepancies or end-to-side anastomosis
- all showed very poor clinical results.

New anastomotic devices should overcome all these limitations to become widely acceptable and the keys to success are reliability and better clinical results.

■ References

1. Callow AD (1982) Historical overview of experimental and clinical development of vascular grafts. In: Stanley JC, Burkel WE, Lindenauer SM, Barlett RH, Turcotte JG (eds) *Biologic and synthetic vascular prostheses*. Grune & Stratton, NY, pp 11–16
2. Carrel A (1902) La technique opératoire des anastomoses vasculaires et la transplantation des viscères. *Lyon Med* 98:859–863
3. Abbe R (1894) The surgery of the hand. *NY Med J* 59:33
4. Nitze M (1897) Kongress in Moskau. *Centralbl Chir* 24:1042
5. Tuffier M (1915) De l'untubation dans les plaies des grosses artères. *Bull Acad Natl Med (Paris)* 74:455
6. Muir ES (1914) A new device for anastomosing blood vessels. *Lancet* 34:211
7. Payr E (1900) Beiträge zur Technik der Blutgefäß- und Nervennaht nebst Mitteilungen über die Verwendung eines resorbierbaren Metalles in der Chirurgie. *Arch Klein Chir* 62:67–93
8. Payr E (1904) Zur Frage der zirkularen Vereinigung von Blutgefäße mit resorbierbaren Prothesen. *Arch Klein Chir* 72:32–54
9. Steichen FN, Ravitch MM (1982) History of mechanical devices and instruments for suturing. In: Ravitch MM, Steichen FM, Austen WG, Scott HW Jr, Fonkalsrud EW, Polk HC (eds) *Current problems in surgery*. Year Book Medical, Chicago, pp 3–51
10. Landon LH (1913) A simplified method of direct blood transfusion with self retaining tubes. *JAMA* 61:490–492
11. Blakemore AH, Lord JW, Stefco PL (1942) The severed primary artery in the war wounded. A non sutured method of bridging arterial defects. *Surgery* 12:488
12. De Bakey ME, Simeone FA (1946) Battle injuries of the arteries in World War II. An analysis of 2471 cases. *Ann Surg* 123:534
13. Androsov PI (1956) New method of surgical treatment of blood vessel lesions. *Arch Surg* 73:902
14. Inokuchi K (1961) Stapling device for end-to-side anastomosis of blood vessel. *Arch Surg* 82:337

15. Goetz R, Rhoman M, Haller J, Dee R, Rosenak S (1961) Internal mammary-coronary artery anastomosis. A non suture method employing tantalum ring. *J Thorac Cardiovasc Surg* 41:378–386
16. Nakayama K, Tamiya T, Yamamoto K (1962) A simple new apparatus for small vessel anastomosis. *Surgery* 52:918
17. Haller JD, Kripke DC, Rosenak SS (1965) Long term results of small vessel anastomoses with a ring technique. *Ann Surg* 161:67
18. Daniel RK, Olding M (1984) An absorbable anastomotic device for microvascular surgery: experimental studies. *Plast Rec Surg* 74(3):329–336
19. Mattox DE, Wozniak JJ (1991) Sutureless vascular anastomosis with biocompatible heat-shrink tubing. *Arch Otolaryngol Head Neck Surg* 117:1260–1264
20. Berggren A, Ostrup LT, Lidman D (1987) Mechanical anastomosis of small arteries and veins with the Unilink apparatus: a histological and scanning electron microscopic study. *Plast Reconstr Surg* 80:274–283
21. Obora Y, Tamaki N, Matsumoto S (1978) Nonsuture microvascular anastomosis using magnet rings: preliminary report. *Surg Neurol* 9(2):117–120
21. Kirsch WM, Zhu YH, Hardesty RA et al. (1992) A new method for microvascular anastomosis: report of experimental and clinical research. *Am Surg* 58:722–727
22. Kirsch WM, Zhu YH, Wahlstrom E, Wang ZG, Hardesty R, Oberg K (1998) Vascular reconstructions with nonpenetrating arcuate-legged clips. In: Yao JST, Pearce WH (eds) *Techniques in vascular and endovascular surgery*. Appleton & Lange, Stamford, CT, pp 67–89
23. Jain KK, Gorisch W (1979) Repair of small blood vessels with the neodymium-YAG laser: a preliminary report. *Surgery* 85:684–688
24. Phillips ABM, Ginsburg BY, Shin SJ, Soslow R, Wilson K, Poppas DP (1999) Laser welding for vascular anastomosis using albumin solder: an approach for MID-CAB Lasers. *Surg Med* 24(4):264–268
25. Grubbs PE, Wang S, Marini C, Rose DM, Cunningham JN (1988) Enhancement of CO₂ laser microvascular anastomoses by fibrin glue. *J Surg Res* 45:112–119
26. Gundry SR, Black K, Izutani H (2000) Sutureless coronary artery bypass with biologic glued anastomoses: preliminary in vivo and in vitro results. *J Thorac Cardiovasc Surg* 120(3):473–477

2

The physiology of blood flow and artery wall

Introduction

Arterial hemodynamics play an important role in the genesis and progression of vascular diseases and anastomoses outcome [1]. Flow dynamics on the vessel bifurcation and on the vascular anastomosis and the mechanical properties of artery wall seem to play an important role in the development of myointimal hyperplasia. Non-physiological or turbulent flow fields like flow stagnation, flow separation, recirculation, as well as intramural stress distributions promote atherosclerotic disease and myointimal proliferation (Fig. 1).

Myointimal hyperplasia can reasonably be considered the leading cause of anastomosis stenosis and eventually occlusion and, therefore, it is the cardiovascular surgeon's number one enemy (Fig. 2).

To better understand the effects of flow dynamics on vascular anastomoses it is necessary to review the principles of fluid mechanics. This chapter reviews the essential concepts of flow dynamics applied to the blood tissue and analyses the mechanical properties of normal artery walls and their methods of quantization, pointing out the areas that deserve further research.

2.1 The physical nature of blood flow

The vascular system has 3 main specific characteristics:

- it has a three-dimensional geometry that involves shape in diameter, spatial bending and twisting;
- it has a tree structure that involves branching and bifurcation with discontinuities at joining points;
- it has a dynamic motion mostly seen in coronary arteries that involves translation, rotation, extension and contraction.

On top of this, one should consider that atherosclerosis and aging processes deeply affect all these characteristics. It can be easily understood

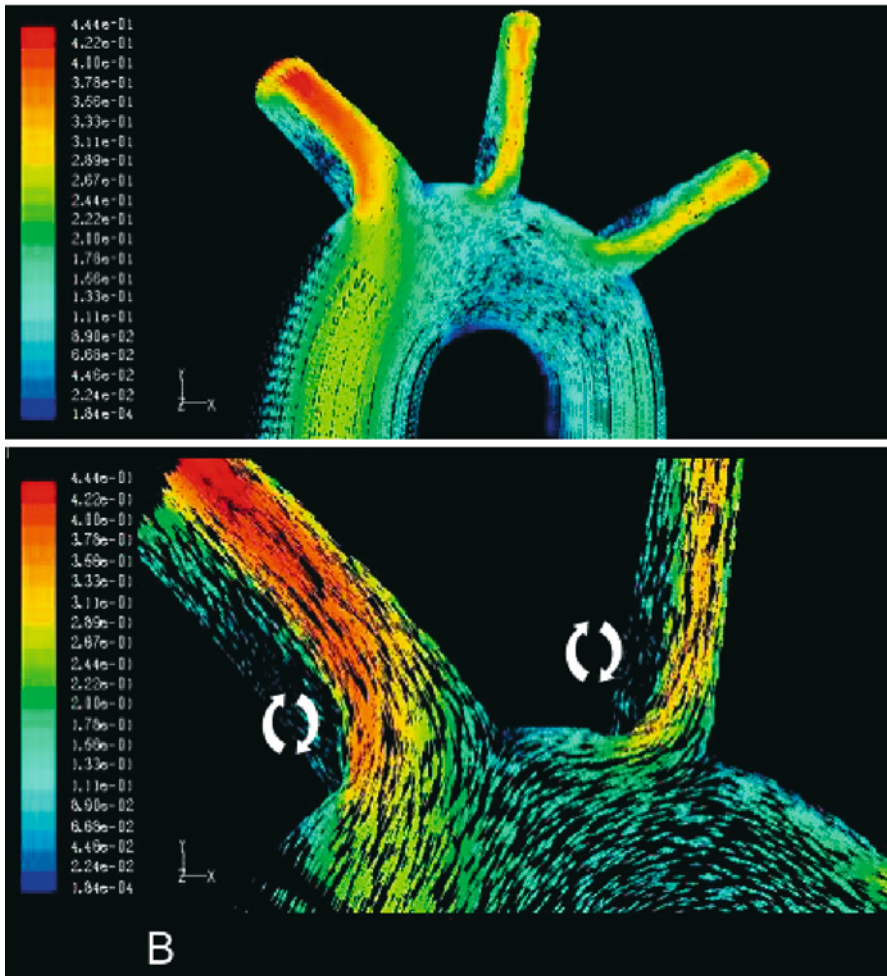


Fig. 1. Computational flow dynamics of blood flow velocities into the aortic arch. **B:** Details of flow velocities and vectors at the origin of brachiocephalic trunk and left carotid artery. Arrows indicate areas where the flow comes apart from the wall generating zones of recirculation. In these areas wall shear stress is very low and this is thought to promote myointimal hyperplasia.

that it is extremely difficult to reproduce an experimental or mathematical model that takes into account all the characteristics of the vascular system and all its changes due to aging and atherosclerosis. Therefore, all the models we describe in this chapter reproduce only a part of the real physical situation, but this is the best we can do today.

The equations most commonly used to describe the blood flow apply to a simple model that is very far from reality: flow is nonpulsatile and laminar, vessels are cylindrical tubes with rigid walls and blood is a Newtonian

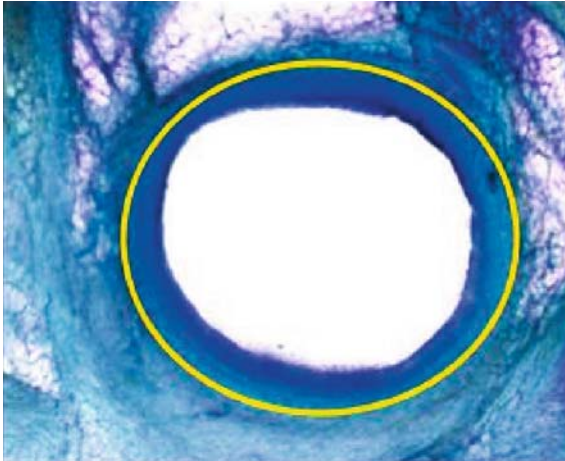


Fig. 2. Left Anterior Descending (LAD) artery of adult sheep 6 months after an off pump coronary artery bypass (left internal mammary artery on LAD). In yellow the lamina basalis. There is a 45% reduction of the coronary cross sectional area due to the proliferation of smooth muscles cells.

fluid. Nevertheless, the equations are extremely useful in understanding flow and how it is altered by pathological or post surgical states.

Bernoulli's Law

Bernoulli described the interaction of pressure, potential energy and kinetic energy in the physics of flow in tubes. Beginning with the equation for total hydraulic energy (E) which represents the sum of all forces contributing to the movement of blood-like fluid

$$E = P + \rho gh + \frac{1}{2} \rho v^2$$

where P is the intravascular pressure, ρ is blood density, g is gravity acceleration, h is distance from the heart and v is blood velocity, Bernoulli demonstrates the conservation of energy in flowing ideal Newtonian fluid moving along a streamline in a frictionless system [2]. Bernoulli's law states that when fluid flows without acceleration or deceleration (steadily) from one point to another, its total energy content along any given streamline remains constant, provided there are no frictional losses, so that if the velocity should decrease downstream, total energy can be conserved by increasing the pressure. This is true in the human body where blood velocity gradually decreases with the increase of vascular cross-sectional area reaching the minimal velocity at the capillary bed. The loss of velocity is converted into intravascular pressure.

It is well known that vascular endothelial cells and smooth muscle cells adapt their biological activity as a function of the force exerted by the flow on the vessel wall: this force is defined as fluid shear stress. From the pressure, diameter, length and flow data, it is possible to calculate a number of

biomechanical and hemodynamics indexes to define the fluid shear stress and the wall strain. Mean fluid shear stress can be calculate with the following expression assuming that the velocity profile is parabolic:

$$\tau = \frac{a}{\sqrt{2}} \frac{\mu \bar{Q}(t)}{\pi R^3}$$

where τ = wall shear stress (dynes/cm²), μ = coefficient of viscosity (dynes-s/cm²), $\bar{Q}(t)$ = flow rate (ml/sec), R = radius (cm) and a = Womersley parameter [3].

The equation for the Womersley parameter is:

$$a = R \sqrt{\frac{2\pi\rho f}{\mu}}$$

where f = frequency (Hz), and ρ = the density (gm/ml) [4].

Reynolds numbers are used to give a quantitative analysis of potential turbulences within the flow system. With few exceptions, it is possible to affirm that low Reynolds numbers are associated with flow stagnation, flow separation and recirculation, or simply non-physiologic flow. Equations for mean and modulation Reynolds numbers are:

$$Rem = \frac{\rho VD}{\mu}$$

where Rem = mean Reynolds numbers, ρ = the density (gm/ml), μ = coefficient of viscosity and D = diameter (cm) [4]

$$Remw = \frac{Re \max - Re \min}{2}$$

where $Re \max$ is the maximum Reynolds number and $Re \min$ is the minimum Reynolds number [4].

Clear evidence exists for a relationship between low flow velocity, low shear stress, low Reynolds numbers and smooth muscle cell proliferation at the anastomotic site. Intimal hyperplasia in experimental vein grafts can be generated by long-term decreased flow.

Normal arteries with a τ of 10 to 70 dyne/cm² remodel in response to high shear by dilatation and thinning [5], whereas chronically low shear stress leads to intimal thickening and contraction [6, 7]. Very low levels of shear stress ($\tau < 2$ dyne/cm²) lead to a variety of pathologic endothelial cellular events including hyperpolarization, adhesion molecule expression, intracellular calcium release, down regulation of prostaglandin I₂ and nitric oxide synthase, and platelet derived grow factor production [8-10].

Low shear stress enhances the hyperplastic response to vessel injury after balloon angioplasty [11]. Areas of low shear and flow separation induce mass transfer and atherosclerosis [12] and the shear stress hypothesis remains one of the prevailing theories of atherogenesis [13, 14].

In a dog model Berguer has demonstrated that reductions in blood flow of 50% to 80% have generally led to a doubling of myointimal hyperplasia [15]. Dobrin has demonstrated in several studies that smooth muscles cells of vein graft increase their mitotic activity and migrate into the vessel lumen through the *lamina basalis* when the vessel wall is exposed to low shear stress [16, 17]. In an elegant study, Meyerson describes the effects of extremely low shear stress on neointimal thickening in the failing venous bypass graft [18]. If the shear stress is lower than 2 dyne/cm^2 the rate of smooth muscles cell proliferation increases with a non linear correlation causing the rapid progression of neointimal lesions that lead to bypass graft occlusion.

2.2 Mechanical properties of artery wall

Arteries change structurally and mechanically during development, maturation and aging. The extensive literature in this area may be summarized as follows: during fetal and neonatal development, artery diameter and wall thickness increase. Histologically, the wall exhibits gradual widening of the media, less cellularity, more elastic lamellae and increasing collagen content. The collagen-to-elastic ratio of arteries increases throughout development and maturation. With age, the arterial diameter dilates and wall thickness and collagen-to-elastine ratio increase. These changes are associated with rising arterial stiffness, as demonstrated by changes in load-length relations of vascular strips and rings, increased pulse-wave velocity and increased vascular impedance.

In vivo arterial motion occurs mostly in the circumferential and radial direction; much smaller changes occur in the longitudinal direction.

Circumferential properties

Extrathoracic systemic arteries change 8–10% in diameter with each cardiac cycle, whereas the diameter of the intrathoracic arteries changes 8–18% with each cardiac cycle [19]. The distensibility of intrathoracic vessels correlates with the relatively high content of elastin in their wall. As suggested by Dobrin, the elastin may determine vessel properties at small diameters and collagen may determine vessel properties at larger diameters. The distensibility characteristics of arteries depend on the extent to which they are stretched which in turn depend on transmural pressure. At low pressures and small diameters the arteries are very distensible, whereas with increasing pressure and diameter they become gradually stiffer. Although there is no sharp inflection point in a volume-pressure and pressure-diameter relationship, the transition from compliant to stiff behaviour occurs

between 80 and 120 mmHg in large arteries [20]. These values tend to decrease with age, so that arteries of aged patients are functionally stiffer at physiological pressures. Also arteries are generally stiffer toward the periphery of the circulation because of the increase in collagen-to-elastin ratio in the distal arterial tree and stiffness may be especially high at bifurcations [21].

The elastic properties of arteries may be numerically expressed by computing strain-stress relations and incremental elastic moduli. Strain (ε) in the circumferential direction is:

$$\varepsilon = \frac{(d - d_0)}{d_0} = \frac{\Delta d}{d_0}$$

where d is the observed diameter and d_0 is the retracted or totally unloaded vessel. ε expresses the change in d as a fraction of some predetermined reference dimension.

The mean circumferential stress σ_θ is:

$$\sigma_\theta = P_t \times \frac{r_i}{h}$$

where r_i is the internal radius, P_t transmural pressure and h wall thickness.

Circumferential stress is comparable to the wall tension given by the law of Laplace but accounts for the finite wall thickness of arteries.

For materials having linear strain-stress relations, the ratio of stress to strain can be used to compute the Young's elastic modulus, a measure of material stiffness. For a cylindrical vessel with wall stiffness that is equal in all directions, the elastic modulus (E) may be computed by:

$$E = \frac{\Delta\sigma_\theta}{\Delta\varepsilon_\theta}$$

where $\Delta\sigma_\theta$ and $\Delta\varepsilon_\theta$ are small changes in stress and strain respectively.

The mean circumferential stress σ_θ is not distributed uniformly across the wall. Several investigators have shown that the point stress is high at the lumen and declines curvilinearly across the wall thickness [22]. This distribution closely resembles the density of the elastic lamellae at different points across the wall; elastic lamellae are close together near the lumen and more widely spaced near the adventitia. This suggests that an adaptive relationship may exist between morphology and mechanical load at different locations across the wall.

Longitudinal properties

Several studies have reported arterial length changes during the cardiac cycle, however no clear relationship with pulse pressure were provided. Lawton [23] reported a 1% increase in length of the thoracic aorta and a 1% decrease in length of the abdominal aorta during cardiac cycles without

identifying any relationship with pulse pressure. Patel reported [24] that the ascending aorta and the pulmonary arteries could modify their length up to 11% but this axial movement resulted from gross motion of the heart. In vivo, there are at least two structures that provide arterial fixation to the surrounding structures: perivascular connective tissues and arterial side branches. The fixation of arterial side branches and the presence of periadventitial connective tissues cause tethering. Patel and Fry [25] suggest that perivascular traction is distributed over the length of the arterial tree. It is minimal at the aortic root and increases with the distance from the aortic valve.

Moreover, arteries are extended in the longitudinal direction. It is reflected by the observation that excising arteries causes them to retract. Dobrin reports that the interaction between pressure and traction stresses keeps the length of artery nearly constant [26]. All these statements are based on experimental data obtained with electromechanical gauges applied to exposed vessels or with roentgenographic and ultrasonic methods [16, 17, 19].

Using high-resolution investigation tools, we recently demonstrated [26] that the axial deformation of a 1 cm-long segment of pig common carotid artery (CCA) is consequential although twice as small as the diameter changes observed during the cardiac cycle. Moreover, during systole the vessel shortens and dilates. We suggest qualifying this arterial motion as axial systolic shortening.

Longitudinal displacement of piezoelectric crystals placed 9–15 mm apart (Fig. 3) is comprised between 0.11 mm and 0.65 mm. Because the distance between the two piezoelectric crystals could not be kept constant due to technical constraints, the results are expressed as relative changes of

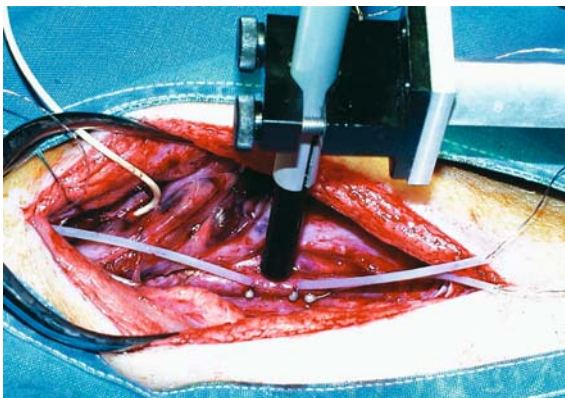


Fig. 3. Pig's carotid arteries have been exposed. Three piezoelectric crystals are sutured on right carotid and the echo-tracking system (NIUS 02) is placed on the carotid between the 2 crystals to calculate carotid diameter and cross-sectional compliance. A high fidelity pressure probe (yellow catheter on the right upper part of the incision) is inserted in the left carotid.

the distance between the crystals: the displacement varies from 1.14% to 5.8%. The behaviour of the vessel did not change significantly during the whole experiment. To exclude interference of pulse waves and blood mass (viscosity and hematocrit) on the ultrasonic waves during measurements, we switched the receiver/transmitter functions of the piezoelectric crystals in all feasible combinations. The results obtained under these conditions did not reveal any significant difference in ΔL . Therefore, blood mass and pulse wave reflections can be considered to have no significant influence on the measurements of this segment of CCA.

Our conclusions hold true provided that the examined arterial segment is straight. Indeed, if the vessel shows a significant curvature, then the convex part would slide over the concave part of the vessel wall. We tested this possibility by measuring axial length at 3 different sites of the vessel circumference and comparing their axial deformation. No difference was observed between the sites implying that the examined vessel segment is straight.

Axial movement is inversely correlated to pulse pressure. This inverse correlation is shown in Figure 4 where regression analysis of the distance between crystals versus blood pressure is plotted. Increasing blood pressure causes vessel length reduction with a highly significant correlation ($R=0.97$; $p<0.001$). This was a characteristic feature observed in all animals in the study; correlation coefficient (R) was always greater than 0.92. The slope in the diastolic pressure range is lower than the mean systolo-diastolic slope which most likely results from the hysteresis due to viscoelastic properties of the material in the axial direction. The same has been observed in the cross-sectional direction [19, 27].

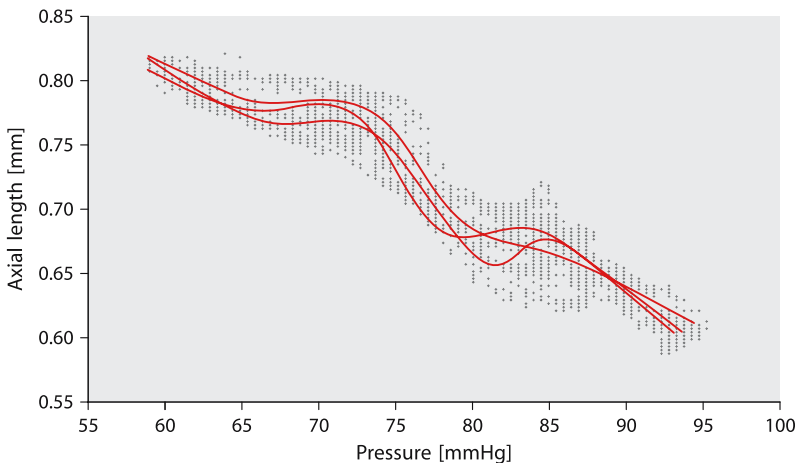


Fig. 4. Correlation between piezoelectric crystal distances and arterial blood pressure in 10 pigs. Blood pressure increase correlates with vessel shortening ($R=0.97$).

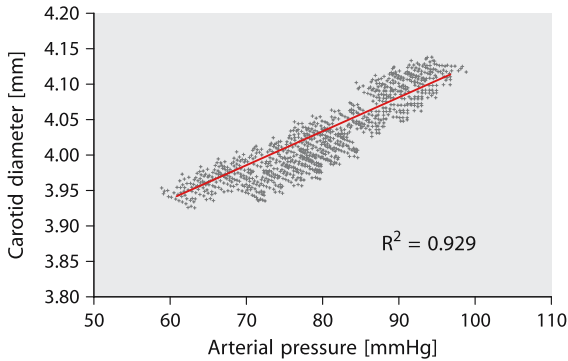


Fig. 5. Correlation between carotid diameter and arterial pressure ($R=0.96$) in 10 pigs.

Whether integrity of the endothelial function plays a role in the behaviour of the axial wall motion and more specifically on the importance of this hysteresis remains to be determined. It is well known that the carotid artery diameter is directly correlated to blood pressure and this was also confirmed in our study. Figure 5 shows the relationship between carotid diameter and arterial pressure: $R=0.96$; $p < 0.001$.

In general it is assumed that axial strain can be neglected compared to the circumferential strain. Our findings confirm that the axial strain is indeed lower than the radial strain. On the average an axial length modification of 2.7% was found for a diameter variation of 4.8%. It is also well known that the mechanical properties of the artery are anisotropic although, for deformations that occur in vivo, the elasticity of arteries can be considered isotropic [28]. However, canine carotid and femoral arteries are stiffer in the circumferential than in the longitudinal direction, whereas the reverse is true for canine and bovine aorta. This may be due to the differences in wall architecture and in load bearing of the wall constituents in each direction. Thus arteries in vivo undergo unequal deformations in each direction, and this differentially stretches and stiffens all constituents.

The systolic arterial shortening represents the capacity of the vessel wall to passively adapt to axial stress (σ_z) and it should clearly be differentiated from an active contraction. These findings contrast with the description of the arterial wall movement observed by Levy et al. [29]. In an elegant experimental study performed in vitro on rat common carotid arteries, the authors report an increase in carotid length in response to pressure. This axial length increase was more important in normotensive than in spontaneously hypertensive rats. However, the measurements were determined by video microscopy and computer-assisted image analysis. Therefore, due to the major differences in experimental conditions, the results cannot be appropriately compared.

The role of the axial movement in the determination of volumetric compliance measurement is not clear. Arterial compliance (C) is expressed as the ratio between vessel volume variation (ΔV) during cardiac cycle and pulse pressure (ΔP)

$$C = \frac{\Delta V}{\Delta P}$$

In clinical practice, a high-resolution echo-tracking system allows to precisely measure local cross-sectional compliance considering only vessel diameter variations. Instead of measuring volumetric changes (Δm^3) only cross-sectional area (Δm^2) is measured. Cross-sectional compliance is thus defined as the ratio between variations in arterial cross-sectional area (ΔA) and blood pressure (ΔP)

$$CC = \frac{\Delta A}{\Delta P}$$

CC is expressed in $\mu m^2/mmHg$ or m^2/kPa [30].

According to our data, it would not appear appropriate to neglect the axial movement in the computation of segmental arterial compliance because it overestimates the volumetric elastic properties of the vessel. If similar axial movement occurs in the human carotid artery, then reappraisal of local arterial compliance measurements would appear necessary. Volumetric compliance assessment based on a method taking into account the postulate of mass continuity may represent an interesting option. In an animal model, we measured the ratio of blood flow gradient through an arterial segment and the derivative of blood pressure over a given time. According to the principle of continuity of mass, arterial compliance can be expressed as:

$$C_d = \frac{\bar{Q}_{in} - \bar{Q}_{out}}{\Delta P / \Delta t}$$

where Q_{in} is the instantaneous blood inflow in a given arterial conduit; Q_{out} is the blood outflow in the same conduit at the same time; the difference between Q_{in} and Q_{out} represents the energy converted in the vessel wall deformation during blood displacement and is identified as phase shift (φ). C_d is what we have called the vessel wall dynamic compliance; $\Delta P / \Delta t$ is the derivative of pressure in a considered interval of time. To calculate carotid maximal dynamic compliance, we considered the maximal phase shift between inflow and outflow and calculated the correspondent $\Delta P / \Delta t$.

Even with many limitations, this method has the prerogative to quantify the impact of axial strain in compliance calculation. Our results correlate with those reported in current literature from the qualitative point of view: as blood pressure increases instantaneous φ decreases (Fig. 6) and, therefore, C_d decreases [28]. The impact of axial strain in compliance calculation could be expressed by the fact that that C_d is smaller than CC because in the equation

$$\frac{\Delta V}{\Delta P} = (L \times CC) + A \times \frac{\Delta L}{\Delta P}$$

the $A \times \frac{\Delta L}{\Delta P} < 0$

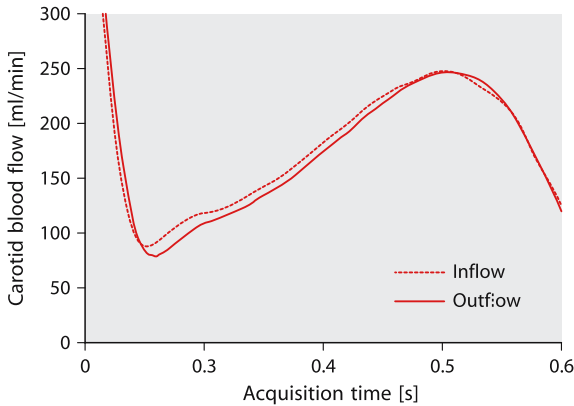


Fig. 6. Inflow (dashed line) and outflow (continuous line) through a 10 cm segment of pig carotid artery measured simultaneously. The difference between the two lines is the phase shift (φ) and it represents the energy converted in the vessel wall deformation during blood displacement.

since vessel shortens when pressure increases. Thus,

$$\frac{\Delta V}{\Delta P} \leq (L \times CC)$$

which means that arterial compliance is smaller than cross-sectional compliance. It can be speculated that for the same pulse pressure, the increase in vessel diameter is associated to the decrease in vessel length and vice-versa. There is probably a correlation between the degree of diameter change versus the degree of shortening, i.e.: the greater the diameter increases the greater the axis shortens. Therefore, vessel volume variations (ΔV) during cardiac cycle seem to be smaller than previously thought.

However, for practical purpose cross-sectional distensibility of the vessel provides valuable information on the elasticity of the vessel wall and when the distensibility is related to wall thickness the elastic modulus of wall material can be assessed.

References

1. Asakura T, Karino T (1990) Flow patterns and spatial distribution of atherosclerotic lesions in human coronary arteries. *Circ Res* 66:1045–1066
2. Hopkins RW (1991) Presidential address. In: Bernoulli D, Young T, Poiseuille JLM, Simone FA (eds) *Energy, Poise, and Resilience*. *J Vasc Surg* 13:777–784
3. Wolf S, Werthenssen N (1979) *Dynamics of arterial flow*. Plenum Press, New York
4. Nichols WW, O'Rourke MF (1990) *McDonald's blood flow in arteries, theoretic, experimental and clinical principles*, 3rd ed. Lea & Febiger, Philadelphia London, pp 38–56
5. Zarins CK, Zatina MA, Giddens DP, Ku DN, Glagov S (1987) Shear stress regulation of artery lumen diameter in experimental atherogenesis. *J Vasc Surg* 5:413–420

6. Zhuang YJ, Singh TM, Zarins CK, Masuda H (1998) Sequential increases and decreases in blood flow stimulates progressive intimal thickening. *Eur J Vasc Endovasc Surg* 16:301–310
7. Gnasso A, Carallo C, Irace C, Spagnuolo V, de Novara G, Mattioli PL (1996) Association between intima-media thickness and wall shear stress in common carotid arteries in healthy male subjects. *Circulation* 94:3257–3262
8. Davies PF, Tripathi SC (1993) Mechanical stress mechanisms and the cell: an endothelial paradigm. *Circ Res* 72:239–245
9. Malek AM, Izumo S (1994) Molecular aspects of signal transduction of shear stress in the endothelial cell. *J Hypertens* 12:989–999
10. Mohan S, Mohan N, Valente AJ, Sprague EA (1999) Regulation of low shear flow-induced HAEC VCAM-1 expression and monocyte adhesion. *Am J Physiol* 276:C1100–1107
11. Hehrlein C, Chuang CH, Tuntelder JR, Tatsis GP, Littmann L, Svenson RH (1991) Effects of vascular runoff on myointimal hyperplasia after mechanical balloon or thermal laser arterial injury in dogs. *Circulation* 84:884–890
12. Zarins CK, Giddens DP, Bharadvaj BK, Sottiurai VS, Mabon RF, Glagov S (1983) Carotid bifurcation atherosclerosis: quantitative correlation of plaque localization with flow velocity profiles and wall shear stress. *Circ Res* 53:502–514
13. Pedersen EM, Oyre S, Agerbaek M, Kristensen IB, Ringgaard S, Boesiger P et al. (1999) Distribution of early atherosclerotic lesions in the human abdominal aorta correlates with wall shear stresses measured in vivo. *Eur J Vasc Endovasc Surg* 18:328–333
14. Malek AM, Alper SL, Izumo S (1999) Hemodynamic shear stress and its role in atherosclerosis. *JAMA* 282:2035–2042
15. Berguer R, Higgins RF, Reddy DJ (1980) Intimal hyperplasia. An experimental study. *Arch Surg* 115(3):332–335
16. Dobrin PB, Littooy FN, Edean ED (1989) Mechanical factors predisposing to intimal hyperplasia and medial thickening in autogenous vein grafts. *Surgery* 105(3):393–400
17. Dobrin PB (1995) Mechanical factors associated with the development of intima and medial thickening in vein grafts subjected to arterial pressure. *Hypertension* 26:38–43
18. Meyerson SL, Skelly CL, Curi MA et al. (2001) The effects of extremely low shear stress on cellular proliferation and neointimal thickening in the failing bypass graft. *J Vasc Surg* 34:90–97
19. Dobrin PB (1978) Mechanical properties of arteries. *Physiol Rev* 58:397–460
20. Cox RH (1978) Passive mechanics and connective tissue composition of canine arteries. *Am J Physiol* 234:H533–H541
21. Schonfeld D, Atabek HB, Patel DJ (1979) Geometry and elastic response of the aorto iliac junction. *J Biomech* 12:483–489
22. Doyle JM, Dobrin PB (1973) Stress gradients in the walls of large arteries. *J Biomech* 6:631–639
23. Lawton RW (1957) Some aspects of research in biological elasticity. Introductory remarks. In: Remington JW (ed) *Tissue elasticity*. Am Physiol Soc, Washington, DC, pp 1–11
24. Patel DJ, Fry DL (1964) In situ pressure-radius-length measurements in ascending aorta of anesthetized dogs. *J Appl Physiol* 19:413–416

25. Patel DJ, Fry DL (1966) Longitudinal tethering of arteries in dogs. *Circ Res* 19:1011–1021
26. Tozzi P, Hayoz D, Oedman C, Mallabiabarrena I, von Segesser LK (2001) Systolic axial artery length reduction: an overlooked phenomenon in vivo. *Am J Physiol Heart Circ Physiol* 280(5):H2300–H2305
27. Arndt JO, Kober G (1970) Pressure diameter relationship of the intact femoral artery in conscious man. *Pflugers Arch* 318:130–146
28. Weizsacker HW, Pinto JG (1988) Isotropy and anisotropy of the arterial wall. *J Biomech* 21(6):477–487
29. Lichtenstein O, Safar ME, Poitevin P, Levy BI (1995) Biaxial mechanical properties of carotid arteries from normotensive and hypertensive rats. *Hypertension* 26(1):15–19
30. Tozzi P, Hayoz D, Corno AF, Mallabiabarrena I, von Segesser LK (2003) Cross-sectional compliance overestimates arterial compliance because it neglects the axial strain. *Swiss Med Wkly* 133:461–464

3

Mathematic modelling of vascular anastomoses

Introduction

The majority of mathematical models of vascular anastomoses assume that blood flow is laminar, the blood is an incompressible non-Newtonian fluid and conduits, arteries and graft as well, have rigid walls that don't react to blood pressure.

If we are looking for a more realistic model, we have to consider that the flow inside an artery is the result of the interaction between a fluid, the blood, and an elastic conduit, the vessel, each governed by a distinct set of partial differential equations. With this approach, we are able to compute pressure and velocities of the fluid, as well as displacement of the structure at any point of the computational domain. The principal quantities that describe blood flow are the velocity V and the pressure P . Knowing these fields, we can calculate the stress to which an arterial wall is subject due to the blood movement. The displacement of the vessel wall due to the action of the flow field is another quantity of relevance. Moreover, pressure, velocity and vessel wall displacement will be function of time and of spatial position, since blood flow is pulsatile. This means that we cannot neglect the time considering a "steady state" solution and, even if with some approximation, we can consider the blood flow to be periodical in time. Unsteady flow is much more complex to define than a steady one. For instance, if we consider the steady flow of a fluid like water inside an infinitely long cylindrical tube, it is possible to derive the analytical steady state solution (Poiseuille flow), characterised by a parabolic velocity profile; the same flow, in a transient regime (Womersley flow) becomes completely different. Figure 1 clearly expresses the difference between the very theoretical and the more realistic and complex mathematical model. However, from the clinical point of view simple geometrical models are still of great importance because they point out the main features of the blood flow and can be easily understood.

There is a general consensus on the fact that local flow dynamics and wall mechanical conditions can induce the development of intimal hyperplasia in vascular graft anastomoses with subsequent graft failure. Beside the thrombogenicity of the surface of synthetic vascular grafts, turbulent flow fields and intramural stress distributions promote intimal thickening

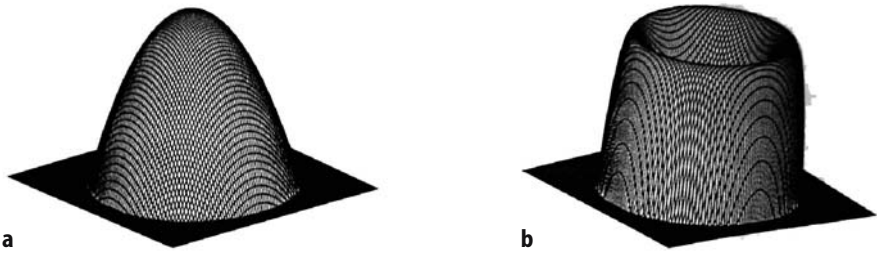


Fig. 1. Difference between theoretical and more realistic blood flow. Profiles of the same flow velocity in a steady state flow (a) (Poiseuille) and in an unsteady pulsatile flow (b) (Womersley) at a given instant.

finally leading to complete luminal occlusion as demonstrated by several experimental and numerical studies [1–5].

Attention is also paid to the migration of stagnation points and secondary motions that are also considered to have an important influence on the disease process. Intimal thickening in end-to-side anastomoses occurs mainly on the artery floor opposite to the connection, along the suture line and especially at the heel and toe of the junction. Experimental studies [6–9] and numerical studies [10–15] underline the correlation between local anastomotic flow characteristics and intimal hyperplasia. Local flow characteristics and wall-shear stress distribution are strongly influenced by the geometrical configuration of the blood vessel. This relationship shows the importance of anatomically correct geometric modelling even if we still don't handle phenomena like the non-planarity of curvature and branching in the arterial systems [16].

In the last ten years, the mechanical properties of the graft and the artery-graft connection have become a field of investigation with respect to the development of intimal hyperplasia, particularly at the suture line. From clinical and in vivo observations, it is known that the mismatch in artery-graft compliance can lead to graft failure [17, 18]. It is assumed that the occurrence of intimal hyperplasia around the suture line is caused by the tissue remodelling as a response to mechanical injury due to the artery-graft compliance mismatch [18, 19]. With the analysis of intramural stress distribution, one can gain a deeper insight into the disease development. In the following we report an example of a numerical study published in 2002 by Leuprecht and co-workers, that reproduces pulsatile flow patterns and vessel wall mechanics in distal end-to-side anastomoses of bypass grafts using expanded polytetrafluoroethylene (e-PTFE) prosthes and investigates the influence of distensible vessel walls on the anastomotic flow field and the occurring stresses [20].

3.1 Realistic mathematical model

Geometric model

The computational geometric model generates a grid that reproduces the luminal cast of a standard end-to-side anastomosis and is based on local optimization of geometric grid properties such as smoothness and orthogonality (Fig. 2).

The flow domain partition applies isoparametric brick elements with eight corners. Each inner grid point represents a common corner point of eight neighboring brick elements (master cell). A local grid function at an inner point P is defined as

$$F = a_s f_s + a_0 f_0 + a_b f_b$$

where the length between P and its six neighbour points is controlled by f_s , f_0 denotes the angle function regulating the orthogonal of the brick edges and f_b governs the orthogonal of the grid near the boundary. Selecting appropriate values for the control parameters a_s , a_0 and a_b the grid generation procedure is started with fixed grid points on the surface and arbitrarily distributed points in the domain. The position of each grid point P is determined by locally minimizing F with respect to P 's co-ordinates resulting in a set of equations for the location of P . Iterating upon the minimization of F finally leads to a proper finite element mesh [14, 15].

Flow model

Newton's law describes the basic physical principles of conservation of mass and momentum and provides the basis for the creation of the three-dimensional, time-dependent Navier-Stokes equations for incompressible fluids. They are valid on any fixed spatial domain at a given time (Fig. 3).

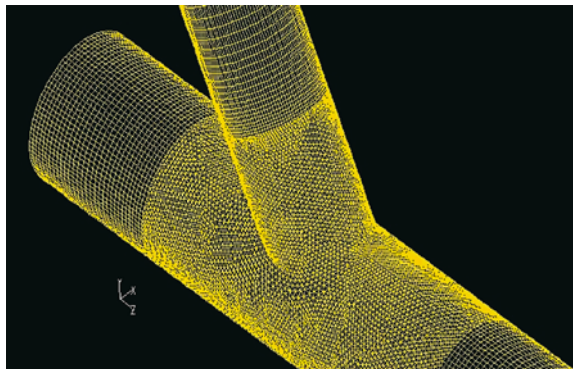


Fig. 2. Computational geometric model of standard end-to-side anastomosis: it represents the luminal cast of the anastomosis.

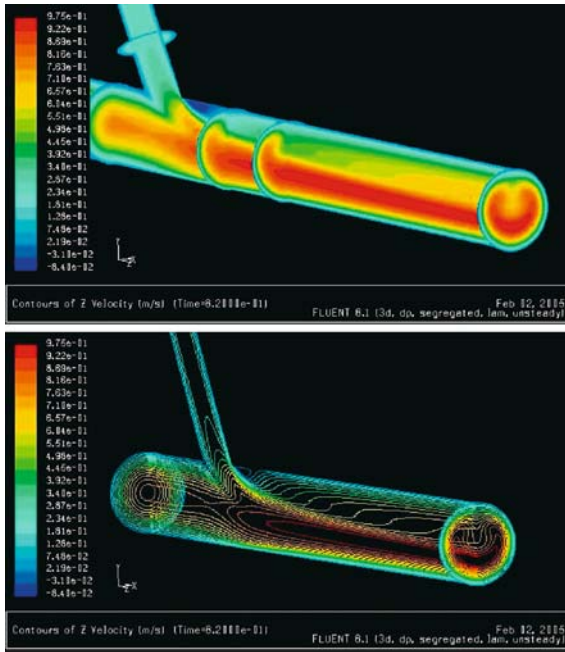


Fig. 3. Computation flow dynamic in end-to-side anastomosis based on three-dimensional, time-dependent Navier-Stokes equations for incompressible fluids. They are valid on any fixed spatial domain at a given time. Different flow velocity configurations can be analysed (high flow top image, low flow bottom image).

The influence of the time-dependent flow domain in distensible models is taken into account by applying an Arbitrary Lagrangian–Eulerian (ALE) kinematical description [21], resulting in a correction of the convective velocity for compliant models with moving boundaries. Under the summation convention, the equations of blood flow without body forces are:

$$\rho \left(\frac{\partial u_i}{\partial t} + \nabla u \times \frac{\partial u_i}{\partial x_j} \right) = \frac{\partial}{\partial x_j} \sigma_{ij}$$

where u_i , $i=1, 2, 3$, are the components of the velocity vector, \vec{u} , \hat{u}_j , $j=1, 2, 3$, denote the components of the domain velocity, $i, j=1, 2, 3$, the components of the Cauchy stress tensor $\rightarrow \vec{\sigma}$ and ρ is the constant for fluid density.

The vessel wall movement that is calculated iteratively at each time step expressing the fluid-structure interaction determines the mesh velocity at an inner point of the flow domain.

The symmetric stress tensor for the Newtonian fluid is expressed by the constitutive equation

$$\sigma_{ij} = -p\delta_{ij} + 2\mu e_{ij}$$

where p is the fluid pressure, δ the Kronecker delta, μ denotes the apparent fluid viscosity and e_{ij} is the component of the rate-of-strain tensor. With regard to the incompressible mass conservation, the extra-stresses can be conveniently inserted into the equation of motion leading to a closed form

of the Navier-Stokes system. Introducing the reference length L_0 , the reference velocity U_0 and the kinematic viscosity $\nu = \mu/\rho$ the equations can be written in non-dimensional form

$$\frac{\partial u}{\partial t} - \frac{1}{\text{Re}} \frac{\partial}{\partial x} \frac{\partial u}{\partial x} + \frac{\partial p}{\partial x} = 0$$

where $\text{Re} = U_0 L_0 / \nu$ is the Reynolds number.

Appropriate boundary conditions must be applied for velocity and pressure. The limit of the flow domain consists of two sections with different types of boundary conditions. Physiologically correct inflow velocity profiles are not available, and thus, fully developed profiles (Womersley profiles) are imposed at the inflow boundary.

At the outflow boundary, the condition describing the surface traction force can be assumed

$$\left(-p\delta + \mu \left(\frac{\partial u_i}{\partial x_j} + \frac{\partial u_j}{\partial x_i} \right) \right) n_j = h_i(t)$$

where n_j , $j = 1, 2, 3$, denote the components of the outward pointing normal unit vector at the outflow boundary. In rigid wall calculations traction-free outflow is assumed. In calculations with moving walls the pressure at the outflow prescribes the normal force $\sigma_n = -p(t)$ and the tangential force is $\sigma_t = 0$.

Wall model

We can assume the vessel wall being a three-dimensional continuous medium for which one dimension, the thickness, is relatively small with respect to the two others. Therefore, with a reasonable approximation, the thickness can be neglected and the vessel wall is represented as a two-dimensional model with two independent curvilinear coordinates approximating the three dimensional structure in the Euclidean space. The mechanical behaviour of the wall is governed by two-dimensional equations that are defined with respect to the middle surface of the structure that serves as a reference surface [22]. The main problem consists in determining the deformation of the reference surface under the physical properties of the vessel wall, the distribution of applied forces and appropriate boundary conditions. Strains and stresses in the wall can then be calculated from the deformation. The description of the wall mechanics applies a functional approach. The function represents the total potential energy consisting of the loading part (applied pressure force) and the deformation part (strain energy). The strain energy in the variational formulation is expressed by a reference surface integral, where the integrand is formed by a quadratic expression of the strain tensor components defining the extensional energy

per unit area, and the tensor of curvature change of the reference surface expressing the bending energy per unit area. The numerical solution applies the principle of minimum potential energy with respect to the chosen finite element subspace. Due to the relatively large displacements in the anastomotic region, the analysis uses geometric non-linear theory.

Elastic behaviour is assumed for the different wall materials (native artery and e-PTFE graft). The corresponding elastic moduli have been determined from experimental deformation results [17]. The validity of the simplified linearly elastic relation has been proven in various computations carried out in pressure loaded cylindrical vessel models with different mechanical characteristics (linearly elastic, hyperelastic and viscoelastic). Numerical experiments showed minor quantitative influence on the vessel wall displacements compared with the elastic results [23].

Numerical approach

The numerical solution of the time-dependent three-dimensional Navier-Stokes system describing the incompressible Newtonian fluid flow applies a developed velocity-pressure correction method [23]. It is based on the decomposition of a sufficiently regular vector field into a divergence-free and a rotation-free field. This technique offers an efficient method for the solution of three-dimensional flow problems by decoupling the occurring variables.

The calculation of the wall displacements and the intramural stresses (principal stresses) can be done using any commercial finite element program package like ABAQUS. The wall model applies a four-node doubly curved, shear flexible shell element with reduced integration and hourglass control and five degrees of freedom: three displacement components and two in-surface rotation components.

The fluid-structure interaction is expressed by an iterative coupling of the fluid motion and the vessel wall deformation at a time level. The algorithm's basic steps are:

- Calculate the wall position and the wall velocity from the total wall pressure and the vessel wall mass forces with the ABAQUS package.
- Update the vessel geometry and the finite element mesh and interpolate the velocity and the pressure at the displaced nodes.
- Update the convective velocity in the equations of motion taking into account the mesh velocity determined by the wall velocity.
- Calculate the kinematic quantities by the algorithm described above.

The stop criterion of the iterative procedure at a time level is based on the difference in successive velocities in the iteration scheme:

$$\max_i \left\{ \frac{u_i^{n+1,m+1} - u_i^{n+1,m}}{u_i^{n+1,m+1}} \right\} \leq 0.01$$

where the $u_i^{n+1,m}$, $i=1, 2, 3$, are the three components of the velocity vector \vec{u} at a velocity node of the finite element mesh at the time level $n+1$ and iteration step m . When it is satisfied for all velocity nodes the iteration process is stopped. The largest errors occur in the region near the suture line. In the remaining flow domain the errors are significantly smaller.

Modelling

Applying mean inflow velocity $U_0=0.42$ m/s, the apparent viscosity $\mu=3.9 \times 10^{-3}$ Pas, the constant density $\rho=1044$ kg/m³ and the reference length $L_0=3.95 \times 10^{-3}$ m results in the Reynolds number $R=380$. The Womersley number is $\lambda=3.13$.

In Figure 4 characteristic axial flow profiles during systolic deceleration ($t/tp=0.42$) are demonstrated for the conventional type anastomosis. Extremely skewed profiles towards the outer (far) wall occur in the anastomotic region and downstream forming a jet flow. Zones of recirculation are found on the artery floor opposite the junction.

Axial and circumferential wall shear stress are demonstrated in Figure 5 at two chosen points on the hood and on the floor of cross-section B indicated in Figure 4 during the cardiac cycle. The comparison between the distensible wall models (bold line) and their referential rigid wall configurations corresponding to the diastolic geometry (thin line) do not show qualitative differences. The wall shear stress on the artery floor is very low and oscillating. The axial wall shear stress on the hood follows the pulse waveform. Circumferential wall shear stress is 1/10 of the axial stress magnitude.

On the basis of the finite element meshes for the fluid flow simulations, shell meshes of the vessel walls can be generated for the wall mechanical studies (Fig. 6).

In the analysis the materials of the synthetic graft and the artery are assumed to be elastic with Young's moduli of $E_g=7.5 \times 10^6$ N/m², $E_a=$

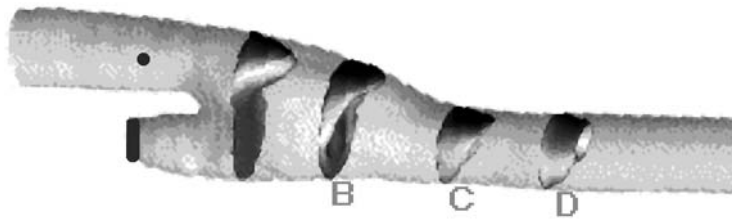


Fig. 4. Axial velocity profiles during systolic deceleration ($t/tp=0.42$) at different cross-sections of conventional type anastomosis.

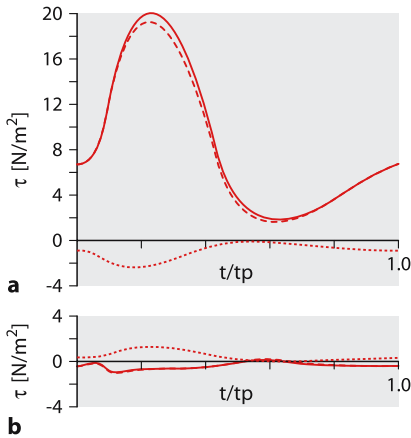


Fig. 5. Conventional type anastomosis: axial (solid line) and circumferential (dashed line) wall shear stress during cardiac cycle; (a) hood and (b) floor point of cross-section B (as indicated in Fig. 4); distensible model (bold lines) and rigid model (thin lines).

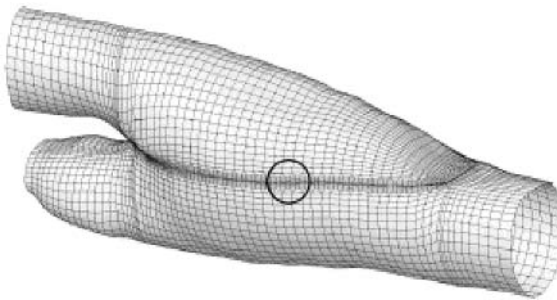


Fig. 6. Geometric wall model: finite element mesh of the anastomotic wall region: conventional type anastomosis.

$4.1 \times 10^5 \text{ N/m}^2$ and $E_v = 8.2 \times 10^5 \text{ N/m}^2$, respectively, and nearly incompressible expressed by the Poisson ratio = 0.49. The thickness of the graft wall is about 10% of its diameter ($h = 3.5 \times 10^{-4} \text{ m}$), the artery has a thickness of $h = 5 \times 10^{-4} \text{ m}$. The parameters listed were determined from experimental data [3]. In the calculation of the vessel wall deformation, the applied pressure load corresponds to the pressure pulse waveform relative to the diastolic reference pressure. The geometry is fixed in axial direction at graft inflow and both ends of native artery to prevent rigid body motion.

The maximum principal stresses at the inner wall surface calculated at the pressure $P = 1.2 \times 10^4 \text{ N/m}^2$ (90 mmHg) is concentrated along the suture line. Steep stress gradients can be observed in the artery-graft junction. The smallest stresses occur in the artery due to its small bulk modulus and large deformation.

The results of the flow studies with distensible vessel walls show a rather small influence on the flow field compared to the rigid wall models. Velocity patterns and magnitude and distribution of wall shear stress do not change considerably despite rather large sidewall deformations in the anastomotic region. Low wall shear stress is found on the artery floor opposite

the anastomotic junction during the entire pulse cycle. This phenomenon has been identified to promote intimal thickening while high shear stress tends to prevent it [24]. The migration of the stagnation point is also considered to have a role in the disease progress [25].

Intimal hyperplasia does not only occur on the artery floor in the anastomotic region but also along the suture lines of the junctions. The vessel wall mechanics and the compliance mismatch of the materials seem to play the major role in the development and progress of intimal thickening in this region [1, 3, 4, 19, 26]. Although the correlation between intimal suture line hyperplasia and tissue injury caused by intramural stress is still not fully understood, it has been found that more compliant grafts result in a reduction of the intimal thickening around the suture line in end-to-side anastomoses.

Of course the hyperplasia at such junctions may not only be affected by mechanical factors, but also by biochemical influences and material interactions [4, 27].

3.2 Simplified mathematical model

It is well known that the geometry of end-to-side anastomoses has a determinant influence on their patency rates. Geometry induces stresses and strains that promote myointimal hyperplasia, thus causing stenosis. In addition to that, experimental tests have been performed that help confirm the strong relationship between disturbed flow and site of myointimal hyperplasia.

One of the most famous surgical techniques known to provide better long term patency rate is the Miller-cuff technique [28, 29]. This procedure consists in positioning an autologous vein as a cuff in between prosthesis and artery. Using a computational fluid dynamics model we examine the consequences of different geometries systematically constructed from a single and controllable parameter, the length of arteriotomy relative to the vessel diameter, trying to evaluate the hemodynamic characteristics of the Miller-cuff anastomosis that are probably the major determinants of its excellent clinical results.

Conventionally, an arteriotomy of 150% of the vascular diameter is recommended. The factor on which the geometry is based, is the length of the arteriotomy as n times the vessel diameter. As an example, we can generate three different anastomotic geometries for the following values $n=1.5, 3,$ and $4.5,$ giving different shapes and sizes to each anastomosis. The diameter ratio between the vessel and the prosthesis is set to 1, and the diameter is set to 6 mm. The angle between the two conduits is set to 45° .

The fluid is Newtonian, incompressible, with a dynamic viscosity of 2×10^{-3} kg/ms. Its density is set at 1060 kg/m³. The flow is considered as

steady with a velocity of 0.05 m/s. Other conditions are: a constant pressure of 76 mmHg and a constant temperature of 37 °C. The vessel and the prosthesis are considered to be rigid walls. The proximal part of the grafted artery is occluded.

In the described condition, we calculate the strain and the velocity fields in the fluid. However, three conditions have to be fulfilled by results before being considered:

They have to be systematic which means they have to appear in each simulation.

They have to be comparable from one simulation to the other

They have to correspond to our knowledge of myointimal hyperplasia sites.

Strains

First, we consider the area at the bottom of the anastomosis where the stresses are high. We measured the length of that area. We want it to be as short as possible to minimize its absolute length. Then, we consider the length of the strain gradient at the bottom of the anastomosis. High gradients also being related to myointimal hyperplasia, we want that region to be as long as possible. Finally, we consider the heel of the anastomosis where strains have an extent in the direction of the flow. We characterize them by measuring the vertical limit above (positive values) or below (negative values) the top of the anastomosis. We are not interested in the values of the strains, but in the extent of the regions that can be considered as harmful to the hemodynamics (Fig. 7). Our motivation in considering absolute distances is due to the fact that these regions do not have less effect if the diameter of the vessel is different. We just want the least strain and gradient as possible.

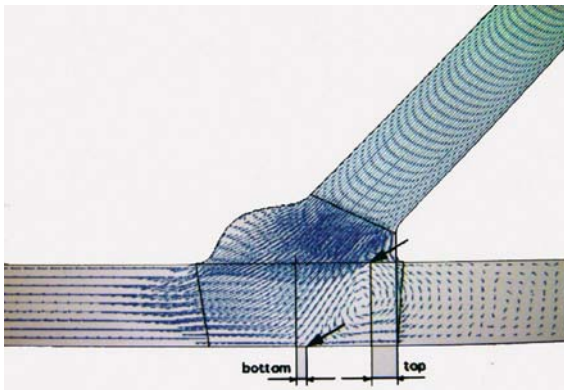


Fig. 7. Two dimension model of end-to-side conventional anastomosis. In the analysis we take into account the extent of the areas in which the strain is higher.

Velocity fields

We observe that recirculation occurs at the bottom of the anastomosis. It influences the flow at the heel as well as at the bottom of the anastomosis. The less the disturbance intrudes the main stream region, the less it influences the flow. We define the extent of the disturbance by considering the points where the velocity changes direction, relative to main flow. These points are shown in Figure 8. Poor hemodynamics at the heel of the anastomosis is believed to cause myointimal hyperplasia. We measured the distance of the border point to the heel and consider its value relative to the length of the arteriotomy, to minimize the relative value.

We then consider the disturbances at the bottom by measuring their distances to the centre of the arteriotomy which corresponds to the middle axis of the prosthesis. As long as the disturbance is on the proximal side of the middle, it has a negative value. Therefore we want to minimize it. Our motivation in considering relative values in this case is the following: we are interested in maintaining the main stream untouched. The main stream is centered around a curve that joins the middle axes of the prosthesis and the vessel, and that passes a little distal to the middle of the opening, at the top plane of the anastomosis. The middle point of the aperture being at different distances to the heel, we cannot consider the absolute distances, but have to consider them relative to this middle point, or to the heel.

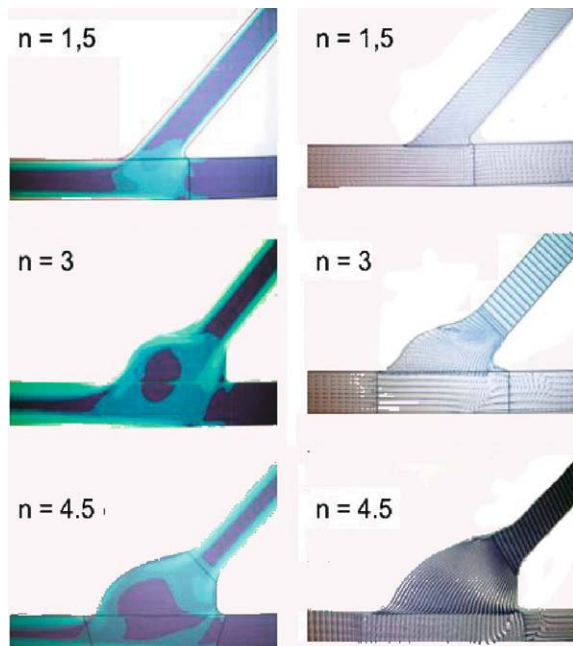


Fig. 8. Two dimensions simulation of 3 different types of end to side conventional anastomosis where the arteriotomy is n times vessel diameter. Results in Table 1.

Table 1. Computational Fluid Dynamics of three different end-to-side anastomoses where the arteriotomy is n times the vessel diameter

Analysis	Best n		Worst n
Extent of high strain at the bottom	4.5	3	1.5
Gradient of the strain at the bottom	4.5	3	1.5
Strain at the heel	4.5	3	1.5
Intrusion of the recirculation region at the heel	4.5	1.5	1.5
Intrusion of the recirculation at the bottom	4.5	3	1.5
Conclusion	4.5	3	1.5

The results of the three analyses performed are summarised in Table 1.

Giving the same weight to each one of these analyses does the general rating. We see that the best geometry appears to be the case of $n=4.5$ which represents an important luminal enlargement. The worst case is $n=1.5$. It is quite intuitive, because the cuff looks more like a bulb than a smooth transition from graft to vessel. This confirms previously obtained results, where cuffed anastomoses give better results than simple vessel-to-vessel junctions did.

The mathematical models presented here demonstrate the considerable influence of asymmetries and local geometric irregularities on flow pattern, especially secondary spiral flow effects, so that differences in hyperplasia between individuals may be partially explainable by mechanical factors.

References

1. Bassiouny HS, White S, Glagov S, Choi E, Giddens DP, Zarins CK (1992) Anastomotic intimal hyperplasia: mechanical injury or flow induced. *J Vasc Surg* 15:708–717
2. Perktold K, Tatzl H, Rappitsch G (1994) Flow dynamic effect of the anastomotic angle: a numerical study of pulsatile flow in vascular graft anastomoses models. *Tech Health Care* 1:197–207
3. Trubel W, Schima H, Moritz A, Raderer F, Windisch A, Ullrich R, Windberger U, Losert U, Polterauer P (1995) Compliance mismatch and formation of distal anastomotic intimal hyperplasia in externally stiffened and lumen-adapted venous grafts. *Euro J Vasc Endovasc Surg* 10:1–9
4. Lemson MS, Tordoir JHM, Daemen MJAP, Kitslaar PJEHM (2000) Intimal hyperplasia in vascular grafts. *Europ J Vasc Endovasc Surg* 19:336–350
5. Hofer M, Rappitsch G, Perktold K, Trubel W, Schima H (1996) Numerical study of wall mechanics and fluid dynamics in end-to-side anastomosis and correlation to intimal hyperplasia. *J Biomech* 29:1297–1308
6. Giddens EM, Giddens DP, White S, Zarins CK, Bassiouny H, Glagov S (1990) Exercise flow conditions eliminate stasis at vascular graft anastomoses. In: Schneck DJ, Lucas CL (eds) *Biofluid Mechanics: Proceedings of the Third*

- Mid-Atlantic Conference on Biofluid Mechanics. University Press, New York, pp 255–267
7. Keynton RS, Rittgers SE, Shu MCS (1990) Hemodynamic effects of angle and flow rate within distal vascular graft anastomoses. In: Schneck DJ, Lucas CL (eds) *Biofluid Mechanics: Proceedings of the Third Mid-Atlantic Conference on Biofluid Mechanics*. University Press, New York, pp 227–236
 8. Schima H, Trubel W, Raderer F, Scherer R, Einav S, Perktold K, Moritz A (1994) Investigation of the flow velocity pattern in distal end-to-side anastomoses and the correlation to intimal hyperplasia. In: Liepsch D (ed) *Biofluid Mechanics, Fortschrittberichte, Biotechnik, Reihe 17*. VDI, Düsseldorf, 107(Suppl):21–26
 9. White S, Zarins CK, Giddens DP, Bassiouny H, Loth F, Jones SA, Glagov S (1993) Hemodynamic patterns in two models of end-to-side vascular bypass anastomoses: effects of pulsatility, flow division, Reynolds number and hood length. *J Biomech Eng* 115:104–111
 10. Ethier CR, Zhang X, Karpik SR, Ojha M (1993) Numerical simulation of flow in a model 3-D end-to-side anastomoses. In: Tarbell JM (ed) *Advances in Bioengineering, BED-Vol. 26*, ASME, New York, pp 83–86
 11. Steinman DA, Vinh B, Ethier RC, Ojha M, Cobbold RSC, Johnston KW (1993) A numerical simulation of flow in a two-dimensional end-to-side anastomosis model. *J Biomech Eng* 115:112–118
 12. Inzoli F, Migliavacca F, Mantero S (1994) Pulsatile flow in an aorto-coronary bypass 3-D model. In: Liepsch D (ed) *Biofluid Mechanics, Fortschrittberichte, Reihe 17, Biotechnik, VDI, Düsseldorf*, 107:455–463
 13. Perktold K, Rappitsch G, Gruber G, Trubel W, Schima H (1996) The interaction of geometry and local flow phenomena in compliant end-to-side anastomoses models. In: Rastegar S (ed) *Advances in Bioengineering*. ASME, New York, 33:77–78
 14. Perktold K, Hofer M, Karner G, Trubel W, Schima H (1998) Computer simulation of vascular fluid dynamics and mass transport: optimum design of arterial bypass anastomoses. In: Papailiou KD, Tsahalis D, Périaux J, Knoerzer D (eds) *Computational Fluid Dynamics '98*. Wiley, New York, 2:484–489
 15. Perktold K, Hofer M, Rappitsch G, Löw M, Kuban BD, Friedman MH (1998) Validated computation of physiologic flow in a realistic coronary artery branch. *J Biomech* 31:217–228
 16. Caro CG, Doorly DJ, Tarnawski M, Scott KT, Long Q, Dumoulin CL (1996) Non-planar geometry and non-planar type flow at sites of arterial curvature and branching implications for arterial biology and disease. In: Jaffrin MY, Caro CG (eds) *Biological Flows*. Plenum Press, London New York, pp 69–81
 17. LoGerfo FW, Quist WC, Nowak MD, Crawshaw HM, Haudenschild CC (1983) Downstream anastomotic hyperplasia: a mechanism for failure in Dacron arterial grafts. *Ann Surg* 197:479–483
 18. Trubel W, Moritz A, Schima H, Raderer F, Scherer R, Ullrich R, Losert U, Polterauer P (1994) Compliance and formation of distal anastomotic intimal hyperplasia in dacron mesh tube constricted veins used as arterial bypass grafts. *ASAIO J* 40:M273–278
 19. Ballyk PD, Walsh C, Butany J, Ojha M (1998) Compliance mismatch may promote graft-artery intimal hyperplasia by altering suture-line stresses. *J Biomech* 31:229–237

20. Leuprecht A, Perktold K, Prosi M, Berk Th, Wolfgang T, Schima H (2002) Numerical study of hemodynamics and wall mechanics in distal end-to-side anastomoses of bypass grafts. *J Biomech* 35:225–236
21. Hughes TJR, Liu WK, Zimmermann TK (1981) Lagrangian–Eulerian finite element formulation in incompressible viscous flows. *Comp Meth Appl Mech Eng* 29:329–349
22. Koiter WT, Simmonds JC (1973) Foundations of shell theory. Proceedings of the 13th International Congress Theory on Applied Mechanics. Springer, Berlin, pp 150–176
23. Hofer M, Perktold K (1995) Vorkonditionierter konjugierter Gradienten Algorithmus für große schlecht konditionierte unsymmetrische Gleichungssysteme, Suppl Vol ZAMM. *Z Angew Math Mech* 75(SII):S641–642
24. Morinaga K, Okadome K, Kuroki M, Miyazaki T, Muto Y, Inokuchi K (1985) Effect of wall stress on intimal thickening of arterially transplanted veins in dogs. *J Vasc Surg* 2:430–433
25. Noori N, Scherer R, Perktold K, Czerny M, Karner G, Trubel W, Polterauer P, Schima H (1999) Blood flow in distal end-to-side anastomoses with PTFE and a venous patch: results of an in-vitro flow visualization study. *Europ J Endovasc Surg* 18:191–200
26. Sottiurai VS, Yao JST, Baston RC, Sue SL, Jones R, Nakamura YA (1989) Distal anastomotic intimal hyperplasia: histological character and bigenesis. *Ann Vasc Surg* 3:26–33
27. Kissin M, Kansal N, Pappas PJ, DeFouw DO, Durán WN, Hobsen RW (2000) Vein interposition cuffs decrease the intimal hyperplastic response of polytetrafluoroethylene bypass grafts. *J Vasc Surg* 31:69–83
28. Miller JH, Foreman RK, Ferguson L, Faris I (1984) Interposition vein cuff for anastomosis of prosthesis to small artery. *Australian and New Zealand J Surg* 54:283–285
29. Taylor RS, Loh A, McFarland RJ, Cox M, Chester JF (1992) Improved technique for polytetrafluoroethylene bypass grafting: long-term results using anastomotic vein patches. *Br J Surg* 79:348–354

4

Determinants of anastomosis long term patency

Introduction

The hope of any surgeon performing vascular anastomosis is that the vascular reconstruction he is performing will last forever and patients will be once and for all set free from ischemic symptoms. Unfortunately, this rarely occurs mostly because the surgical procedure doesn't treat the cause of vessel occlusion, such as the atherosclerosis and the atherosclerotic process will probably continue to progress, the anastomosis not being spared. Based on clinical experience, cardiac surgeons know, for instance, that to achieve 100% graft patency at 10 years they should use arterial grafts as conduits on a 3 mm coronary artery with proximal sub-occlusion, without distal disease, with large runoff in patients taking antiplatelet drugs and statins and no hypercoagulability (Fig. 1). On the other hand, 100% of graft occlusion at 10 days occurs when a large vein is anastomosed on 1 mm coronary artery with moderate proximal stenosis, with distal disease and poor runoff, in a diabetic patient taking no drugs. However, in this chapter, we systematically review the elements and parameters clearly affecting the outcome of any vascular reconstruction in order to give a general view of what cardiiovascular surgeons should take into account in order to give a realistic expectation of anastomosis patency.

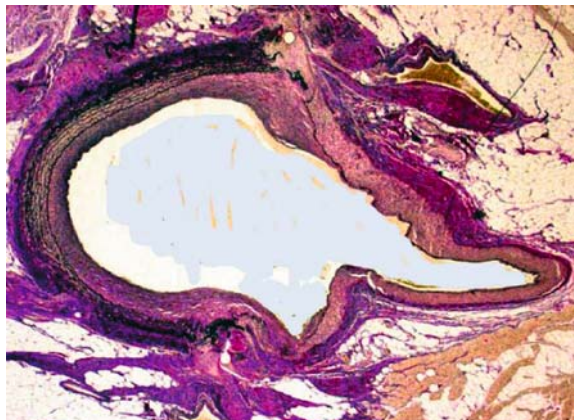


Fig. 1. One year histology of LIMA on LAD conventional anastomosis in sheep model. The transition between graft and coronary is extremely smooth and no sign of myointimal hyperplasia is evident.

The long-term patency of any vascular reconstruction depends on the combination of three different elements: surgical, hemodynamic and biological. The surgical element includes surgical techniques (interrupted vs running suture), graft material (vein, artery, prosthetic graft), anastomosis geometry (shape and dimension) and surgeon's dexterity. The hemodynamic element includes anastomotic inflow, runoff and flow characteristics (turbulent flow with stagnation, separation, and recirculation), as well as the degree of stenosis of the grafted conduit. The biological element comprises the diseases associated with aggressive atherosclerosis progression (such as diabetes, hypertension, etc.), with hypercoagulability (lack of Antithrombin III factor, etc.) and the pharmacological treatment in case the patient takes antiplatelet agents and or statins.

4.1 Surgical element

There are two main types of suture techniques: the continuous or running suture and the interrupted suture. Running versus interrupted suture can be reasonably considered one of the most frequent subjects of discussion since vascular surgery took its first steps. To date, this is still an open issue despite many scientific works published world-wide. The suture material selected and the suture technique employed can influence the size and the distensibility of the anastomotic lumen. Cross-sectional compliance in the perianastomotic zone, wall shear stress, axial stress, and their relationship with intimal hyperplasia are the most frequently considered parameters for comparing the two different techniques. If we try to resume the *pros* and *cons* of each technique we conclude that running suture is faster and somehow easier to do but it can produce a purse-string effect that can impair the hemodynamic performance of the anastomosis. Multiple stitch technique avoids the purse-string effect but requires more time and is often characterised with bleeding from the suture line.

Anastomosis compliance

Anastomosis alters vessel wall mechanical properties no matter which technique has been used to perform it [1]. Continuous or interrupted sutures increase vessel wall rigidity on the anastomotic site and alter the circumferential elastic modulus [2, 3]. We have recently carried out several experimental studies to assess the cross-sectional compliance at the anastomotic site and the movement of the anastomosed vessel's edges with respect to the suture technique. In a pig model, end-to-end anastomoses on both carotid arteries were performed using either running or interrupted polypropylene 6-0 sutures. To generate detailed cross sectional arterial profiles in

Fig. 2. Lateral view of pig's left carotid artery. Piezoelectric crystals were sutured on artery wall in order to evaluate axial vessel wall displacement due to pulse pressure. A high resolution echo-tracking system (NIUS 02) was used to generate detailed cross sectional arterial profiles.

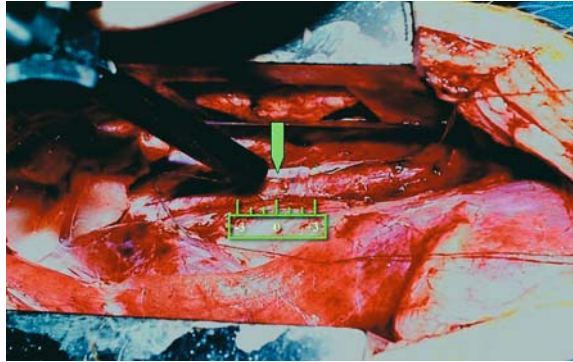


Table 1. Running Vs interrupted suture technique. Mean values of cross-sectional compliance proximal (Cprox), distal (Cdist) and on the anastomosis (Canas) measured with echo-tracking system. ΔP is mean pulse pressure.

Suture technique	Cross sectional compliance ($10^{-7} \text{ m}^2/\text{KPa}$)			ΔP (mmHg)
	Proximal to the anastomosis	On the anastomosis	Distal to the anastomosis	
Interrupted	2.11 ± 0.2	-0.4 ± 0.2	1.7 ± 0.2	39 ± 12
Running	2.32 ± 0.2	-1.2 ± 0.6	2.1 ± 0.3	42 ± 2

the proximity and on the anastomosis we used a high resolution echo-tracking system (NIUS 02) (Fig. 2).

The computation of the carotid artery cross sectional compliance in the para anastomotic area confirms the existence of the so called para-anastomotic hypercompliant zone (PHZ) probably due to turbulent blood flow [3, 4, 5]. Unexpectedly, we find a reduction of the anastomosis cross sectional area during systole which means that the vessel diameter decreases when blood pressure increases [6, 7]. The vessel cross-section reduction for a pulse pressure going from 5 to 32 mmHg ranges from 0.9 to 2% of diastolic vessel cross-section (Table 1). Therefore the arterial compliance on the anastomosis is negative regardless of the technique used.

This anastomotic behaviour generates a dynamic stenosis whose magnitude seems to depend on blood pressure level. We find an inverse correlation between pulse pressure and anastomosis diameter as represented by the regression curve illustrated in Figure 3. Smooth muscular fibre interruption could contribute to determining this behaviour, because at the anastomotic site, vessel wall acts as a free end under the influence of pulse waves. Increasing blood pressure causes the retraction of vessel ends which causes vessel lumen reduction.

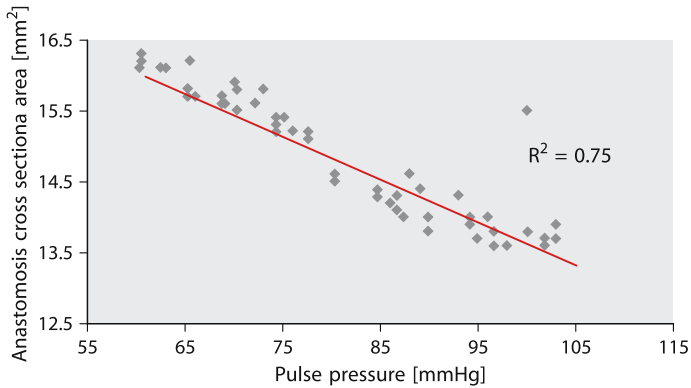


Fig. 3. Regression curve of vessel diameter vs pulse pressure on carotid anastomosis (continuous suture with 6/0 polypropylene). Regression coefficient (R^2) of 0.75 means that they are inversely correlated with high statistic relevance.

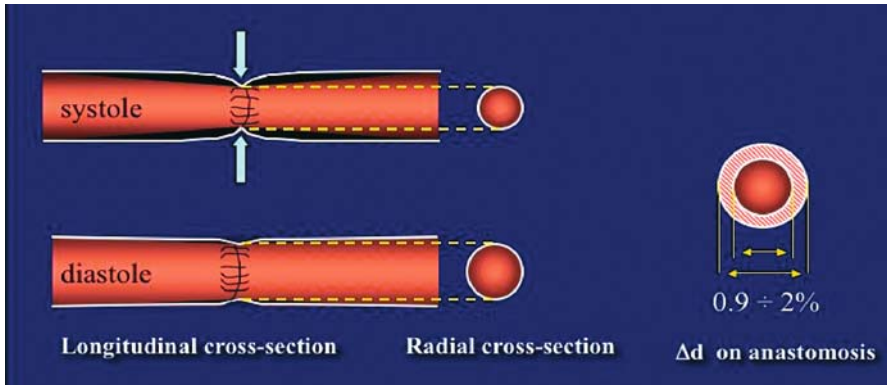
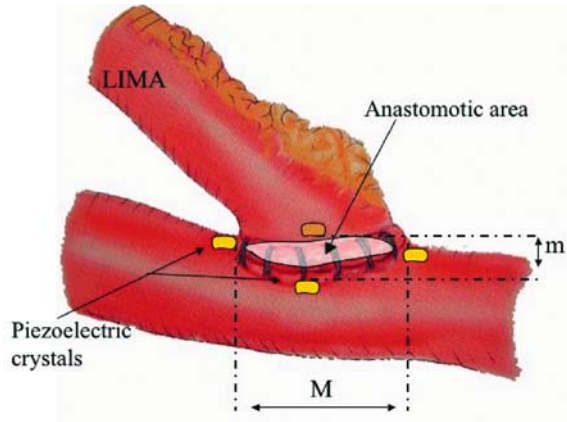


Fig. 4. Schematic representation of systolic movement of vessel edges at the anastomotic site soon after end-to-end anastomosis construction with running suture technique.

These results suggest that suture does not provide the continuity of mechanical properties of arterial conduit, at least soon after surgical restoration of vessel continuity. We don't know if this phenomenon disappears with the healing process of the vessel wall. In Figure 4 we resume the vessel movement at the anastomotic site.

In another experimental set, using piezoelectric crystals sutured on each side of an end-to-end carotid artery anastomosis, we detected an inversion of longitudinal artery wall movement. In the acute phase following an end-to-end anastomosis, an increase in blood pressure causes an increase in vessel length with an exponential correlation. Therefore anastomosis is constantly subjected to longitudinal traction whose magnitude depends on pulse pressure [7].

Fig. 5. End-to-side anastomosis between left internal mammary artery (LIMA) and carotid artery. Piezoelectric crystals (in yellow) are sutured on toe, heel, and both sides of the anastomosis in order to measure the anastomotic diameters for computation of anastomosis cross sectional compliance.



To assess the effects of suture technique on end-to-side anastomosis luminal dimensions and compliance, we designed an animal model in which both internal mammary arteries are anastomosed to the carotid arteries using either running or interrupted suture technique. Cross sectional anastomotic area has been assessed suturing piezoelectric crystals at the toe, heel and both sides of anastomoses [8] as shown in Figure 5.

Assuming that the anastomosis has an elliptical shape, the Cross Sectional Anastomotic Area (CSAA) can be calculated as:

$$CSAA = \pi \frac{mM}{4}$$

where m and M are the minor and major axes of the anastomosis. CSAA is expressed in mm^2 . Cross-Sectional Anastomotic Compliance (CSAC) is the ratio between variations in Anastomotic Cross-Sectional Area ($\Delta CSAA$) and blood pressure (ΔP):

$$CSAC = \frac{\Delta CSAA}{\Delta P}$$

CSAC is expressed in m^2/kPa .

Using this method we calculated a CSAC for a running suture of $4.5 \times 10^{-6} \text{ m}^2/\text{kPa}$ and for an interrupted suture of $11 \times 10^{-6} \text{ m}^2/\text{kPa}$, demonstrating that suture technique has a substantial effect on CSAC of end-to-side anastomoses. Interrupted suture provides a considerably higher CSAC than continuous suture and can be reasonably considered the most “physiological” suture because it keeps the biomechanical properties of the arterial wall as close as possible to those of the native vessel [9]. This anastomotic behaviour appears to result mainly from the elastic recoil of the arterial wall

constituents which are better preserved with interrupted suture [10]. Therefore, the notion that differences in hemodynamic properties of end-to-side anastomoses performed with the two considered techniques are negligible [3], deserves reappraisal. Furthermore, even if there are few limitations such as the anastomosis has a perfect elliptical shape and that distances calculated with piezoelectric crystals correspond to the maximal and minimal diameters of this ellipse, it seems that the systolic increase of cross-sectional anastomotic area is definitely bigger if interrupted suture is used and this behaviour may theoretically improve the systolic flow through the anastomosis as hypothesised the first time in 1960 by Szilagyi [11].

Better anastomotic compliance means less suture-line stress [12, 13], reduces flow disturbances and may reduce the disposition toward the development of intimal hyperplasia or thrombosis [14, 15]. Geometrical simulation demonstrates that a more compliant anastomosis is associated with a smaller stagnation point due to flow separation (typically on heel, toe and the hood of the graft) giving rise to low wall shear stress that is associated with intimal hyperplasia [16]. Interrupted suture may maximise the anastomotic lumen and provides a considerably higher CSAC than continuous suture which reduces flow turbulence, shear stress and intimal hyperplasia.

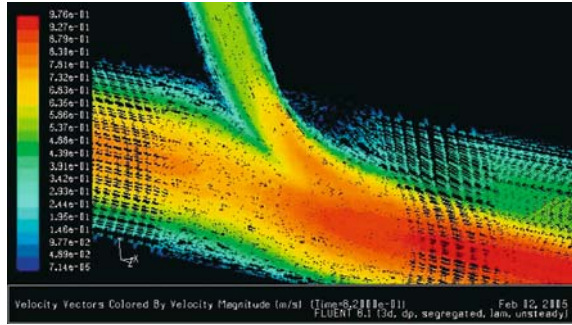
Anastomotic angle and design

Several numerical and experimental studies have extensively assessed the influence of anastomotic angle and shape to anastomotic flow and patency. The ideal take off angle for a side-to-end or landing angle for an end-to-side anastomosis is between 30° and 45° (Fig. 6). It has been demonstrated that angles over 120° are associated with an immediate reduction of the expected flow of up to 50% [17] and the 30° angle provides less flow resistance than steeper angles [18]. Separated flow regions are seen along the inner arterial wall (toe region) for angles $\geq 60^\circ$ while a stagnation point exists along the outer arterial wall (floor region).

Shear stress rates along the arterial wall vary widely throughout the anastomotic region with negative values in the separation zones and upstream of the stagnation points which increases in magnitude with the angle. The shear stress increases with distance downstream of the stagnation point and with magnitudes that increase with the angle [19]. The inclusion of a patch or a cuff moves the stagnation point at the floor region distally and reduces the strength of the recirculation region opposite the heel of the anastomosis up to 50% [20].

Various cuff and patch designs for vessel-graft anastomoses have been developed in an attempt to increase the patency rate of ePTFE grafts used for lower-extremity bypass procedures. In 1984, Miller [21] reported a new vein cuff design that produced good patency in femoral-distal grafts. Brumby [22] found that grafts implanted with the vein cuff technique had

Fig. 6. Computational flow dynamics of end-to-side anastomosis. The ideal anastomotic angle seems to be between 30° and 45° as shown by the flow velocity near vessel wall.



significantly better patency than those for which a noncuffed anastomosis was employed in both above-knee and below-knee popliteal bypasses. Other studies suggested that use of Miller cuff improved patency only in belowknee grafts [23, 24].

The patched geometry promotes earlier recovery of the flow in the distal outflow segment than for the unpatched model. Also, the helical flow patterns associated with the cuffed geometry are stronger. The net effect of these changes are that peak wall shear stress values for the patched and cuffed geometries are three times lower than those for the uncuffed geometry [16, 20]. On the other hand, the improved patency rates of cuffed end-to-side anastomoses may be simply due to an increased ability of the cuff to accommodate myointimal hyperplasia before causing a significant stenosis [22].

Conduit characteristics

It is well known that arterial conduits for coronary revascularization have better long term patency rates with respect to vein grafts and seem to improve patient's survival [26]. Recently, a clinical study compared the anastomotic shear stress of internal mammary artery to left anterior descending artery to that of saphenous vein to right coronary artery: when an arterial conduit is used the shear stress at the anastomotic site is about 4 times greater than that associate with the vein graft ($16.0 \pm 4.8 \text{ dyn/cm}^2$ Vs $4.8 \pm 1.6 \text{ dyn/cm}^2$) [27].

It is also well known that synthetic conduits, either e-PTFE or Dacron, provide results as good as vein grafts only when the graft diameter is 6 mm or bigger. For diameters below 6 mm, results are generally very poor. This is the reason why there are no synthetic grafts for coronary artery revascularization so far and it is not recommended to use a synthetic conduit for vascular reconstructions below the knee.

Surgical dexterity

The construction of any vascular anastomosis is a highly technical demanding procedure and even if surgeons are trained for years before being certified, there still is an individual variability or “personal touch” certainly affecting results. Unfortunately, it is not simple to quantify this parameter, and, above all there is always the risk of hurting surgeon’s feelings. Conduits manipulation to preserve the integrity of the intima, the precise positioning of sutures with correct intima-to-intima apposition, the regularity of the suture line, are only a few examples of domains subject to individual variability. The introduction of mechanical and automatic suture devices should reduce the impact of individual dexterity on the anastomosis outcome and standardize the surgical procedure.

4.2 Flow element

Inflow

Many authors have demonstrated that low anastomotic inflow seems to promote myointimal hyperplasia and thrombus formation, leading to the occlusion of the anastomosis [28]. Clear evidence exists for a relationship between low flow velocity (LFV), low shear stress (SS) and circumferential stress (δ), smooth muscle cell proliferation and myointimal hyperplasia (MIH) at the anastomotic site. MIH in experimental vein graft can be generated by long term low flow. In a dog model Berguer demonstrates that reductions in blood flow of 50% to 80% have generally led to a doubling of intimal hyperplasia [28]. Dobrin demonstrates intimal hyperplasia in venous graft is best associated with low flow velocity which is correlated to low blood-artery shear stress [10]. In an elegant study, Meyerson describes the effects of extremely low shear stress on neointimal thickening in the failing venous bypass graft [29]. If the shear stress is lower than 2 dyne/cm² the rate of smooth muscle cell proliferation increases with a non linear correlation causing the rapid progression of neointimal lesions that lead to bypass graft occlusion.

Run off

There is a general consensus on the role of the run off in keeping the graft open. It is assumed that each bypass has its critical run off: when the graft flow is lower than the critical value, the bypass has very few chances of staying open. For coronary arteries, for example, a run off allowing a distal flow lower than 10 ml/min is associated with early graft occlusion. Poor

Fig. 7. Surgical technique: left posterior thoracotomy to expose thoracic descending aorta (A) and left pulmonary artery (B). Pulmonary artery was ligated in its proximal part and transected; its distal part is sutured with 6-0 polypropylene to descending aorta.

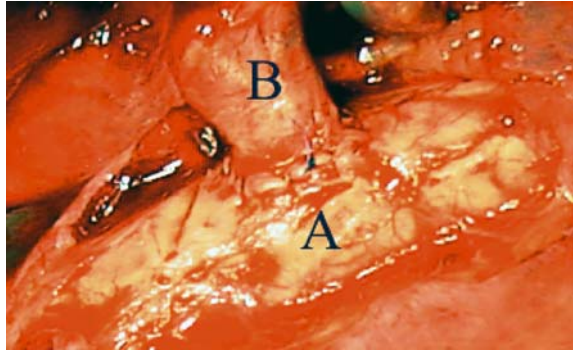
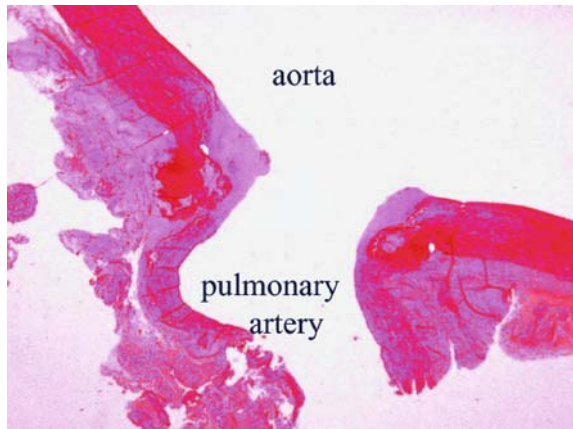


Fig. 8. Thoracic descending aorta to left pulmonary artery anastomosis at 12 weeks (magnification 2 \times). No significant myointimal hyperplasia is noted.



runoff reduces late patency rate of coronary anastomoses and contributes to anastomotic intimal thickening as demonstrated in a canine model [14, 15].

Poor runoff is associated with high anastomosis occlusion. In a multivariate analysis of factors affecting patency of femoro-popliteal bypass grafting, Ljungman concludes that the status of distal runoff, the graft material and the site of distal anastomosis independently and significantly influence the patency rate [14]. However, we developed a chronic animal model of low inflow and low runoff anastomosis to demonstrate that in specific experimental conditions those parameters are not predictors of intimal hyperplasia and anastomotic failure [30]. In adult pigs, descending thoracic aorta to left pulmonary artery anastomoses in a side-to-end configuration have been performed (Fig. 7).

After 12 weeks an angiography and IVUS were performed and data concerning aortic, left and right pulmonary artery pressure and flow were collected. Anastomosis was harvested for histology (Fig. 8). Mean circumferential stress and mean wall shear stress at the anastomotic site were calculated (Table 2).

Table 2. Side-to-end anastomosis between descending thoracic aorta and left pulmonary artery after 12 weeks (10 pigs). *LPA MT* is the left pulmonary artery media thickness; *Aa* \varnothing is the mean anastomotic diameter; *MIH* is the mean myointimal hyperplasia.

Side-to-end anastomosis						
Mean wall shear stress (T_w) (L/min mm ³ 10 ⁻⁴)				Circumferential stress (δ) (mmHg 10 ²)		
2.79				1.73		
Mean Pressure (mmHg)				Histology (mm)		
Ascending Aorta	Pulmonary artery	Left pulm. artery	<i>Aa</i> \varnothing	Wall thickness	LPA MT	MIH
73 \pm 8	13 \pm 2	73 \pm 8	6.4 \pm 0.3	1.5 \pm 0.02	0.2 \pm 0.02	0.08
Angiography			Flow measurements (L/min)			
Stenosis	Inflow	Runoff	Ascending Aorta	Right pulm. art.	Left pulm. art.	
No	Low	poor	5.6 \pm 0.2	5.4 \pm 0.1	0.2 \pm 0.02	

All animals developed severe pulmonary hypertension limited to the left lung, the right lung being normal. Anastomoses inflow and runoff have been extremely low for 2 months, with a mean inflow estimated at 0.2 l/min. When these mean pulmonary artery flows and anastomotic radii are entered into the Poiseuille equation, the resulting wall shear stress is quite low, seemingly to favour myointimal hyperplasia formation, therefore we expected to find a high degree of luminal stenosis due to intimal hyperplasia, but this was not the case.

Histology showed no evidence of stenosis except for a thin layer of intimal proliferation on the suture line that could be considered as physiological. We noted the thickening of the media layer which is probably associated with the increased deformation of the artery wall in the circumferential direction [30] due to systemic artery pressure existing in the left pulmonary artery. There is an important compliance mismatch between the aorta and the pulmonary artery. Biomechanical elastic coefficients for the aorta are 3 to 4 times higher than those of the pulmonary artery which means the aorta is 3 to 4 times stiffer than the pulmonary artery. This compliance mismatch could be compared to that between synthetic graft (PTFE or Dacron) and native arteries [32] making the model probably valid for prosthetic bypass.

This model did not follow some of the most accredited hypothesis on intimal hyperplasia induction. This is probably due to the particular biomechanical and biochemical properties of the pulmonary artery. Endothelial cells clearly exist in a dynamic state and respond to forces associated with mechanical stretch and strain. Many of these responses and the stimuli that elicit them are just beginning to be understood. Furthermore, recent works [33] indicate that vascular endothelial cells represent a phenoty-

pically heterogeneous population. Thus it is possible that the responses of endothelial cells to mechanical stresses will differ depending on their vessel origin. It is likely that stimuli that can induce myointimal hyperplasia depending on biomechanical and biochemical properties of the vessel and these are probably not the same in all vessels. If this data is confirmed, we should look deeper into pulmonary endothelial cell biology to eventually find the key to minimize myointimal hyperplasia at any anastomotic site.

Severity of stenosis of the target vessel

Graft failure has been reported when an arterial conduit is grafted to a lower grade coronary artery stenosis. Although controversy exists, it has been hypothesized that competitive flow between the graft and the native coronary artery may produce late arterial graft failure when the native coronary artery has a mild stenosis [15, 34]. In this setting the arterial graft can gradually diminish in size and graft failure may occur. It has also been demonstrated that the arterial conduit can increase its diameter and flow when stenosis of the native coronary artery increases. A recent clinical study conducted on over 100 patients scheduled for coronary artery bypass grafting [29] shows that if a native coronary artery has a stenosis of 50 to 75%, the graft flow is significantly reduced with respect to the native coronary artery being suboccluded, promoting the development of the so called string sign that corresponds, from a hemodynamic point of view, to arterial graft occlusion. Moreover, intermediate stenosis is associated to lower anastomotic shear stress, at least when vein graft is used for coronary artery bypass.

4.3 Biological element

Diabetic patients that do not require insulin treatment show a higher incidence of major adverse cardiac events (MACEs), defined as cardiac mortality, myocardial infarction, or revascularization of a previous target vessel, after CABGs when a connector is used for the construction of the proximal anastomosis [35]. The cause of this predisposition for early MACEs to occur primarily in connector patients with diabetes is unknown, but it bears resemblance to results seen in this population with percutaneous coronary interventions. Activated protein kinase C can inhibit the expression of endothelial nitric oxide synthase, thus leading to impaired endothelial vasodilatory regulation. The protein kinase C can also increase cytokine induced tissue factor gene expression and procoagulant activity in endothelial cells [36], thereby increasing the production of proinflammatory cytokines and proliferation of vascular smooth muscle cells. Diabetes is recognized to be

an important risk factor for poor outcome after percutaneous coronary interventions [37, 38]. Potential mechanisms include an upregulated inflammatory response that may result in chronic constrictive remodeling, an allergic reaction to the metallic elements of the stent, or a device design that may increase the amount of stent induced vascular wall injury [38, 39].

References

1. Hasson JE, Megerman J, Abbot WM (1985) Increased compliance near vascular anastomoses. *J Vasc Surg* 2(3):419–423
2. Dobrin PB (1980) *Vascular Mechanics*. In: *Handbook of physiology the cardiovascular system*, Vol. 2. Bethesda, Maryland, Am Phys Soc, pp 65–102
3. Baumgartner N, Dobrin PB et al. (1996) Influence of suture technique and suture material selection on the mechanics of end-to-end and end-to-side anastomoses. *J Thorac Cardiovasc Surg* 111(5):1063–1072
4. Hasson JE, Megerman J, Abbott WM (1986) Suture technique and para-anastomotic compliance. *J Vasc Surg* 3:591–598
5. Schajer GS, Green SI, Davis AP, Hsiang NH (1996) Influence of elastic nonlinearity of arterial anastomotic compliance. *J Biomech Eng* 118:445–451
6. Tozzi P, Hayoz D, Mueller XM, M'Baku C, Mallabiabarrena I, von Segesser LK (2000) Decreased compliance on arterial anastomoses. *Swiss Surg* 6(2):77–79
7. Tozzi P, Hayoz D, Mueller XM, M'Baku C, Mallabiabarrena I, von Segesser LK (2000) Anastomotic longitudinal stress due to modification of arterial longitudinal properties after anastomosis. *Swiss Surg* 6(2):74–76
8. Tozzi P, Hayoz D, Ruchat P, Corno A, Oedman C, Botta U, von Segesser LK (2001) Animal model to compare the effects of suture technique on cross-sectional compliance on end-to-side anastomoses. *Eur J Cardiothorac Surg* 19(4):477–481
9. Klein SR, Goldberg L, Miranda RM (1982) Effect of suture technique on arterial anastomotic compliance. *Arch Surg* 117(1):45–47
10. Dobrin PB (1994) Mechanical factors associated with the development of intimal hyperplasia with respect to vascular grafts. In: Dobrin PB (ed) *Intimal hyperplasia*. RG Landes, Austin, pp 85–109
11. Szilagyi DE, Whitcomb J, Schenker W (1960) The laws of fluid flow and arterial grafting. *Surgery* 47:55–67
12. Ballyk PD, Walsh C, Butany J, Ojha M (1998) Compliance mismatch may promote graft-artery intimal hyperplasia by altering suture-line stresses. *J Biomech* 31(3):229–237
13. Hasson JE, Megerman J, Abbot WM (1985) Increased compliance near vascular anastomoses. *J Vasc Surg* 2(3):419–423
14. Ljungman C, Ulus AT, Almgren B, Bergstrom R (2000) A multivariate analysis of factors affecting patency of femoropopliteal and femorodistal bypass grafting. *Vasa* 29(3):215–220
15. Chow MST, Sim E, Orszulak TA et al. (1994) Patency of internal thoracic artery grafts: comparison of right versus left and importance of vessel grafted. *Circulation* 90:129–132
16. Harris Peter, How T (1999) Haemodynamics of cuffed arterial anastomoses. *Crit Ischae* 9(1):20–26

17. Zhang L, Moskovitz M, Piscatelli S, Longaker MT, Siebert JW (1995) Hemodynamic study of different angled end-to-side anastomoses. *Microsurg* 16(2): 114–117
18. Leva C, Engstrom KG (2003) Flow resistance over technical anastomoses in relation to the angle of distal end-to-side connections. *Scand Cardiovasc J* 37(3):165–171
19. Fei DY, Thomas JD, Rittgers SE (1994) The effect of angle and flow rate upon hemodynamics in distal vascular graft anastomoses: a numerical model study. *J Biomech Eng* 116(3):331–336
20. Walsh MT, Kavanagh EG, O'Brien T, Grace PA, McGloughlin T (2003) On the existence of an optimum end-to-side junctional geometry in peripheral bypass surgery – a computer generated study. *Eur J Vasc Endovasc Surg* 26(6): 649–656
21. Miller JH, Foreman RK, Ferguson L, Faris I (1984) Interposition vein cuff for anastomosis of prosthesis to small artery. *Aust NZ J Surg* 54:283–285
22. Brumby SA, Petrucco MF, Walsh JA, Bond MJ (1992) A retrospective analysis of infra-inguinal arterial reconstruction: three-year patency rates. *Aust NZ J Surg* 62:256–260
23. Stonebridge PA, Prescott RJ, Ruckley CV (1997) Randomized trial comparing infrainguinal polytetrafluoroethylene bypass grafting with and without vein interposition cuff at the distal anastomosis. *J Vasc Surg* 26:543–550
24. Raptis S, Miller JH (1995) Influence of a vein cuff on polytetrafluoroethylene grafts for primary femoropopliteal bypass. *Br J Surg* 82:487–491
25. Wijesinghe LD, Mahmood T, Scott DJ (1999) Axial flow fields in cuffed end-to-side anastomoses: effect of angle and disease progression. *Eur J Vasc Endovasc Surg* 18(3):240–244
26. Zacharias A, Habib RH, Schwann TA, Riordan CJ, Durham SJ, Shah A (2004) Improved survival with radial artery versus vein conduits in coronary bypass surgery with left internal thoracic artery to left anterior descending artery grafting. *Circulation* 109(12):1489–1496
27. Shimizu T, Ito S, Kikuchi Y, Misaka M, Hirayama T, Ishimaru S, Yamashina A (2004) Arterial conduit shear stress following bypass grafting for intermediate coronary artery stenosis: a comparative study with saphenous vein grafts. *Eur J Cardiothorac Surg* 25(4):578–584
28. Berguer R, Higgins RF, Reddy DJ (1980) Intimal hyperplasia. An experimental study. *Arch Surg* 115(3):332–335
29. Meyerson SL, Skelly CL, Curi MA et al. (2001) The effects of extremely low shear stress on cellular proliferation and neointimal thickening in the failing bypass graft. *J Vasc Surg* 34:90–97
30. Corno AF, Tozzi P, Genton CY, von Segesser LK (2003) Surgically induced unilateral pulmonary hypertension: time-related analysis of a new experimental model. *Eur J Cardiothorac Surg* 23(4):513–517
31. Pevac WC, L'Italien GJ, Megerman J, Cambria RP, Abbott WM (1993) Abnormal wall strain at distal end-to-side anastomoses. *Ann Vasc Surg* 7(1):14–20
32. Salacinski HJ, Goldner S, Giudiceandrea A, Hamilton G, Seifalian AM, Edwards A, Carson RG (2001) The mechanical behaviour of vascular grafts: a review. *J Biomater Appl* 15(3):241–278
33. King J, Weathington T, Creighton J, McDonald F, Gillespie M et al. (2001) Characterization of phenotypically distinct endothelial cells population from rat lungs. *FASEB J* 15:A492

34. Suma H (1999) Arterial grafts in coronary bypass surgery. *Ann Thorac Cardiovasc Surg* 5(3):141–145
35. Dewey M, Crumrine K, Herbert MA, Leonard A, Prince SL, Worley C, Edger-ton JR, Magee MJ, Mack MJ (2004) First-year outcomes of beating heart coronary artery bypass grafting using proximal mechanical connectors. *Ann Thorac Surg* 77:1542–1549
36. Terry CM, Callahan KS (1996) Protein kinase C regulates cytokine induced tissue factor transcription and procoagulant activity in human endothelial cells. *J Lab Clin Med* 127:81–93
37. Abizaid A, Kornowski R, Mintz GS et al. (1998) The influence of diabetes mellitus on acute and late clinical outcomes following coronary stent implan-tation. *J Am Coll Cardiol* 32:584–589
38. Elezi S, Kastrati A, Pache J et al. (1998) Diabetes mellitus and the clinical and angiographic outcome after coronary stent placement. *J Am Coll Cardiol* 32:1866–1873
39. Kornowski R, Hong MK, Tio FO et al. (1998) In-stent restenosis. Contribu-tions of inflammatory responses and arterial injury to neointimal hyperpla-sia. *J Am Coll Cardiol* 31:224–230

5

Key issues in sutureless vascular anastomoses

■ Introduction

Since the beginning of cardiovascular surgery, anastomoses have been performed with hand-held sutures basically based on the principles of suture technique described by Alexis Carrel in 1902 [1]. Even if in the last 100 years many other techniques have been proposed to join two vessels, the comfort to surgeons in performing a reliable anastomosis with the suture technique and the excellence of its long term results have led to its adoption as the gold standard. Therefore we should ask ourselves if we really need an alternative way to construct the vascular anastomosis. A key element to perform a safe and accurate hand-sutured coronary anastomosis is to have a bloodless operating field and an arrested heart. Surgical environment is becoming more and more challenging since off-pump CABGs and minimally invasive approach have been introduced. Surgeons have to deal with more and more diseased vessels since patient's age and comorbidities continue to increase. Automated anastomotic technologies will enable the creation of rapid, precise and consistent anastomoses and this perfectly match the surgeon's needs. We are looking for alternative ways to construct a coronary or any vascular bypass in order to reduce the technical demand, standardise the quality of the surgical procedure, reduce the individual surgical dexterity as a determinant factor for anastomosis outcome and possibly, expediting the procedure and reduce costs of the surgical treatment.

This chapter reviews the basic principles of the different technologies and methods applied to the construction of vascular anastomoses and clearly defines the key technical elements common to almost all sutureless devices. The comprehension of these elements will help the reader to better analyse and evaluate each of the devices described in the next chapters.

5.1 Criteria of sutureless device evaluation

Medical device companies propose a wide range of products that intend to face the anastomotic quest using different technological approaches and original, sometimes eccentric, strategies. For schematic purpose only, we can identify:

- sutureless devices based on:
 - 1) stainless steel
 - 2) memory shape metal alloys
 - 3) biological or synthetic glue combined or not with metallic scaffold
 - 4) laser welding with or without organic solder
- suture delivery devices
- new suture materials
- anastomotic assist devices.

Any vascular reconstruction obtained without using hand sewing or hand-tying knots could be considered a mechanical or sutureless anastomosis. If we accept this definition, there are 83 fundamental patents concerning sutureless vascular anastomosis devices, updated to December 2004. Most of them are only ideas and will probably never become reality; others are prototypes still far from clinical use.

In order to evaluate a sutureless anastomotic device, 3 aspects need to be taken into consideration: device-vessel wall connection, graft preparation and anastomosis biomechanical properties.

■ Device-vessel wall connection

Basically, there are 3 different technical solutions providing the coupling of the sutureless device to the vessel wall: pins, wall eversion and wall squeezing and all these solutions could simultaneously be present in the same device.

■ **Pins.** Pins pierce through the graft wall either from intima to adventitia direction or from the opposite direction (Fig. 1).

The number of pins is generally between 5 and 12 and depend on connector diameter. When pins penetrate the vessel from the inside to the outside the risk of generating an intimal flap or a dissection is very low because the pin itself pushes the intima against the wall and avoids the blood penetration into the wall. On the other hand, if pins penetrate from the outside of the vessel, they can produce intimal lesions leading to flaps or dissections. In order to minimize the risk of these dreadful complications, biomedical engineers have developed clever solutions to keep pins into the wall width avoiding any lesion of the intima layer and any contact between the device and the blood stream as well (Fig. 2).

Fig. 1. Two examples of devices having pins coupling the vessel (**a**=CorLink by J&J, **b**=Q-CAB by SJM)

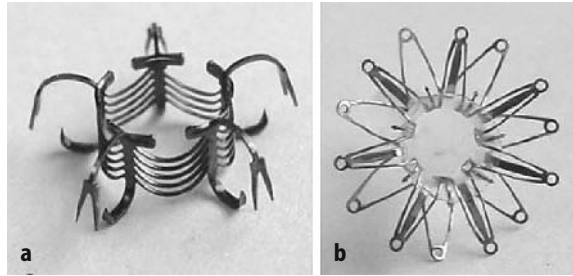
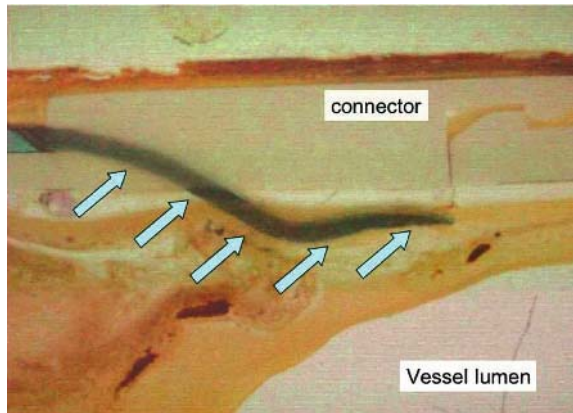


Fig. 2. The Vascular Join. The end-to-end carotid artery anastomosis has been cut following the blood flow direction. Pins penetrate vessel wall from the outside and they stay into the vessel width (arrows) avoiding any lesion of the intima and having no blood-exposed surface. This technical solution minimizes the risk of intimal flap or wall dissection.



The pin's traumatic action on vessel wall can be compared to that of a 5-0 needle or smaller. Pins guarantee an excellent connection in terms of strength because the break point depends on the vessel wall firmness: disconnection occurs when vessel wall is torn and this is exactly what happens with suture technique. It may be interesting to remind the reader that the breaking strain of 2 mm diameter coronary artery in a patient over 60 years old is about 0.45 calculated as

$$\text{Coronary} \times \text{Strain} = \frac{\text{Circumference (stretched - relaxed)}}{\text{Circumference} \times \text{relaxed}}$$

It is reached when the vessel wall is stretched by a factor of 2 (1-2).

If pins are the only means connecting the device to the vessel, the device's blood-exposed surface can be lower than suture technique or even nil.

The first limiting factor for using pins to ensure the device-vessel wall connection is wall stiffness. For a device made of Nickel-Titanium alloy (Nitinol), that has memory shape properties, the calcified artery is a great challenge because, as a general assumption, Nitinol doesn't have enough strength to penetrate a stiff wall and the anastomosis construction can not succeed. Moreover, this is the main reason why connectors made of Nitinol can not be used with synthetic graft made of e-PTFE or Dacron; these ma-

terials are too stiff and cannot be penetrated by memory shape alloys at least in the current devices' configuration. Biomedical engineers have overcome this limitation by using stainless steel (L 300 series) which provides much higher strength than Nitinol, but, unfortunately, doesn't have thermal memory shape properties.

The second limiting factor in using pins consists in the fact that, with few exceptions, vessel edges have to be trimmed if the anastomosis aborts, because removing the pins can easily scratch and destroy the vessel.

■ **Wall eversion.** This solution generally requires the use of an anvil (metallic or plastic) to achieve the eversion. Wall eversion is the oldest method used for creating a vascular anastomosis (see Chapter 1) and is still used in many of the current anastomotic devices (Fig. 3).

The eversion of the vessel assures a perfect intima-to-intima apposition as well as the fact that no adventitia will be left in the lumen, therefore reducing the risk of acute anastomosis thrombosis. Other functions of the anvil are to create enough overlapping area for easy application of bonding elements, to prevent movement of wall segment when bonding elements penetrate the vessel wall and to enable the bonding elements to be fixated by deformation. Such a type of connection probably provides the best tensional force since the disconnection of the device from the vessel occurs only if the vessel is cut. However, this method shows several potential limitations. The first limitation resides in the fact that the vessel wall has to be small and very soft in order to be turned around the anvil. Vessels having a diameter of 5 mm or more and stiffer than normal because of atherosclerosis, can seldom be eligible for this procedure because the vessel wall tends to rupture when folded. The eversion of a 2 mm sclerotic coronary artery causes a wall strain of 0.87, exceeding the braking strain of 0.45 [1, 2] and excessive wall strain can promote early anastomosis occlusion. Another limitation consists in the technique used to accomplish the eversion:

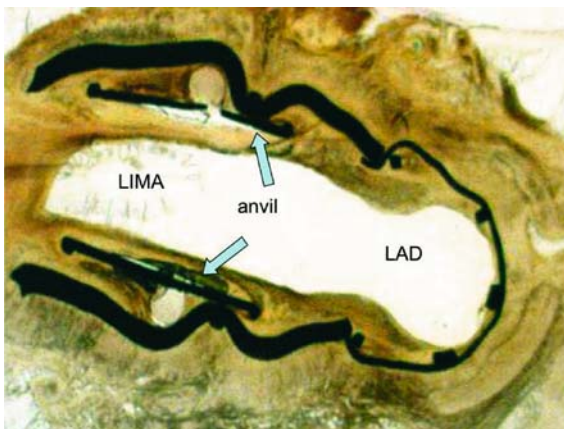


Fig. 3. The Graft Connector. The end-to-side *LIMA* on *LAD* anastomosis on adult sheep has been cut following the direction of the blood flow. *LIMA* has been everted onto the *anvil* and tied to it with the same technique first described by Payr in 1900.

it is necessary to use forceps to position the vessel around the anvil and this is a potential source of intimal lesion mostly on the edge which could lead to myointimal hyperplasia.

Even if an anvil is not used, folding the vessel's wall together and fastening them by a mechanical device has not been proven successful enough to be regularly performed in human beings. The main problem experienced with wall eversion is the atrophy of the vessel walls which are folded together. The atrophy occurs because in the folded part of the wall, there is no blood flow therefore, the energetic supply is significantly reduced. Necrosis of the everted vessel has been the primary cause of failure of the previous generation of anastomotic devices [3–6].

■ **Wall squeezing.** The vessel wall is squeezed between the inner and the outer device's surface (Figs. 4 and 5). This technique is generally non-traumatic for the vessel wall if the two surfaces are designed in such a way as to allow wall feeding. This also means that very little intima surface is covered by metallic parts and, theoretically, no occlusion of vasa-vasorum should occur. Such a connection provides limited strength: there is a consistent risk of accidental disconnection with catastrophic consequences. On the other hand, redoing the anastomosis generally does not require trimming the vessel edges.

A potential limiting factor is the presence of foreign material (for instance metal) in the vessel lumen that could promote myointimal hyperplasia. This has been exhaustively demonstrated by the experience acquired with coronary stents (Fig. 6). Another limiting factor is wall thickness: it has to be in a precise range, generally between 2 and 4 mm according to

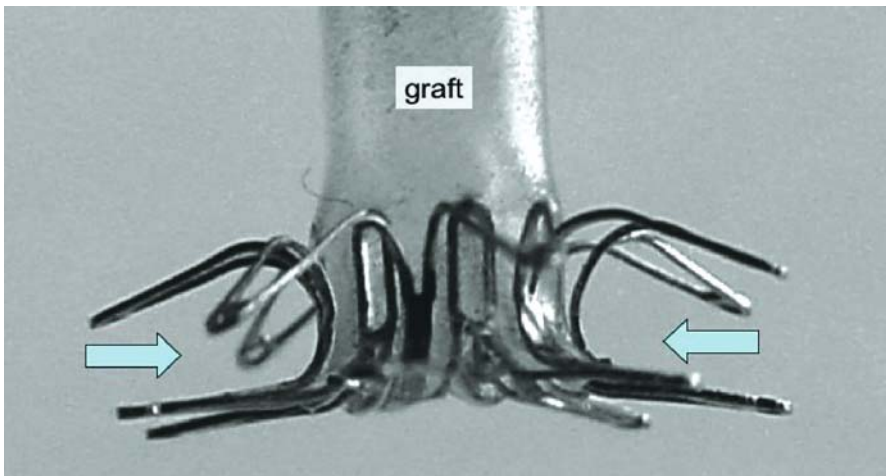


Fig. 4. The Q-CAB. Arrows show the area where the aortic wall is squeezed in between the Nitinol struts.

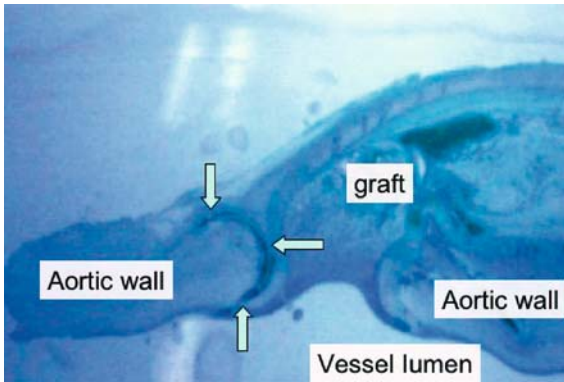


Fig. 5. The Q-CAB. The end-to-side aortic anastomosis on adult pig has been cut in the axial direction. Arrows indicate the connector' struts that squeeze aortic wall.

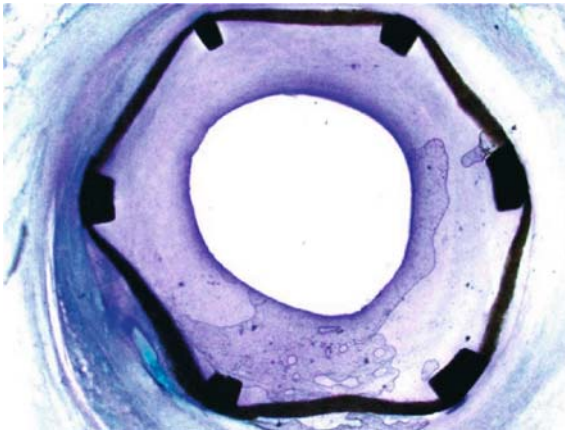


Fig. 6. Example of in stent stenosis. Cross-section image of sheep coronary artery 6 months after the implantation of covered stent. Lumen width is significantly reduced due to tremendous myointimal hyperplasia.

the device design. Very thick or very thin vessel walls can compromise the strength of the connection. This is a key point for anastomosis outcome and it could be helpful to measure aortic wall thickness with an ultrasound or equivalent techniques before deploying the device.

No matter which type of device-wall connection is used, all devices guarantee the intima-to-intima apposition, in agreement with Carrel's principles enunciated at the beginning of the 20th century.

■ Graft preparation

One issue that we should take into account to evaluate any anastomotic device is the manipulations the graft has to go through to be loaded on the deploying system. In some devices the graft has to be mounted on a *transfer sheet* and this could cause intimal lesions that could potentially affect the long-term patency. Other devices require manipulation of the graft end

that has to be inserted into pins, everted, or crimped with forceps and, at the end of the manipulation, this part of the graft is not trimmed or excluded from the blood circulation. Even if this has not been proven by dedicated experimental or clinical investigations, we can speculate that the use of a transfer sheath and or excessive manipulation of the graft end can eventually induce myointimal hyperplasia leading to early graft occlusion.

Some delivery systems do not tolerate the use of metallic clips for graft side branch occlusions, therefore only sutures can be used to ensure the hemostasis on the vein graft.

In some devices, the graft preparation first requires the construction of the proximal anastomosis, and this could be felt as a limitation by some cardiac surgeons.

■ Anastomotic biomechanics

Elastic properties of the vessel wall are altered by vascular anastomoses and there are several studies that underline the importance of anastomotic compliance in the vascular reconstruction outcome as it has been discussed in Chapters 3 and 4. As a general assumption, the more the vascular anastomosis is compliant, the less the probability that it could develop a stenosis due to myointimal hyperplasia is [7, 8]. Unfortunately, there is no experimental study on sutureless anastomotic compliance. Baguneid found an improvement in para-anastomotic compliance when vascular reconstruction was performed with non-penetrating clips versus polypropylene running suture, but these results have not been confirmed by other authors [7]. We could speculate that sutureless anastomosis is more compliant than a running suture anastomosis since materials like Nitinol is more elastic than polypropylene, but the device itself probably makes the anastomosis more rigid than the one constructed with the interrupted suture technique. The relative stiffness of the connector could be a potential cause of vessel wall atrophy. Daniel reported severe vessel wall atrophy inside a rigid foreign body, and they postulate that this could occur each time a rigid body encloses a dynamic dilating structure [8].

Another point concerns the anastomotic angle. In Chapters 3 and 4 we stressed the role of the takeoff anastomotic angle in affecting anastomoses durability. Flow velocity in the proximity of the wall is the main determinant of the shear stress which is associated with intimal hyperplasia. Low velocity means low shear stress which is considered as the first determinant of myointimal hyperplasia. A take off angle between 30° and 45° is considered ideal for end-to-side or side-to-end anastomoses. Unfortunately, only a few anastomotic devices take into account this important issue. Almost all the existing connectors developed for the construction of the proximal anastomosis in CABGs have a take off angle of 90° . Not only is this angle not considered optimal, but it can also predispose the graft to kink once the pericardium is closed.

■ Blood-exposed non-intimal surface

In an elegant experimental study, Scheltes introduced the concept of the Blood Exposed Non Intimal Surface (BENIS) and its correlation to coronary wall stress. This study compares the area of blood-exposed non-intimal surface in sutureless anastomoses with the conventionally sutured anastomosis and examines the technical feasibility of 0 blood-exposed non-intimal surface anastomosis configurations using finite element modelling. The sutured anastomosis BENIS area is about 1.3 mm^2 and this value is considered as the reference value. Approximate BENIS of several connectors varies from 4.3 mm^2 to 80 mm^2 , depending on anastomotic orifice size, wall thickness, and bonding components' location and size.

Theoretically, the ideal anastomotic device should have the lowest BENIS as possible in order to reduce the risk of myointimal hyperplasia. Authors investigate the possibility of creating an anastomosis having $\text{BENIS}=0$ and, surprisingly, the anastomotic device providing it is associate with a 90° coronary wall eversion only exposing intima. They hypothesized that these deformations would induce wall stress that may exceed the threshold tear stress of the artery, leading to tears and leakage. The mean peak porcine coronary wall stress in 0 BENIS anastomosis configurations with greater

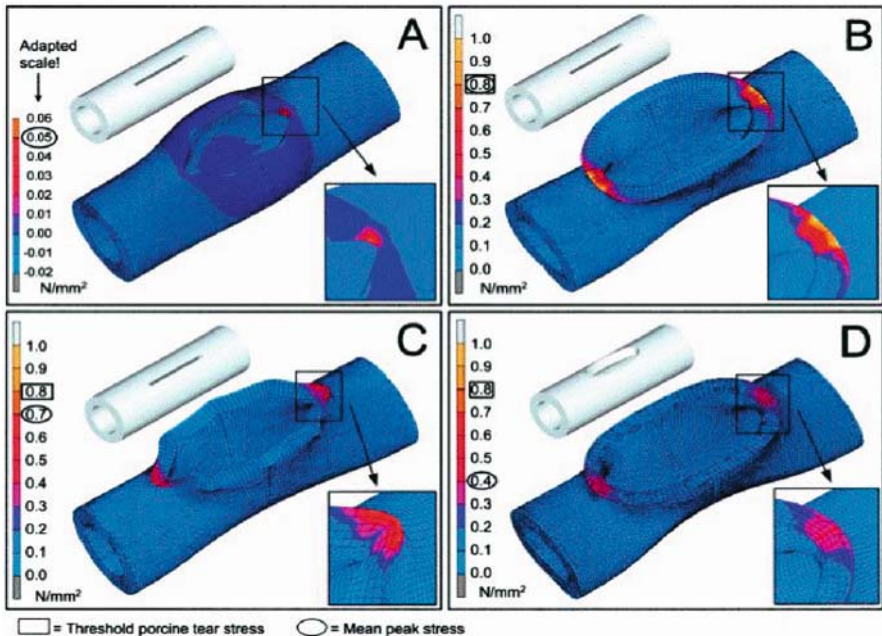







Fig. 7. Geometrical model to calculate anastomosis shear stress. In order to have $\text{BENIS}=0$, vessel's edges have to be everted with 90° angle leading to dangerously high stress concentrations at the toe and hill of the anastomosis (red spots).

Table 1. BENIS of some sutureless anastomosis devices.

Device	BENIS (mm ²)	Device	BENIS (mm ²)
Intima-to-intima	0		1.3
	0.3		27
	1.8		80

than 90 degrees arteriotomy edge eversion, ranges from 0.4 to 0.8 N/mm² compared with the mean porcine coronary tear stress of 0.8 N/mm². Deforming the coronary wall to most of the 0 blood-exposed non-intimal surface anastomosis configurations leads to dangerously high stress concentrations in the coronary arteriotomy corners (Fig. 7).

This theory should be revisited because, later in this book, an anastomotic device that provides zero BENIS without everting vessel wall will be presented (Vascular Join).

In Table 1 we report the BENIS of several sutureless anastomotic devices.

■ Welding and gluing techniques

Lasers (neodymium-YAG laser and CO₂ laser) have been used to repair arteries since 1979 [10–13]. The basic principle of the laser technique resides in using thermal energy to create protein bonds. Despite the fact this is a very simple and generally straightforward procedure, it has major drawback in the anastomosis strength: since the early beginning of the experimental studies there was clear evidence that the joined vessel could be easily disconnected, making this technique unsafe. The introduction of albumin solder [11–16] has significantly improved the anastomosis strength, but this technique still has some important limitations: thermal injury to the vessel wall can lead to pseudoaneurysm formation and anastomotic failure [12]. Moreover, the acute histology suggests entry of albumin into the arterial lumen [11] and the role this has on long-term patency has not yet been determined.

The adhesives used clinically may be categorized into two groups, fibrin glues and cyanoacrylate glues. Fibrin glue consists of two components and imitates the final step of blood coagulation. The first component contains, factor XIII and plasma proteins; the second usually consists of calcium,

thrombin and aprotinin. Fibrin glue was first introduced in 1977 by Matras as a material for the creation of vascular anastomoses. A sutureless end-to-side vascular anastomosis in animal models, has been created inserting the angled end of femoral artery into the femoral vein, sealing the gap between the vessels wall with fibrin glue. Long-term results were not reported, but narrowing of the vessel lumen at the anastomotic site can be expected with this technique.

The second group of surgical glues comprises the synthetic cyanoacrylates (methyl-, ethyl- and buthyl-cyanoacrylates). Gottlob and Blumel in 1968, used alkyl-cyanoacrylate to secure bushing that were used for experimental vascular anastomosis in vessels ranging from 1.0 to 5.0 mm in diameter. They reported satisfactory short-term patency rates, but already stated in the same paper that they had changed the type of cyanoacrylate because of hystotoxicity [30]. When biological [18] or synthetic [19, 20] glues are used to bond vessels, sleeve elements are needed to keep vessels' edges in the correct position during the glue injection phase in order to guarantee the intima to intima apposition as well as the anastomotic geometry. The sleeve element problem has been approached in different ways using inflated balloons or extraluminal frames (Fig. 8), but, at the present time, there is no solution which can simplify and speed up the procedure.

Somehow, the use of adhesive technique makes the anastomosis construction more difficult and time consuming than standard running tech-

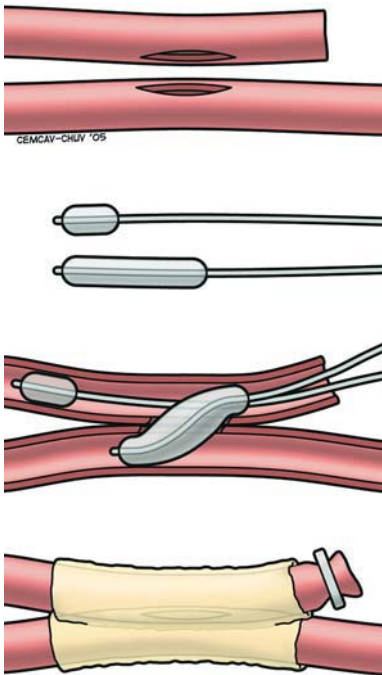


Fig. 8. Laser welding and adhesive anastomoses. The use of sleeve elements (i.e. balloons) is mandatory to guarantee the correct intima-to-intima apposition and the optimal anastomotic geometry.

nique. Moreover, pathological examination shows acute and chronic inflammatory reaction (foreign body giant cells occasionally seen) at the adventitial application site of the synthetic glue (octyl-cyanoacrylate) and more intimal hyperplasia is found in the crinoline-adhesive anastomoses than in sutured control anastomoses, even if this has been considered the result of streamline filling of anastomotic wall recesses by neointima formation. None of these techniques has been used in the human being, so far.

■ Suture material

Polypropylene dominates the market of vascular sutures mainly because it provides excellent results, is easy to use and, above all, is not expensive. The only potential alternative that currently exists is the Nitinol wire. The U-ClipTM (Coalescent Surgical, Sunnydale, CA) [21] features a simple yet elegant design that eliminates the usual suture management and knot tying. The device consists of a self-closing clip made from shape memory alloy which is attached to a conventional suture needle through a flexible suture-like Nitinol member (Fig. 9).

The U-clip is placed via a conventional needle. Squeezing the release mechanism immediately adjacent to the clip, with the needle-holder separates the member and releases the clip allowing it to immediately recoil to its preferred closed-loop configuration. The Nitinol wire, once detached from the flexible member, functions to approximate and hold tissue together similarly to an interrupted suture. The superelastic properties of the Nitinol wire are used to allow precise delivery and positioning of the clip and produce strong but atraumatic tissue approximation. The anastomosis is performed as usual interrupted suture with clips applied around the anastomosis (Fig. 10).

It can be used to perform proximal and distal coronary anastomoses with all types of conduits during CABG as well as for arterial and venous anastomoses in pediatric cardiac surgery, arterio-venous hemodialysis shunts, and peripheral vascular anastomoses [22, 23]. Anastomotic time is similar to or less than that for continuous suture anastomosis. Clinical patency has been excellent and the ratio of anastomotic diameter to the LAD diameter was good (1.17, ranging from 0.93–1.93) [24, 25].



Fig. 9. The U-Clip is a self-closing clip made from shape memory alloy, which is attached to a conventional suture needle through a flexible suture-like Nitinol member.

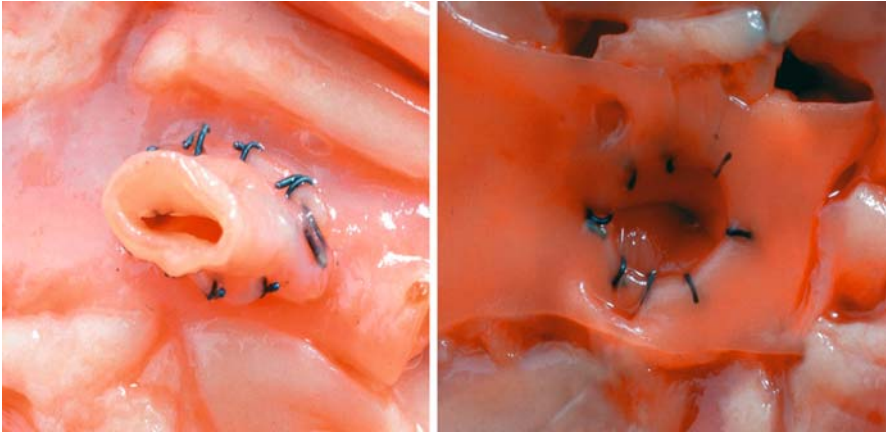


Fig. 10. Inside and outside macroscopic view of coronary anastomosis performed with U-clip (sheep model).

Interrupted anastomoses are the least restrictive and consistently produce an internal configuration with minimal deformity and potential for increased flow rates, compliance, and growth [26, 27]. Therefore, clips may be of particular value in pediatric cardiac surgery helping to preserve growth potential and prevent anastomotic stricture and late stenosis. Because of the elimination of knot-tying the U-clip may also be suitable for minimally invasive, thoracoscopic, and robot-assisted procedures [28, 29].

■ The hybrid approach: combine anastomotic device and tissue adhesive

The Buijsrogge and Borst group from Utrecht developed a hybrid anastomotic technique that combines mechanical coupling and adhesive bonding without the need for dedicated application tools [19].

This technique is based on the use of an extravascular stainless steel frame having 4 downward axially extended hooks, called crinoline because it looks like a basket, that facilitates the positioning of extraluminal octylcyanoacrylate glue. The frame has an outside diameter of 6 mm and the hook elements are 8 mm in length and are bendable (Fig. 11). The end of the graft is passed into the frame, everted and inserted onto the hooks. Thickenings near hook tips prevent the graft from sliding upward. The mounted crinoline is then inserted into the target vessel where a 3 mm arteriotomy has been performed. Two crinoline hook elements at 3 and 9 o'clock positions relative to the anastomosis are first inserted into the target vessel wall using standard forceps; then the heel and toe hook elements are inserted and an intima-to-intima apposition is obtained. Once the correct vessels' apposition is confirmed, and moisture is removed with an air

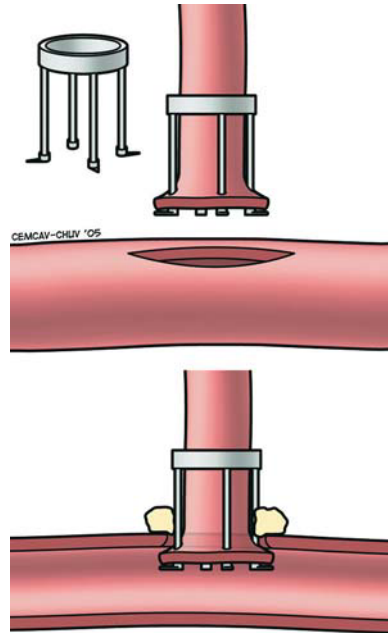


Fig. 11. Crinoline-adhesive anastomotic procedure. The stainless steel ring shaped frame (outside diameter 6 mm) has 4 hooks extended axially (length 8 mm) with thickenings at the end. Hook elements are elastic and can be bended during the insertion. Anastomotic line is slightly stretched radially because of the crinoline hooks. Vessels apposition is consolidated by adhesive (cyanoacrylate).

blower, about 0.3 μL octyl-cyanoacrylate adhesive is applied to consolidate the apposition.

This surgical technique has been the object of several animal studies. In a pig model, LIMA on LAD on beating heart was performed in 8 animals. Anastomosis construction required 6–7 min and no significant leak was detected. At five weeks all anastomoses were patent with minor narrowing in some cases (Fitz Gibbon grade A). In 6 of 8 anastomoses complete intima–intima apposition was established along the full circumference. In 2 cases a small part of the graft rim at either the heel or toe of the anastomosis was exposed to blood. Streamlining intimal hyperplasia coverage of the hooks was found together with complete filling of anastomotic recesses between everted graft and coronary artery. The authors concluded that extraluminal frame structures are relatively easy to apply and minimize foreign-body exposure to the blood. A full view of every anastomotic quadrant facilitates proper positioning. In case of misalignment repositioning of one or more hook elements requires little time. Some limitations were addressed, e.g., by critical arteriotomy length, external ring frame too high, and the fact that the adhesive is approved for topical wound closure only.

5.2 Anastomotic assist devices

Anastomotic assist devices have been recently introduced in the market mainly to avoid the use of aortic side clamp for the construction of the proximal anastomoses in off pump CABGs. Although, they cannot be considered as sutureless anastomotic devices because the anastomosis is constructed using the standard technique, we will briefly describe two of them. The Heartstring® Proximal Seal System (Guidant, CA) consists of polyurethane suture fashioned in a spiral structure, inserted into the anastomotic hole providing a clampless hemostatic seal allowing the construction of a side-to-end anastomosis in any artery with a diameter greater

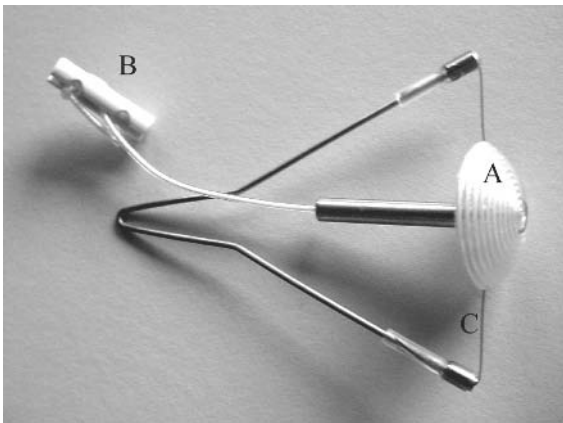


Fig. 12. The Heartstring consists of polyurethane suture fashioned in a spiral structure (A), inserted into the anastomotic hole and providing a clampless hemostatic seal allowing the construction of a side-to-end anastomosis in any artery with a diameter greater than 2 cm. Once the anastomosis construction is completed and before tying the suture, the device is removed by pulling the polyurethane suture (B) and cutting the tension spring (C).

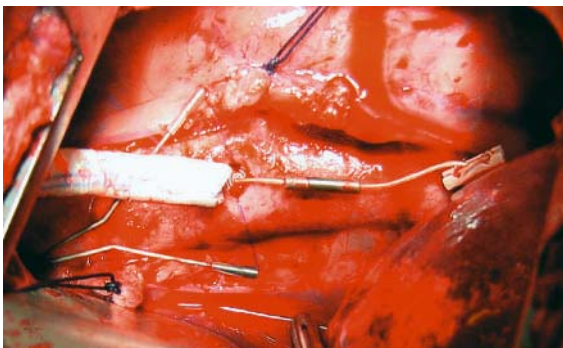


Fig. 13. Animal study. Operative view. The Heartstring has been inserted into the descending thoracic aorta to avoid aortic clamp during the construction of end-to-side anastomosis (PTFE 6 mm prosthesis).

Fig. 14. The Enclose acts by squeezing the aortic wall encircling the anastomotic hole. The white part is inserted into the aorta through a side hole and the basket is open and stitched to the aortic wall isolating the anastomotic area from the blood stream. Once the anastomosis is completed, the basket can be moved following a radial direction with respect to the side hole, to perform another anastomosis or be retrieved.

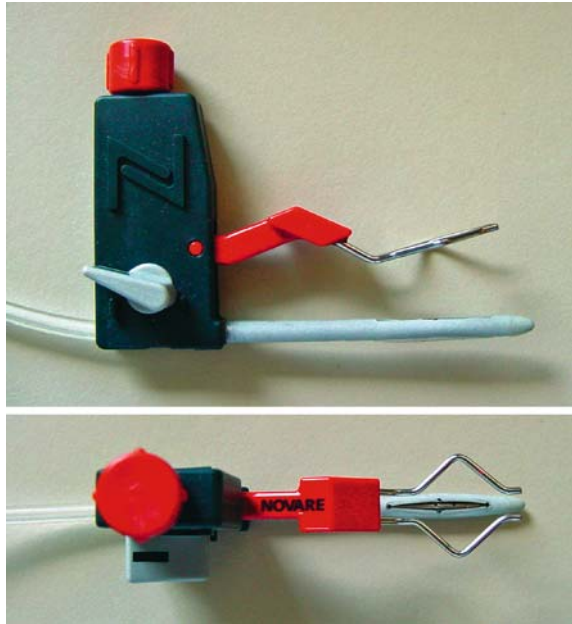
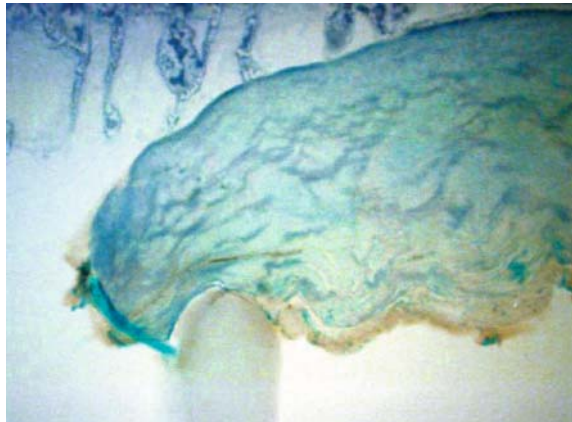


Fig. 15. Animal study (adult pig). Histology of aorto-PTFE graft anastomosis constructed using the Novare anastomotic assist device, 4 h after the procedure. The intima layer has disappeared and this is probably due to the traumatic action of the device.



than 2 cm. Once the anastomosis construction is completed and before tying the suture, the device is removed by pulling the polyurethane suture and cutting the tension spring (Figs. 12 and 13).

The Enclose® (Novare Surgical Systems, CA) acts by squeezing the aortic wall encircling the anastomotic hole. The device is inserted into the aorta through a side hole and the intra-arterial part consists of an expandable basket that is stitched to the aortic wall isolating the anastomosis site from the blood stream (Fig. 14). Once the anastomosis is completed, the

basket can be moved following a radial direction with respect to the side hole, to perform another anastomosis or be retrieved.

We have tested these devices in a sheep model of aorto-coronary bypass and in clinics as well. Our feeling is that both devices seal the aortotomy, are easy to handle and do not impair the anastomosis construction. The Heartstring causes no endothelial lesions. The enclosure can be used several times in the same patient but it causes intimal lesions (Fig. 15) and requires an additional aortotomy to be inserted.

■ References

- Scheltes JS, Heikens M, Pistecky PV, van Andel CJ, Borst C (2000) Assessment of patented coronary end-to-side anastomotic devices using micromechanical bonding. *Ann Thorac Surg* 70(1):218–221
- Yoshimatsu N (1970) Study of strength of parts of human heart. *J Kyoto Pref Med Univ* (1958) 641:553. In: Yamada H, Evans FG (eds) *Strength of biological materials*. Williams & Wilkins, Baltimore, p 113
- Nakayama K, Tamiya T, Yamamoto K (1962) A simple new apparatus for small vessel anastomosis. *Surgery* 52:918
- Mattox DE, Wozniak JJ (1991) Sutureless vascular anastomosis with biocompatible heat-shrink tubing. *Arch Otolaryngol Head Neck Surg* 117:1260–1264
- Androsov PI (1956) New method of surgical treatment of blood vessel lesions. *Arch Surg* 73:902
- Daniel RK, Lidman D, Olding M, Williams JA, Matlaga BF (1984) An anastomotic device for microvascular surgery: evolution. *Ann Plast Surg* 13:402
- Stansby G, Knez P, Berwanger CS, Nelson K, Reichert V, Schmitz-Rixen T (2001) Does vascular stapling improve compliance of vascular anastomoses? *Vasc Surg* 35(2):115–121
- Dobrin PB, Littooy FN, Edean ED (1989) Mechanical factors predisposing to intimal hyperplasia and medial thickening in autogenous vein grafts. *Surg* 105(3):393–400
- Scheltes JS, van Andel CJ, Pistecky PV, Borst C (2003) Coronary anastomotic devices: blood-exposed non-intimal surface and coronary wall stress. *J Thorac Cardiovasc Surg* 126:191–196
- Jain KK, Gorisch W (1979) Repair of small blood vessels with the neodymium-YAG laser: a preliminary report. *Surgery* 85:684–688
- Phillips ABM, Ginsburg BY, Shin SJ, Soslow R, Wilson K, Poppas DP (1999) Laser welding for vascular anastomosis using albumin solder: an approach for MID-CAB. *Lasers Surg Med* 24(4):264–268
- Grubbs PE, Wang S, Marini C, Rose DM, Cunningham JN (1988) Enhancement of CO₂ laser microvascular anastomoses by fibrin glue. *J Surg Res* 45:112–119
- Phillips AB, Ginsburg BY, Shin SJ (1999) Laser welding for vascular anastomosis using albumin solder: a new approach for MIDCAB. *Lasers Surg Med* 24:264–268
- Weissberg D, Goetz RE (1964) Necrosis of arterial wall following application of methyl-2-cyanoacrylate tissue adhesive in the rat. *Surg Gynecol Obstet* 119:1248–1252.

15. Tulleken CAF, Verdaasdonk RM, Beck H (1997) Nonocclusive excimer laser-assisted end-to-side anastomosis. *Ann Thorac Surg* 63:S138-142
16. Chikamatsu E, Sakurai T, Nishikimi N, Yano T, Nimura Y (1995) Comparison of laser welding, interrupted sutures and continuous sutures in growing vascular anastomoses. *Lasers Surg Med* 16:34
17. Detweiler MB, Detweiler JG, Fenton J (1999) Sutureless and reduced suture anastomosis of the hollow vessels with fibrin glue: a review. *J Invest Surg* 12(5):245-262
18. Gundry SR, Black K, Izutani H (2000) Sutureless coronary artery bypass with biologic glued anastomoses: preliminary in vivo and in vitro results. *J Thorac Cardiovasc Surg* 120(3):473-477
19. Buijsrogge MP, Scheltes JS, Heikens M, Grundeman PF, Pistecky PV, Borst C (2002) Sutureless coronary anastomosis with an anastomotic device and tissue adhesive in off-pump porcine coronary bypass grafting. *J Thorac Cardiovasc Surg* 123(4):788-794
20. Buijsrogge MP, Verlaan CW, van Rijen MH, Grundeman PF, Borst C (2002) Coronary end-to-side sleeve anastomosis using adhesive in off-pump bypass grafting in the pig. *Ann Thorac Surg* 73(5):1451-1456
21. Hill AC, Maroney TP, Virmani R (2001) Facilitated coronary anastomosis using a nitinol U-clip device: bovine model. *J Thorac Cardiovasc Surg* 121: 859-870
22. Berdat PA, Kipfer B, Immer FF, Pfammatter JP, Carrel T (2002) Facilitated vascular interrupted anastomosis in cardiovascular surgery with a new clip device. *J Thorac Cardiovasc Surg* 124:1256-1258
23. Berdat PA, Pfammatter JP, Pavlovic M, Carrel T (2003) A new clip device for construction of interrupted anastomosis in congenital cardiac surgery. *The Heart Surgery Forum* (submitted)
24. Caskey MP, Kirshner MS, Alferman EL, Hunsley SL, Daniel MA (2002) Six-month angiographic evaluation of beating-heart coronary artery graft interrupted anastomoses using the coalescent U-clip anastomotic device: a prospective clinical study. *The Heart Surgery Forum* 5:319-327
25. Ono M, Wolf RW, Angouras D, Schneeberger EW (2002) Early experience of coronary artery bypass grafting with a new self-closing clip device. *J Thorac Cardiovasc Surg* 123:783-787
26. Baumgartner J (1996) Influence of suture technique and suture material selection on the mechanics of end-to-end and end-to-side anastomoses. *J Thorac Cardiovasc Surg* 111:1063-1072
27. Stansby G, Knez P, Berwanger CS, Nelson K, Reichert V, Schmitz-Rixen T (2001) Does vascular stapling improve compliance of vascular anastomoses? *J Vasc Surg* 35:115-121
28. Kappert U, Cichon R, Schneider J et al. (2001) Technique of closed chest coronary artery surgery on the beating heart. *Eur J Cardiothorac Surg* 20:765-769
29. Mohr FW, Falk V, Diegeler A et al. (2001) Computer-enhanced robotic cardiac surgery; experience in 148 patients. *J Thorac Cardiovasc Surg* 121:842-853
30. Gottlob R, Blumel G (1968) Anastomoses of small arteries and veins by means of bushings and adhesive. *J Cardiovasc Surg* 9:337-341

6

Coronary surgery: devices for proximal anastomosis

Introduction

In this chapter we review the most recent technologies allowing the construction of the side-to-end anastomosis between ascending aorta and conduit, either vein or artery. For each device, we describe the technical characteristics (*device design*), report the published results of the most important experimental and clinical studies (*experimental work up and clinical results*) and conclude the device's presentation with specific observations that could help the reader to better understand its values and limits (*comments*).

All the described devices do not require aortic clamp and, therefore, can be used on beating heart surgery. However, in some clinical studies and for different reasons, some of them have been used on cross-clamped aorta.

6.1 Symmetry aortic connector, first generation system

The Symmetry Aortic Connector is a part of a family of connectors designed and manufactured by the St. Jude Medical Anastomotic Technology Group (St. Paul, MN). It has the privilege to be the pioneer of Nitinol based connectors, the first to come onto the market and the first to receive FDA approval, and, therefore, this is the connector with the largest clinical experience.

Device design

It is made of Nitinol (Fig. 1), a memory shape alloy of Nickel and Titanium that spontaneously and quickly recovers a given shape once it reaches the body temperature, no matter the shape it has when loaded into the delivery system (crimped configuration).

The manufacturer recommends using the connector only with saphenous vein graft and it is available in 4 sizes from 4.5 to 7.0 mm outer di-

Fig. 1. The first generation of SJM aortic connector. Aortic wall is squeezed in between internal and external struts. The connection with the vein graft is provided by hooks.

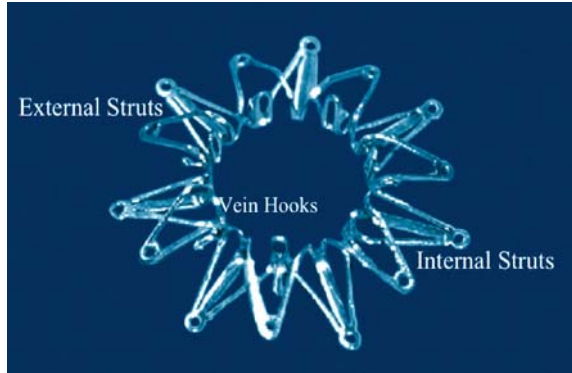
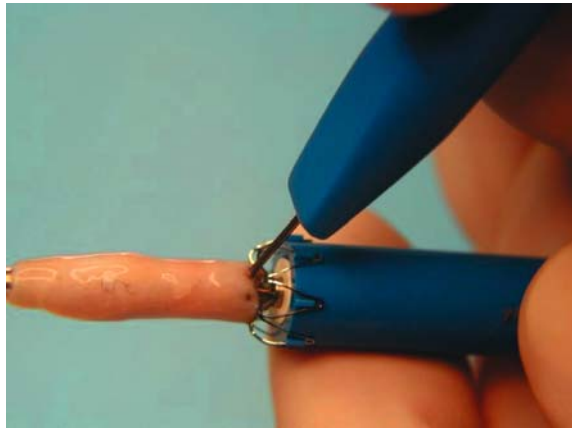


Fig. 2. SJM proximal connector I generation (Q-CAB). Vein is charged onto a transfer sheath and the surgeon manually pierces vein wall to insert device's hooks. The hooks provide the device-vein wall connection.



ameter. Once deployed, it has a double star-like shape squeezing the aortic wall that ensure the connection between the device itself and the aortic wall. A short chimney with hooks at the tips provides the connection between the graft and the device. The use of clips to close side branch holes is not allowed because it can hamper the device loading and no side branches should exist within the last 5 mm of the end of the vein to be attached to the connector. The graft is sized under pressure to select appropriate size connector.

The end of the vein is cut approximately at a 90° angle. It is then transferred on to the delivery system maintaining the direction of flow. Vein edges are pulled over the hooks to pierce the vein ensuring that the vein is not everted (Fig. 2). The connector is then inverted and the delivery system is attached to the handle. The nosecone is inserted and rotated until slots are aligned with vein hooks and the vein is ready for deployment. This procedure requires a learning curve of 10 h and a trained surgeon needs about 10 min to complete it.

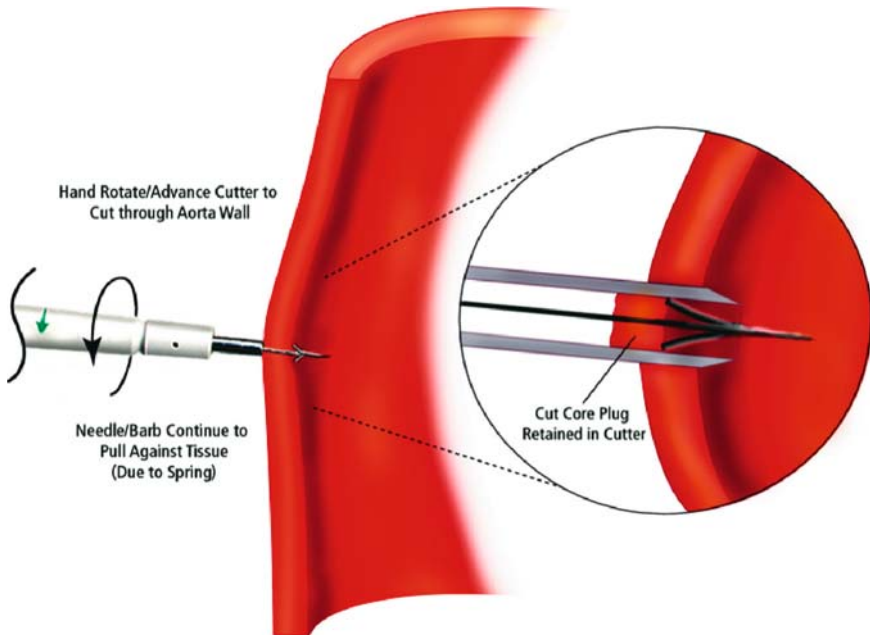


Fig. 3. Dedicate punch for precise arteriotomy.

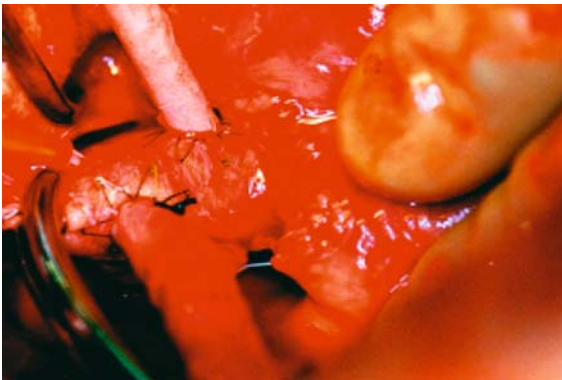


Fig. 4. Intraoperative picture. The Q-Cab has been used for the construction of two proximal anastomoses.

Aortotomy is done with a dedicate punch illustrated in Figure 3.

Figures 4 and 5 show the external and internal aspect of the sutureless anastomosis.

There is a limitation in the CABG timing construction because the proximal anastomosis has to be performed before the distal. The site of a proximal anastomosis must be precisely determined since the take-off angle of the vein graft out of the aorta will be in a 90° angle. This requires an adequate support of the proximal vein graft segment (with the pulmonary ar-

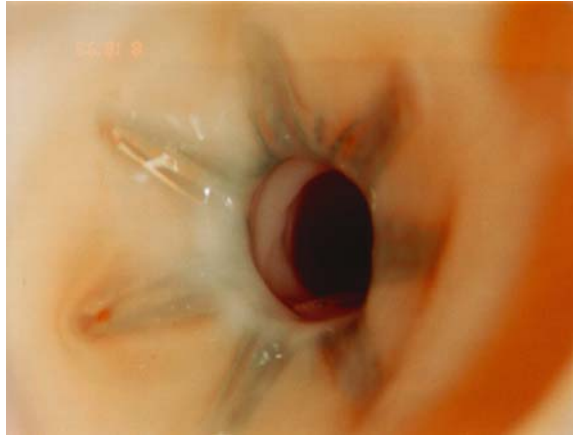


Fig. 5. Sheep model, one month follow-up. Thin layer of neointima cover inner struts of the proximal connector.

tery for those grafts to the circumflex coronary artery and with the right ventricle for those to the right coronary artery) to avoid graft kinking. The final position of the vein graft is still unpredictable once the mediastinal fat tissue and/or the pericardium have been closed and this will also be dependent on the distance between the sternum and the ascending aorta. Thus, for proper alignment and to prevent torsion, the graft to right coronary or posterior descending artery should be connected on the right side of the aorta while the graft for diagonal or obtuse marginal should be connected more to the left side of the aorta. The optimal mean arterial pressure during delivery is about 50–60 mmHg, and in all cases below 100 mmHg. The system uses a unique rotating blade that creates a perfectly round hole without damaging the adjacent aortic wall. Delivery takes less than 10 s. Haemostasis is usually adequate and instantaneous. In case of anastomotic leakage, placement of an adventitial extra-stitch can be performed but is not recommended by the company.

Experimental work up and clinical results

Since receiving CE market label and FDA approval in May 2001, more than 40,000 Symmetry Aortic Connector Systems have been used worldwide and preliminary results were very favourable in terms of consistency of the anastomosis, reliability of the device, immediate haemostasis and flow rate through the graft [1, 2]. However, results of clinical studies assessing the long-term patency of proximal anastomoses constructed with the first generation of SJM connector have dramatically reduced the initial enthusiasm [3]. Traverse [4] reported clinical, angiographic and interventional follow-up of 74 consecutive patients having undergone elective CABGs in which a total of 131 of 144 proximal vein graft anastomoses were performed with this device. A total of 11 patients were readmitted with unstable angina in

the first 6 months after CABG. At angiography, 20 saphenous vein bypass grafts containing 18 connectors were found to have severe stenosis ($n=12$) or occlusion ($n=6$), and were treated with angioplasty and stenting or medical therapy.



In another series of 206 connectors deployed in 132 patients technical problems arose in 5.5% of the cases. Moreover, 19 patients that had received a total of 32 venous bypasses underwent postoperative angiography at eight weeks revealing the occlusion of 4/32 grafts (12.5%) although intraoperative transit time flow measurement was satisfactory in all cases [5].

Assuming that, before widespread acceptance, new techniques must be compared to standard procedures and critically evaluated, we designed a clinical study to assess the 1 year patency rate of this connector and compare it to the patency rate of the standard technique in such a way that each patient was a case and control simultaneously. We designed a one arm, two centers, prospective, non-randomised clinical trial, enrolling patients over 65 year old, with severe 3 coronary vessel disease and vascular co-morbidities, scheduled for elective on pump CABGs. Eighteen patients were enrolled (15/18 had peripheral vasculopathy Fontaine IIB or more, and 6/18 had asymptomatic carotid artery stenosis) each receiving at least 2 venous bypasses: one on the right coronary artery and one on the circumflex artery. Therefore, each patient had one proximal anastomosis constructed with the symmetry device and the other one with the standard technique (5-0 polypropylene running suture). After weaning the pump, graft flow was measured using the ultrasound transit-time method (Medi-Stim system®) and the pulsatility index (PI) was calculated as well. PI is defined as the difference between systolic peak flow and diastolic flow divided by the mean flow [6]. All patients received Aspirin 100 mg per day starting on the day of the operation.

The connector was used in 10 grafts on the right coronary artery and 8 on the circumflex artery and *vice versa* for the running suture. Mean coronary diameter was 1.5 ± 0.5 mm. Twelve patients (86%) also underwent LIMA onto LAD grafting. Mean venous graft flow was 27 ± 11 ml/min in the connector and 31 ± 12 ml/min in the running suture group. The mean pulsatility index was 2.8 ± 0.5 (range 2.5–3.5) for both groups. All patients survived the procedure and the post-operative period was uneventful for all of them. They received Aspirin 100 mg per day. One year after the procedure they were all alive and asymptomatic, without significant ECG modification and all underwent elective coronary angiogram to assess graft patency. Six grafts mechanically anastomosed (33.3%) and 4 grafts sutured manually (22.2%) were occluded. One connector had proximal stenosis of 75% (5.1%). Seven out of 10 occluded grafts were on the right coronary system. Patency rate of LIMA grafts was 92% (11/12) (Table 1).

Overall results were not as good as they were expected to be. It is generally accepted that venous grafts have a 1 year patency rate of about 90% [7]. In our experience only 67% of the venous bypasses constructed with

Table 1. 18 patients underwent off pump CABGs receiving at least 2 vein grafts one on the right coronary artery (RCA) and one on the circumflex artery (CA). One of the 2 proximal anastomosis was constructed with the connector and the other one using the running suture technique. One year after the procedure, the angiogram showed that 6/18 in the connector group and 4/18 in the running suture group were occluded. Data are expressed as mean and standard deviation.

	RCA	CA	Coronary Ø	Graft flow ml/min	1 year angiogram	
					occlusion	stenosis
	10	8	1.5 ± 0.5	27 ± 11	6/18 33%	1
	8	10	1.5 ± 0.5	31 ± 12	4/18 22%	–

the sutureless device and 78% of the venous bypasses constructed using the running suture technique were fully patent one year after the procedure. Patient selection criteria have probably affected the outcome: old patients with severe systemic vasculopathy usually have the worst prognosis. An additional factor that has probably caused the early graft occlusion was the poor run off of the coronary system. The mean graft flow of the occluded bypasses was less than 30 ml/min and, even if the diastolic pattern was satisfactory with a pulsatility index between 2.5 and 3.5, it still is a negative prognostic factor for long term anastomosis outcome [8]. Moreover, 7 out of 10 occluded bypasses were on the right coronary artery, strongly reinforcing the evidence that the bypass on the right coronary system lasts for a shorter period of time. Fortunately, none of the patients with occluded bypass complained of angina. The question of whether the connector has played a role in determining the unfavourable evolution of this sutureless anastomosis, still has an open answer and we can only formulate general hypothesis.

Based on the experience of 10 years of coronary artery stenting, we can speculate that the presence of foreign material in the vessel lumen may promote myointimal hyperplasia which causes stenosis and graft occlusion. The symmetry connector has a BENIS (see Chapt. 5) of 1.8 mm² compared to 0.6 mm² of the running suture, therefore, there is a stronger stimuli to myointimal hyperplasia eventually leading to graft occlusion. However, if this is the main cause of the graft failure, we should expect to find the majority of the stenosis at the level of the connector where all the nitinol is, thus at the anastomotic site, and this is not the case. As reported by other authors and confirmed by our clinical experience almost all stenoses are located a few millimetres distal to the connector's metallic pins and struts (Fig. 6).

This is the reason why other mechanisms for early graft occlusion can be evoked. The take-off angle of the vein graft from the ascending aorta is 90° and this may induce graft kinking and abnormal fluid dynamics.

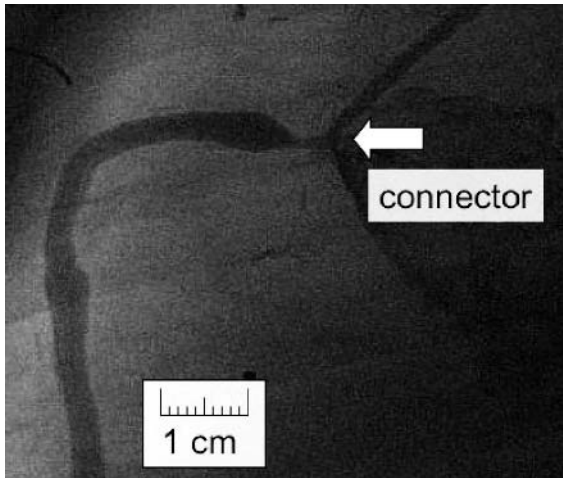


Fig. 6. Coronary angiogram of 1 year follow up SJM proximal connector. The graft sub-occlusion is at least 5 mm from the metallic connector.

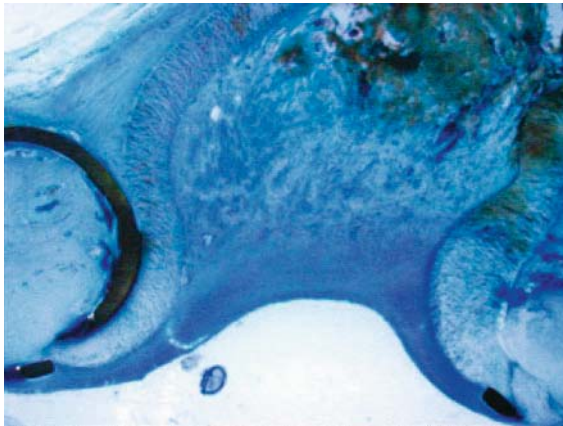


Fig. 7. In an animal model, the SJM proximal connector has been used for constructing the proximal anastomosis of aorto-to-femoral bypass. The pathological examination on the occluded graft reveals a thrombus a few millimetres distally to the connector and this is probably due to graft kinking caused by an anastomotic take off angle of 90° .

Therefore, it is important to correctly estimate the vein graft length before deploying the device. Inappropriate graft length may result in significant vein graft stenosis which typically develops at the connector site when the vein graft is too short.

In an animal study conducted to assess the feasibility of descending thoracic aorta to femoral artery bypass using a thoracoscopic approach, the proximal anastomosis was constructed using the first generation SJM proximal connector [9]. The pathological examination of the occluded grafts showed the thrombus formation a few millimetres distally to the connector as shown in Figures 7 and 8, and this was probably due to the graft kinking caused by an anastomosis take off angle of 90° and the shortness of the graft.

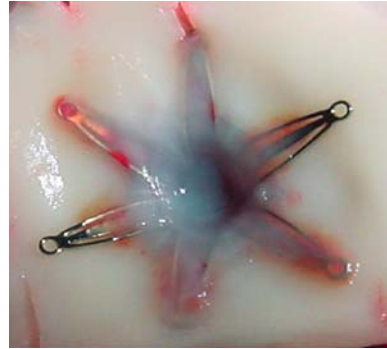


Fig. 8. Animal study. Gross pathology 6 weeks after the construction of the proximal anastomosis with SJM proximal connector. Anastomosis is occluded and covered with a thin myointimal layer.

A 90° angle anastomosis is thought to cause turbulent flow that is associated with areas of low wall shear stress promoting early thrombosis and myointimal hyperplasia. However, if the specific hemodynamic conditions of the ascending aorta to vein graft anastomosis with a 90° take off angle are simulated using a computational flow dynamic approach, the results are somehow, surprising. In an elegant experimental study, Alfieri and co-workers [10] investigated the fluid dynamic patterns at the proximal graft. Four models of hand-sewn anastomoses and two models of automated anastomoses were constructed and a finite volume technique was used to simulate realistic graft fluid dynamics, including aortic compliance and proper aortic and graft flow rates. The anastomosis geometry performance was analyzed by calculating time-averaged wall shear stress and the oscillating shear index at the toe and heel regions of the proximal graft. Time-averaged wall shear stress was significantly lower in the hand-sewn anastomosis models than in the two models that simulated the use of the aortic connector (0.38 ± 0.07 Pa vs 1.32 ± 0.4 Pa). Higher oscillating shear index values were calculated in the hand-sewn anastomosis models (0.15 ± 0.02 Pa vs 0.06 ± 0.02 Pa). They concluded that symmetry anastomosis geometry is associated with less critical fluid dynamics than with conventional hand-sewn anastomosis: the shape of the proximal graft induces more physiological wall shear stress and less oscillating flow, suggesting a lower risk of atherosclerotic plaque and intimal hyperplasia as compared with conventional anastomosis geometry.

The vein graft manipulation during the loading of the vein onto the connector delivery system could play a major role in the anastomosis occlusion. During this phase, the endothelium of the vein can be damaged or even destroyed and this is one of the most powerful stimuli to myointimal hyperplasia.

Another prospective study evaluated the relationship between major adverse cardiac events (MACE), defined as cardiac mortality, myocardial infarction, or revascularization of a previous target vessel, and the use of the connector in two cohorts: 162 patients receiving at least 1 proximal anastomosis constructed with the connector and 159 patients receiving run-

ning suture technique as control [2]. This study demonstrates that in comparison with an equivalent control group, patients having received anastomotic connectors had an increased incidence of early MACEs. The majority of the events were related to the need for target vessel intervention. Multiple factors may negatively impact graft survival and freedom from target vessel reintervention, including technical problems at the time of surgery, poor quality conduit, diminished distal vessel run off, and progression of native vessel disease. In this study, early MACEs were most common in the patients with diabetes and significantly more frequent in patients on oral hypoglycemic medications as opposed to those on insulin. In fact, there were no observable differences in MACEs between the control group and the nondiabetic connector cohort or the connector patients on insulin. Two anastomotic connectors of this series were explanted in a previously bypassed nondiabetic patient undergoing cardiac transplant. Grossly, both anastomoses were subtotally occluded at the ostia with patent distal saphenous vein. Histology of the specimens demonstrated necrosis in the area at which the vein wall abuts the aorta and fibrous tissue occluding the orifice of the anastomosis within the aorta. These findings were indicative of an enhanced fibrotic reaction elicited by deployment of the connector. This response could be exaggerated by the procoagulant and pro-inflammatory predisposition of the diabetic patient, thus leading to reduced graft patency.

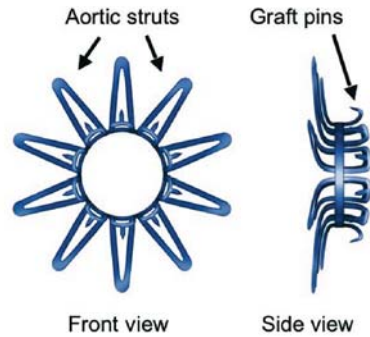
Comments

In summary, there are several critical points concerning the first generation of SJM proximal connectors. The mounting of the vein over the delivery device is one of the most critical steps for the quality of the connection; inaccurate mounting could end up with anastomotic leakage or with a stenotic connection. With this device the proximal anastomosis has to be performed first which means a change for a majority of surgeons. The design of the connector implies a 90° take-off angle of the vein graft from the ascending aorta. This means that the anterior surface of the ascending aorta should be avoided because of the risk of kinking and compression by mediastinal tissue and the sternum. The optimal length of the vein has to be evaluated very precisely to avoid kinking of the graft or tension on the connector.

6.2 Symmetry aortic connector, second generation system

To address some limitations and pitfalls of the first generation proximal connectors, in particular the graft manipulation and the take off angle, the St. Jude Medical developed a second generation system with the following main changes (Fig. 9).

Fig. 9. Second generation of SJM proximal connector. External struts have been taken off and replaced with longer pins. The cross sectional anastomotic area is bigger than first generation's device. There is no graft manipulation during the loading phase and the anastomosis has a side-to-side configuration with an acute take off angle.



First the concept allows a side-to-side anastomosis avoiding manipulations in the vein graft during the loading process. Second, there is no concern about the take-off angle in this configuration. Third there is a fixed size of the connector as compared to self-expansion with the first generation device.

Device design

A sizing/incision tool is advanced 1–3 cm into the proximal end of the graft. A scalpel blade is used to create an opening in the side wall of the graft at the anastomosis site; the delivery system, with the pre-mounted connector, is then placed in this aperture. The attachment knob of the delivery system is then rotated to release the connector graft hooks thereby securing the graft to the connector. The delivery system is then introduced into the target aortic site (cutting process same as with first generation system). The delivery system handle push button is pressed and the delivery system is removed. The graft stub end is ligated or clipped (Fig. 10).

Despite the fact that preliminary clinical results seem to confirm that the second generation of connectors is a consistent improvement, St. Jude Medical Inc. has stopped the manufacturing and distribution of the Symmetry Aortic Connector on January 2005 for reasons apparently not linked to the clinical results.

6.3 The CorLink

The Aortic Anastomotic Device (AAD Bypass, Ltd, Herzelia, Israel) which has been commercialized by J&J Ethicon (Cardioventions, a company of Ethicon, Somerville, NJ) as CorLink, allows the creation of an anastomosis between ascending aorta and saphenous vein graft in a side-to-end configuration.

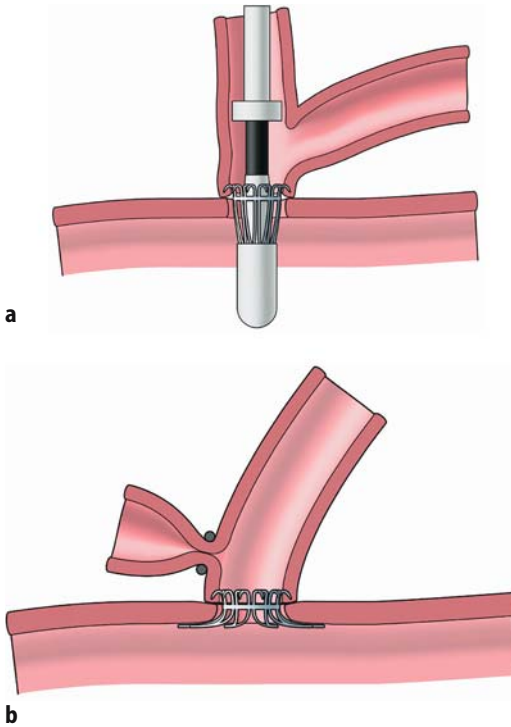


Fig. 10. **a** Proximal St. Jude Medical Symmetry™ second generation aortic connector. Introduction of the delivery instrument is through the proximal end of the graft. **b** Completed side-to-side anastomosis with the proximal end of the graft being clipped. Note that there is no introduction of a delivery system nor a connector within the graft itself.

Device design

The AAD is a self-expanding nitinol extraluminal device that consists of a central cylindrical body made of interconnected elliptical arches and two sets of five pins radiating from each end. The graft is pulled through the inserter by means of a snare or a 4.0 suture passed through the adventitia. The vein graft has to be everted over the distal end of the system and this procedure is cumbersome and could damage the intima layer. The five intimal pins are deployed from the cartridge of the delivery system, making them protrude and penetrate the everted segment of the vein. Full penetration of the pins through the vein tissue is a mandatory precondition for a

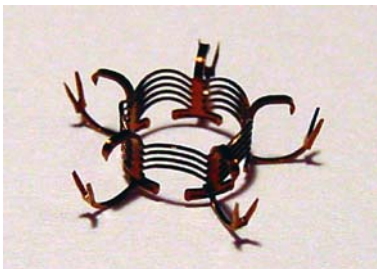


Fig. 11. Front view of the Corelink anastomotic device.

successful procedure. A special punching instrument is inserted in the handle and creates a round hole in the unclamped aorta. After punching, the punch cone is driven into the aorta while the device is rotated 360° in both directions to ensure a complete punching. The punching device is withdrawn from the handle and the delivery system is advanced into the aorta and the AAD is released. At this time the inner pins partially penetrate the aortic wall whereas the outer pins stabilize the device by anchoring into the aortic adventitia. The inserter together with the overtube split open and release the anastomosed vein graft (Fig. 11).

Experimental work up and clinical results

Preliminary animal studies were carried out to assess the reliability of the system. Forty-seven vein-to-aorta anastomoses using the CoreLink and 27 control hand-sutured anastomoses were constructed in 28 sheep [12].

The distal part of these grafts were connected either to the main pulmonary artery or to the sheep's brachiocephalic trunk. Procedural details focusing on deployment, leakage, and early patency rates were examined. Sheep were sacrificed after periods ranging from 1 to 180 days. Specimens were examined grossly and histologically. All anastomoses were patent immediately after their construction. There was no difference between control and sutureless anastomoses with respect to flow rates at the end of operation and before sacrifice. No metal breaks were detected. Fourteen of the 47 sutureless anastomoses and 6 of the control anastomoses (29.8% versus 22.2%, $P = \text{ns}$) were occluded at autopsy. Intimal thickening was found in a notable number of anastomoses, but without any significant difference between the sutureless and sutured controls (44.7% versus 40.7%, $P = \text{ns}$).

Two major clinical studies concerning the CorLink have been conducted. In the first trial 17 patients were enrolled [13] and received one proximal anastomosis constructed with this device. In one patient the device was not deployed and in 2 patients an additional suture was necessary to achieve perfect hemostasis. There was neither mortality nor device-related morbidity in this series and in 6 patients control angiogram showed patent anastomosis after a mean follow-up of 48 days.

In a second prospective randomized trial 11 patients receiving at least one CorLink device were compared to 10 control patients. In one case eversion of the vein graft was not possible and in 2 patients additional sutures were necessary to control minor anastomotic leakage. In the same group one patient had a myocardial infarction and another one had to be reoperated because of a kinked internal thoracic artery (ITA) graft. The 6-month followup with CT-scan showed that all grafts were patent [14].

Comments

Even if graft manipulation is quite important, the amount of foreign material exposed to blood flow is rather small: there are only 5 pins on the aortic side of the anastomosis and nothing on the vein side. The majority of the connector is outside the vessel and, therefore, only very limited intimal hyperplasia should be expected. The take off angle is not fixed and can be adapted to patient's anatomy. However, results of experimental and clinical preliminary studies reduced the enthusiasm for this promising device and, at the present time, the CoreLink is not distributed in Europe or the USA.

6.4 The PAS-Port™ proximal anastomosis system

The PAS-Port proximal anastomosis system (Cardica Inc., Menlo Park, CA) has been cleared by the European Community, receiving the CE mark in September 2004. This device creates a sutureless automatic side-to-end anastomosis between aorta and vein conduit in a side-to-end configuration (Figs. 12 and 13).

Device design

The major improvement that characterizes the PAS-Port is that it consists of a single tool allowing the surgeon to create the aortotomy and the deployment of the connector with one single turn of a knob. This device

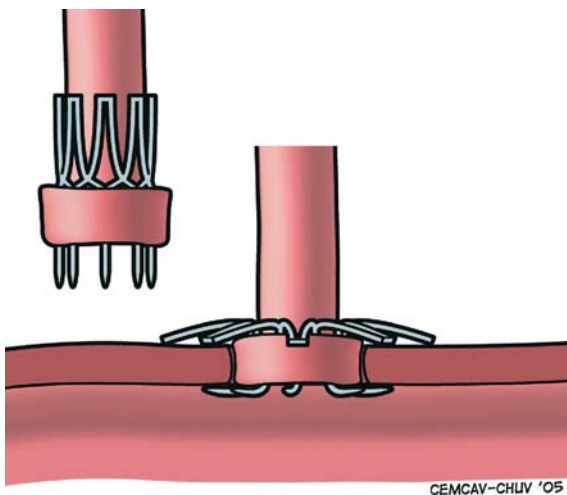


Fig. 12. Schematic representation of the PAS-Port.

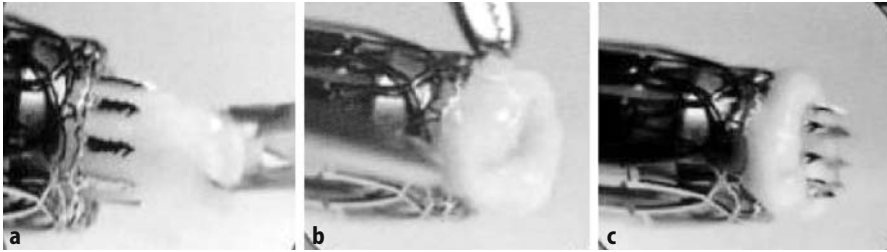


Fig. 13. The PAS-Port proximal anastomotic device. The vein is inserted into the connector (a), then everted (b) and the pins pierce the vein (c) to ensure the connector – graft connection.

eliminates the need of exchanging the aortic puncher with the delivery system and seems to be ideal for endoscopic use. In a three-step process the vein graft is first pulled through the implant, then manually everted over the end of the implant and, with the help of a poke-through tool, the everted vein is attached to the connector with a single action [3]. The deployment tool is placed onto the aorta exactly where the anastomosis will take place and the surgeon rotates a knob at the end of the tool. This design requires the surgeon to perform the proximal anastomosis first and then attach the graft to the target vessel at a 90° angle. Therefore the surgeon has to carefully select the site on the aorta for placement of the proximal anastomosis and correctly measure the appropriate graft length in order to avoid graft kinking.

Experimental work up and clinical results

This device has been evaluated in a multi-center European study. Results of the clinical trial have been recently presented which include data from 50 patients scheduled for elective CABG surgery [15]. Sixty-three PAS-Port devices were deployed. Two deployments were unsuccessful. A purse string suture was used to secure hemostasis in 6 deployments. There were no redo operations for bleeding or ischemic problems. Two patients died of causes unrelated to the device. Patency evaluation at discharge was performed by angiography in 49 implants and CT in 2 implants (86% follow-up). At discharge all controlled grafts were patent (100% early patency rate). The angiographically evaluated implants were all rated FitzGibbon A. At 6 months there was no additional mortality. Forty-seven implants were evaluated by angio, 4 by CT (85% 6 months follow-up). All grafts but one were patent (98%). One graft had proximal stenosis (FitzGibbon B) successfully treated with percutaneous balloon dilatation.

This is the largest series reported in literature and it confirms the unpublished preliminary results. Early and mid term patency are excellent and these data compare favourably to data from historical hand sewn controls.

Comments

The connector is made of stainless steel and this results in a firm attachment of the implant to the aorta. On the other hand, stainless steel can be deformed during anastomosis manipulation resulting in complete and permanent modification of the anastomotic geometry. The blood exposed surface of this connector is very small and is limited to the aortic side of the anastomosis. No metal is present into the graft. Other key improvements over previous generations include minimized endothelial trauma during loading and large effective orifice area. The PAS-PortTM System exists in only one size and is compatible with vein grafts from 4–6 mm outer diameter and aortas greater than 18 mm outer diameter. If used in smaller aorta, the delivery system can injury the opposite side of the aortic wall.

A larger and more widespread use of this device and report on the results might be necessary to judge the value of the device and convince the cardiac surgeon community about the usefulness of routine proximal aortic anastomosis.

6.5 The Spyder

The Spyder (Coalescent Surgical, Sunnyvale, CA) is a novel application of nitinol sutures (U-clips) enabling the construction of graft vein to aorta anastomosis. The vein graft having diameter bigger than 5 mm, is previously mounted onto the delivery system (Fig. 14). After creating a precise aortotomy with dedicate aortic punch, the loaded delivery system is positioned in the aortotomy and six nitinol sutures are deployed simultaneously. The result is an end-to-side anastomosis constructed with interrupted suture technique without the disadvantages of the tying the knots.

This anastomotic device has recently received the FDA approval and the CE mark. It has been the object of clinical study [16] and preliminary results are very promising.

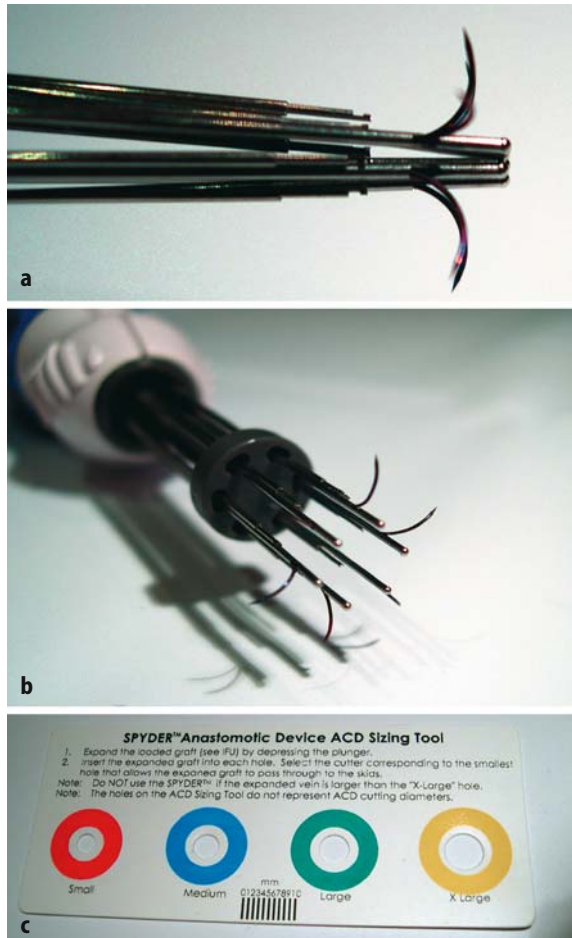


Fig. 14. The Spyder proximal anastomosis device in its closed (a) and open (b) configuration. Nitinol wires are partially deployed for purpose demonstration only. The vein sizer (c) is fundamental for successful application of the device.

References

1. Eckstein FS, Bonilla LF, Engleberger L et al. (2002) The St. Jude symmetry aortic connector system for proximal vein graft anastomoses in coronary artery bypass grafting. *J Thorac Cardiovasc Surg* 123:777–782
2. Dewey TM, Crumrine K, Herbert MA et al. (2004) First year outcomes of beating heart coronary artery bypass grafting using proximal mechanical connectors. *Ann Thorac Surg* 77:1542–1549
3. Carrel T, Eckstein F, Englberger L, Berdat P, Schmidli J (2004) Clinical experience with devices for facilitated anastomoses in coronary artery bypass surgery. *Ann Thorac Surg* 77:1110–1120
4. Traverse JH, Mooney MR, Pedersen W et al. (2003) Clinical, angiographic, and interventional follow-up of patients with aortic-saphenous vein graft connectors. *Circulation* 108:452–456

5. Katariya K, Teharani H, Yassin S, Masroor S, Salerno TA (2003) Initial experience with sutureless proximal anastomoses performed with a mechanical connector leading to clampless OPCAB. STS Ann Meet Proceedings, p 160
6. Morota T, Duhaylongsod FG, Burfeind WR, Huang C-T (2002) Intraoperative evaluation of coronary flow anastomosis by transit-time ultrasonic flow measurement. *Ann Thorac Surg* 73:1146–1150
7. Puskas JD, Williams WH, Mahoney EM et al. (2004) Off-pump vs conventional coronary artery bypass grafting: early and 1 year graft patency, cost and quality of life outcomes. *JAMA* 291:1841–1849
8. D'Ancona G, Karamanoukian H, Ricci M et al. (2000) Graft revision after transit time flow measurement in off-pump coronary artery bypass grafting. *Eur J Cardiothorac Surg* 17:287–293
9. Tozzi P, Corno AF, Marty B, von Segesser LK (2004) Sutureless videoendoscopic thoracic aorta to iliac artery bypass: the easiest approach to occlusive aorto-iliac diseases. *Eur J Vasc Endovasc Surg* 27(5):498–500
10. Redaelli A, Maisano F, Ligorio G, Cattaneo E, Montevocchi FM, Alfieri O (2004) Flow dynamics of the St. Jude Medical Symmetry aortic connector vein graft anastomosis do not contribute to the risk of acute thrombosis. *J Thorac Cardiovasc Surg* 128(1):117–123
11. Terry CM, Callahan KS (1996) Protein kinase C regulates cytokine induced tissue factor transcription and procoagulant activity in human endothelial cells. *J Lab Clin Med* 127:81–93
12. Bar-El Y, Tio FO, Shofti R (2003) CorLink sutureless aortic anastomotic device: results of an animal study. *Surg Res* 115(1):127–132
13. Calafiore AM, Bar-El Y, Vitolla G et al. (2001) Early clinical experience with a new sutureless anastomotic device for proximal anastomosis of the saphenous vein to the aorta. *J Thorac Cardiovasc Surg* 121:854–858
14. Riess FC, Helmold H, Hilfer I et al. (2002) Clinical experience with the Cor-Link device for proximal anastomosis of the saphenous vein to the aorta: a clinical, prospective, and randomized study. *Heart Surg Forum* 5:345–352
15. Gummert JF, Demertzis S, Matschke K, Kappert U, Anssar M, Siclari F, Falk V, Alderman EL, Harringer W (2006) Six month angiographic follow-up of the PAS-Port Clinical Trial. *Ann Thorac Surg* 81(1):90–96
16. Hamman BL, White CH (2004) A novel device for clampless proximal anastomosis in OPCAB surgery: the IPAD. *Heart Surg Forum* 7(5):E374–375

7

Coronary surgery: devices for distal anastomoses

Introduction

In this chapter we review anastomosis devices that allow the construction of end-to-side coronary anastomosis. Several distal devices using different technologies have been developed and are currently under clinical investigation to assess their potential benefits in terms of enabling limited access coronary surgery like totally endoscopic coronary surgery, reducing the technical demand for the anastomosis construction and standardizing anastomosis quality. Some of these devices can be also used with arterial graft, the majority are compatible with beating heart surgery and almost all show good results in terms of early graft patency. All patients receiving distal connectors are under thrombocyte aggregation inhibition with aspirin and/or clopidogrel for at least 1 month after the operation.

For each device, we describe the technical characteristics (*device design*), report the published results of the most important experimental and clinical studies (*experimental work up and clinical results*) and conclude the device's presentation with specific observations that could help the reader to better understand its values and limits (*comments*).

7.1 St. Jude Medical Coronary Connector

The St. Jude Medical Coronary Connector is a balloon-expandable, stainless steel device first mounted on the vein graft and then inserted into the target coronary artery to achieve a side-to-side anastomosis. The side-to-side technique allows accommodation of the device to different conduit sizes, produces a uniform anastomosis diameter and provides an optimal takeoff angle to prevent kinking.

Device design

The first generation of coronary connector has been quickly replaced with a more reliable version. The second generation has been designed in 2 sizes: 2 mm and 2.5 mm. It has external pins securing the vein graft and internal struts engaging the internal coronary artery lumen. A nose cone covers the internal fingers to prevent coronary artery endothelial trauma during deployment (Fig. 1). The connector is loaded on a balloon catheter. When the balloon is inflated, it expands the connector reducing its length and firmly apposing the two vessels to create a hemodynamic seal. The connector body also acts as a scaffold for the anastomosis. An opening is made into the vein wall approximately 1 cm from the distal end of the graft with a preformed 1.25 mm cutting device and a 1.5 mm Teflon-coated dilator. The delivery system is passed through the distal end of the vein, and

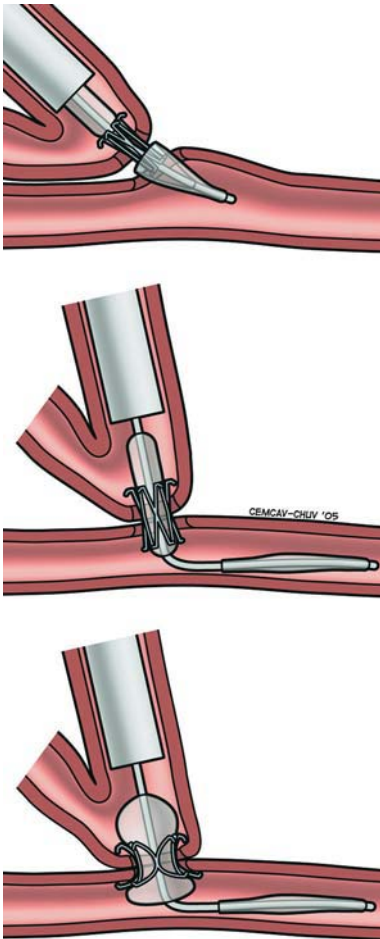


Fig. 1. St. Jude Medical Coronary Connector. The stainless connector is mounted on balloon expandable delivery system. Description in the text.

the external connector struts engage the graft endothelium as the nosecone emerges from the new ostium. The arteriotomy on the target coronary is performed with the same cutting device and dilator sheath. The delivery system is then introduced axially through the arteriotomy until the graft ostium perfectly touches the coronary artery wall. The nosecone is then advanced uncovering the internal struts, and the delivery system is repositioned perpendicular to the long axis of the coronary artery. The balloon is inflated and pressurized to 18 atmospheres, expanding the connector to a uniform cylindrical configuration. After delivery the catheter is pulled back and the distal end of the vein graft is occluded with clip or a similar technique.

Experimental work up and clinical results

This anastomosis device has been extensively studied in animal and controlled clinical studies [1–6]. In a prospective study [6] enrolling 32 patients receiving each 1 distal connector (on the right coronary artery in 14 patients, the posterior descending branch in 12 patients, the obtuse marginal in 5 patients, and the posterolateral branch in 1 patient), 3 connectors were removed because of minor leakage at the connection site, and 1 connector was removed because it was accidentally deformed after successful deployment. Intraoperative flow was assessed by the transit time method and averaged 71 ± 24 mL/min. One patient died of neurological injury; the connector was patent at autopsy. One patient had a perioperative myocardial infarction. There were no adverse cardiac event in the remaining patients. Twenty-one patients were followed up with angiogram at 6 months: 4/21 (19%) grafts were occluded.

In another randomized, controlled study [7] a total of 60 patients scheduled for elective on pump, arrested heart, CABGs were randomly assigned: one vein graft-coronary artery anastomosis per patient was either performed with the connector ($n=30$ patients) or hand sewn ($n=30$ patients). Inclusion criteria required a coronary outer diameter of 2.5 mm at the anastomotic site, corresponding to an estimated inner coronary diameter greater than 2 mm. The internal vein graft diameter had to exceed 3.5 mm. There were no significant differences between groups regarding preoperative demographic data. One patient was excluded from the connector group because of a plaque in the back wall, resulting in dislocation of the connector. Six sutureless anastomoses were leaking and required one additional suture each. The mean time required to load the vein graft onto the delivery system was 2 min and the time for deploying the connector was less than 1 min. The intraoperative graft blood flows after weaning from extracorporeal circulation were about 47 mL/min in both groups indicating that all anastomoses were patent at the end of the procedure.

At the 6-month follow up, one patient has complained of angina and had stenosis of the sutureless anastomosed graft requiring reoperation.

Fifty-seven patients were controlled either with angiography or MRI at 6 months: all the grafts in the control group were patent. Seven of the grafts that received the connector were occluded (26%).

In this study, the SJM connector had a 6-month patency rate of 74% which could be considered equivalent to historical patency rate for vein grafts. However, if we compare this result to the control group in this study in which all sewn anastomoses were open, it is not acceptable. This stresses once again the importance of the study design in the early phase of the evaluation of any new device or drug.

Comments

The complexity of the whole connector system may strongly contribute to these poor results. Anastomoses performed with the SJM coronary connector are round rather than oval leading to the angiographic observation that these anastomoses appear to be smaller than hand-sewn ones (Fig. 2). The use of stainless steel for coupling devices implies the need for a more careful handling of the system during loading and delivery to avoid irreversible deformation. The deformation of the connector during the deployment could be the main cause of bleeding at the anastomosis site.

Besides that, there could be several reasons to explain the high incidence of early graft occlusion when this connector is used. Foreign material is introduced into the vessel with a BENIS of 1.3 mm^2 and the loading process could damage the intima layer. The distal part of the vein has to be ligated after the deployment of the connector, and this can create a cul-de-sac close to the anastomotic site in which a thrombus eventually will form completely remodelling the intimal layer because of changes in the flow pattern.

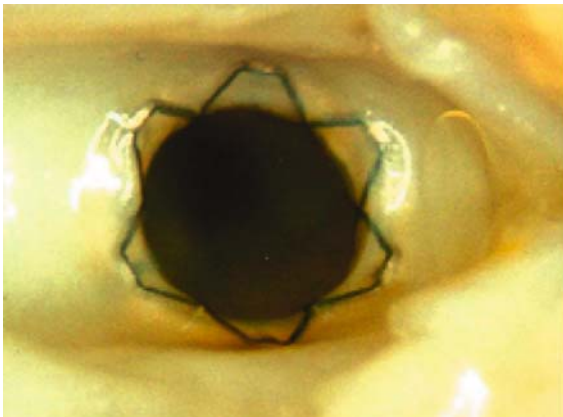


Fig. 2. Coronary view of the SJM coronary connector. The anastomosis has a round shape.

Anastomotic bleeding has always been managed by adding extra stitches because, even if the removal of a failing connector is feasible and easy this will damage the coronary artery and jeopardize the quality of the subsequent hand sewn anastomosis. In the situation of a technical failure, such as a leaking anastomosis, it is easier and somehow safer to add a suture instead of anastomosing a damaged target vessel. However, adding a stitch can potentially compromise the long-term result.

We believe this connector is not ready for extensive clinical use because the incidence of anastomosis bleeding is too high and the graft patency too low.

7.2 The Graft Connector

By means of modern stent technology, Jomed International AB, Helsingborg, Sweden, has developed the Graft Connector (GC) that represents an alternative way to construct the coronary anastomosis by reducing the technical demand with respect to the total number of manual manoeuvres and the required manual dexterity. The GC reduces the performance time of an end-to-side anastomosis and it facilitates a consistent and reproducible sutureless coronary artery anastomosis for minimally invasive and beating heart surgery as Solem has exhaustively demonstrated in an animal model [8]. Moreover, he has demonstrated that GC is a less technically demanding procedure requiring low manual dexterity as compared to a running suture.

Device design

A dedicated coronary artery Nitinol stent is covered by a 10 μm thick layer of polytetrafluoroethylen (PTFE) and has a side branch, called tower, of 4 mm PTFE vascular graft as shown in Figure 3. The tower is where the internal mammary artery (IMA) is inserted and fixated by means of a ligature after it has been first inserted through and then everted over the outside of a Nitinol ring. The covered stent is then inserted in the receiving coronary artery through a 4–6 mm arteriotomy. To facilitate the device insertion in the coronary artery, it is kept in a crimped loaded configuration (1-mm outer diameter) by means of a plastic handle. Once in the correct position, the release mechanism is activated and the covered stented graft self-expands in the receiving vessel and fixates the conduit (IMA) to the coronary artery. There is a minimal coronary size of 1.5 mm and a maximal of 3.5 mm for GC use.

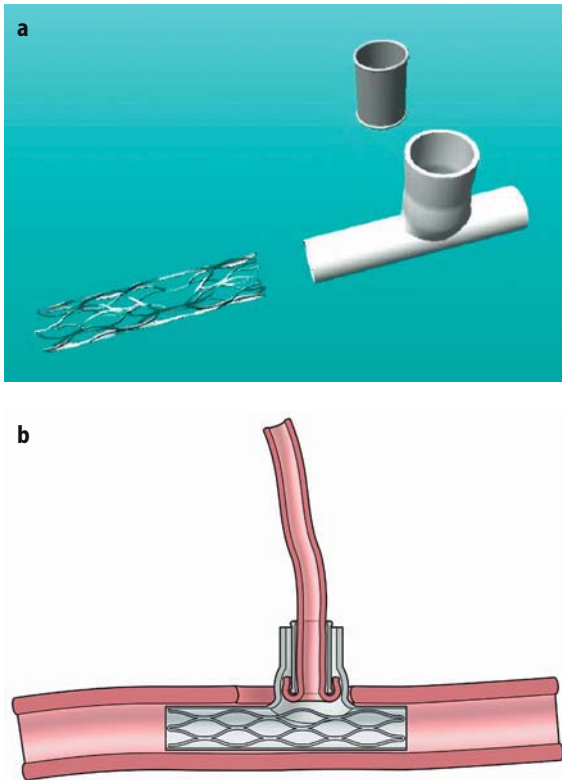


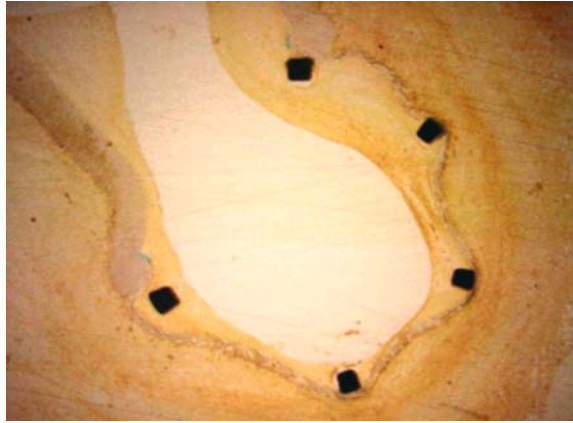
Fig. 3. **a** The GraftConnector components. The anvil, the e-PTFE T tube and the coronary nitinol stent. **b** Schematic view of the deployed GraftConnector.

Experimental work up and clinical results

We designed an animal study to compare histology and luminal width of end-to-side coronary artery anastomoses performed with GC to standard running suture technique [9]. In a sheep model, LIMA on LAD off pump CABG was performed: 25 animals received the connector and 5 running suture as a control group. We have followed up animals for 6 months since in animal models for such devices, the most interesting reactions occur between the 1st and 3rd months. Histological data showed that all the anastomoses examined were patent after 6 months. The thickness of myointimal hyperplasia was the first difference that came up between groups: 0.21 ± 0.1 mm in the device group vs 0.01 mm in the control group (Fig. 4).

Statistical analysis demonstrated that difference is highly significant: $p < 0.001$. As myointimal hyperplasia is the first cause of anastomotic stenosis, we would expect it to cause a reduction of anastomotic diameter, but this was not the case. Mean anastomotic diameter is 1.7 mm in the GC group vs 1.6 mm in the control group (p -value = NS). Mean anastomotic diameter in the GC group corresponded to mean LAD diameter of adult sheep. In other words, there was no histopathological sign of stenosis in

Fig. 4. GraftConnector for IMA to LAD on beating heart in sheep model. Pathology of the anastomosis after 6 months follow-up. Axial cross section. Magnification 2 \times . Thin layer of myointimal hyperplasia covers the connector.



any of the groups even if myointimal hyperplasia was more important in the GC group, because anastomotic luminal width corresponded to the normal adult sheep LAD diameter.

Myointimal hyperplasia was less predominant in the tower but no statistical difference has been noted in the different parts of the GC (tower and stent). Even if myointimal hyperplasia did not affect anastomosis patency, it is a matter of fact that it was significantly higher in the GC group. Vessel injury, stent material and stent geometry are known factors that correlate closely with late neointimal thickening in experimental models [10, 11]. The degree of hyperplasia has been linearly related to the degree of stent-induced vessel wall injury [10], but the specimens of the GC group had intact internal elastic lamina and we can reasonably assume that GC did not provoke any significant vessel injury during deployment.

Animal studies [11] demonstrate that stent design can cause late neointimal thickening to optimize fluid flow at the blood/metal interface, without affecting vessel patency. At deployment, the stent stretches the vessel, imposing a cross-sectional polygonal luminal shape that depends on the stent design. The lumen therefore initially assumes the geometric shape of a polygon, with the struts marking each vertex. Altered stent-imposed fluid dynamics may cause regions of turbulence and/or stagnation in the immediate vicinity of stent struts and provide a basis for the observation that restoring the lumen to a circular shape will optimise fluid flow characteristics at the blood/metal interface. In Figure 4 it appears clearly that stent struts alter vessel geometry and the restoration of luminal circularity by neointimal growth seems to be the physiological response to optimise flow at the blood/metal interface. The oversizing of the device at the implantation has also played a role in the degree of intimal proliferation. We can imagine that the difference between GC and native vessel diameter has been filled up with myointimal proliferation in order to optimise blood flow. Figure 5 illustrates the histological reaction at the GC edges (transi-

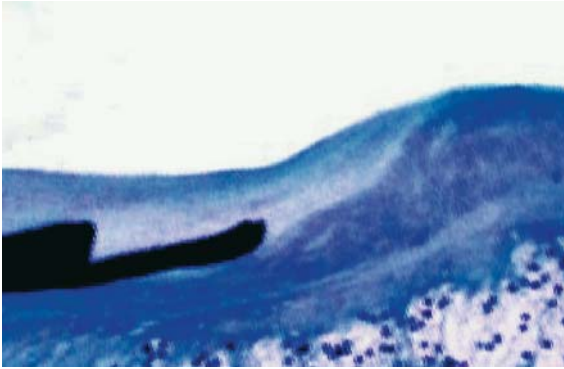


Fig. 5. GraftConnector 6 month follow up. Detail of the transitional area from the connector to normal coronary artery. The connector has overexpanded the coronary artery and the difference in diameter has been filled up with intimal tissue.

tional area) and clearly elucidates this phenomenon: neointimal growth optimizes blood flow characteristics reducing turbulence in the proximity of the GC edges.

The over sizing phenomenon may also explain the reduction of the cross-sectional anastomotic area, 35.6% of distal LAD in the device group versus 5% in the control group. These values were calculated assuming that the native vessel cross-sectional area corresponds to the GC cross-sectional area as reported in Figure 4. This assumption, however, is only valid if the GC is oversized with respect to the native LAD diameter. The consequence of the GC oversizing is an overestimation of the cross-sectional anastomotic area reduction. Therefore, the mean anastomotic cross sectional area reduction of 35.6%, corresponding to a 15% reduction of anastomotic diameter, is overestimated.

No sign of artery wall degeneration has been found. Signs of mild chronic inflammatory reaction have been found in some specimens mostly in the proximity of PTFE layer. This tissue reaction has already been described by other authors and seems to be related to the PTFE itself [12, 13]. There is no evidence in current literature that this tissue reaction has ever affected the anastomosis patency.

The segment of the IMA having been everted and tied onto a rigid structure (tower) was still viable even if it is not possible to recognise an intimal layer and the media has signs of chronic inflammatory reaction.

Carrying out the histological analysis, we also focused our attention on the rim of PTFE which is between the end of the IMA and the endothelium of the coronary: this PTFE was covered with myointimal cells as were the other parts of the GC.

One of the potential drawbacks of the GC is that the covered stent may occlude side branches, like septal branches with obvious unfavorable consequences.

Comments

The GC provides a consistent and reproducible coronary artery anastomosis and reduces technical demand and manual dexterity in coronary surgery. Long-term results in an animal model, demonstrated that off pump CABGs performed with GC had 100% patency rate. The mean anastomotic luminal width corresponds to mean LAD's adult sheep diameter. We may speculate that myointimal hyperplasia occurred as a result of local device oversizing. More precise GC sizing could reduce myointimal hyperplasia even if, in our experience, it doesn't cause stenosis.

The production and distribution of the GC is, at the present time, suspended.

7.3 Magnetic Vascular Positioner™

The nature and origin of magnetic fields is still unknown: they interact with cellular biology but the details of such interaction and the consequent results are far from clear. However, the concept of using magnetic force to create a vascular anastomosis is original and, somehow, fascinating because it is based on a very simple idea. As presented in Chapter 1, Obora has published the first scientific work describing the use of magnetic force to create an end-to-end microvascular anastomosis in 1978, but results were not encouraging. The Magnetic Vascular Positioner (MVP) developed by Ventrica Freemont, CA, represents the first successful attempt to create a vascular anastomotic device that works using magnetic force. The technique of application looks very easy, and this is the basis for a reproducible and standardized application.

This connector can be used with vein and arterial graft as well.

Device design

The MVP system consists of two pairs of magnetic rings mounted on a delivery device to facilitate placement (Fig. 6). One pair of magnets forms the anastomotic docking port within the graft, and the other pair forms an identical anastomotic docking port within the target vessel. One ring lies in the vessel lumen and the other one lies on the adventia in such a way that the vessel wall is squeezed between the two rings. In the second generation device, the magnet size and shape have been modified in order to reduce the amount of foreign material exposed to blood. In the new device the internal magnets are held in place by two external magnets which are placed outside the vessel on the lateral wall. This allows an increase of the effective anastomotic area (now 6.0 mm²). The new delivery system sepa-

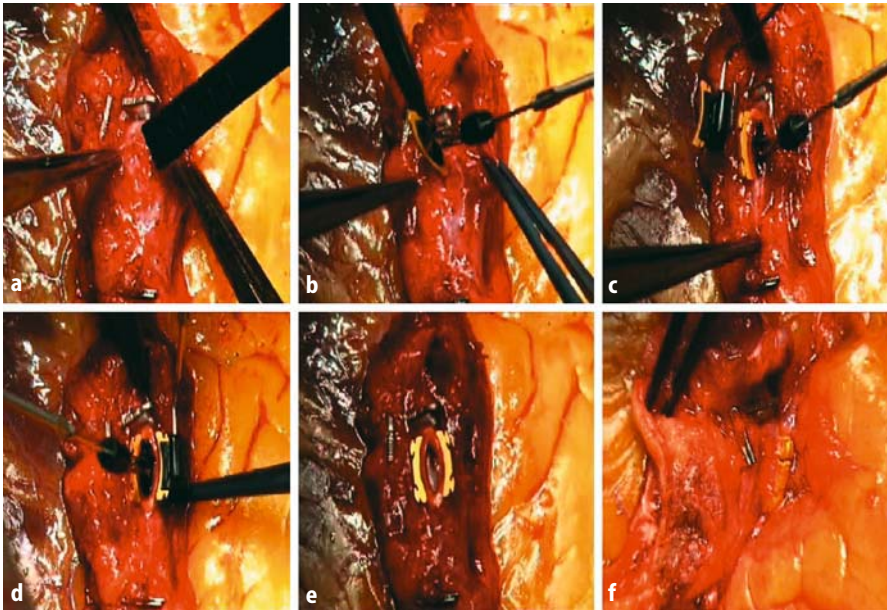
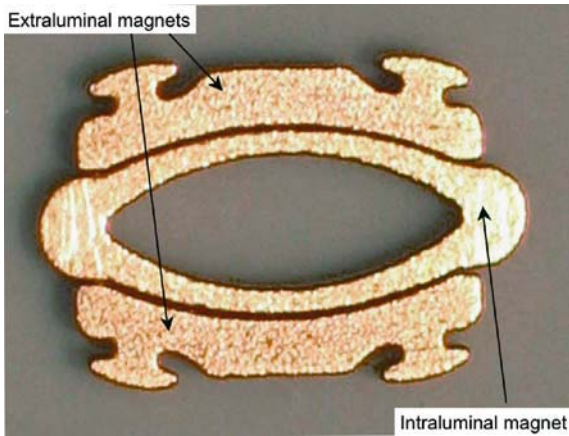


Fig. 6. **a** MVP II generation. The vessel wall is squeezed in between the intraluminal and extraluminal element. **b** The MVP system (II generation) consists of 6 magnetic gold-plated rings and 2 delivery systems for completion of the connection. Pictures show and LIMA on LAD anastomosis. **a** Sizing of LIMA arteriotomy. **b** The intravascular magnet is positioned inside the LIMA. **c** and **d** External magnets ensure the device vessel connection. **e** LIMA is ready to be connected to LAD. The same procedure is done on the target coronary. **f** The 2 ports are then brought together, and the magnetic field maintains the apposition and forms a reliable side-to-side anastomosis.

rates the actuating trigger from the actual delivery platform; this decreases the likelihood of unintended motion of the platform during the manipulation [17].

To allow perfect alignment of the 2 rings lying on the opposite side of the vessel wall, the arteriotomy or venotomy has to have very precise lengths, otherwise some tissue can protrude into the anastomotic lumen and compromise the flow. The 2 magnetic ports are then brought close to each other to complete the anastomosis and the coupling process is realized by the magnetic attraction between the two ports. The anastomosis can, of course, be disrupted if enough force is applied to the graft in any direction. However, the coupling force seems strong enough to prevent inadvertent disruptions.

It exists in 2 sizes: for coronary arteries of 1.5 and 2 mm in diameter.

The MVP system has multiple advantages which include ease of use, reproducibility, and a brief learning curve. Also, the device does not exert radial stress on the vessel wall or the anastomosis, nor does it require vessel wall eversion which could produce vessel distortion. The deployment system is rapid, precise, and applicable to both venous and arterial conduits. One of the major benefits of this technology is that if, after completion of the arteriotomy, the placement of the magnets is not satisfactory, they can be removed atraumatically. In the majority of cases, the same magnets can be redeployed after the adjustment of the arteriotomy size, or the surgeon can revert to a hand-sewn anastomosis.

Experimental work up and clinical results

This connector has been the object of extensive animal and clinical studies. Animal studies conducted in pig models, showed 1 month angiographic patency of IMA on LAD or RCA of 33 out of 34 anastomosis, corresponding to 97% [15]. Six animals were followed up to 6 months. All patent anastomoses had TIMI III flow showing no stenosis. Gross inspection of implants demonstrated complete neointimal coverage and histologic studies confirmed complete neointimal coverage of the endoluminal magnetic surface. No significant luminal obstruction as late as 6 months. Signs of chronic inflammatory reaction as foreign-body giant cells and mature collagen fibrils were seen in contact with the magnets. However, very few signs of acute inflammation were found. There were no polymorphonuclear leukocytes or lymphocytes present and no signs of tissue necrosis (Fig. 7 a,b).

The last, is a very important point since one of the major concerns resides in the fact that the vessel wall participating the anastomosis construction receives very low blood supply because it is squeezed between the 2 magnetic rings. As seen in other devices requiring wall eversion, this can induce necrosis or atrophy of anastomosis edges with potentially catastrophic consequences.

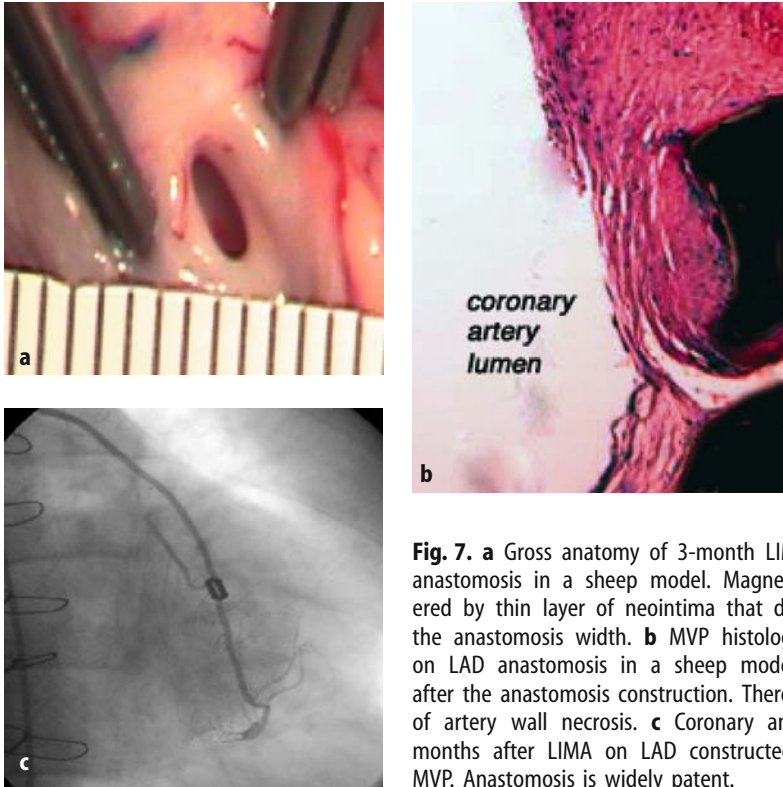


Fig. 7. **a** Gross anatomy of 3-month LIMA on LAD anastomosis in a sheep model. Magnets are covered by thin layer of neointima that doesn't affect the anastomosis width. **b** MVP histology of LIMA on LAD anastomosis in a sheep model 4 weeks after the anastomosis construction. There is no sign of artery wall necrosis. **c** Coronary angiogram 3 months after LIMA on LAD constructed with the MVP. Anastomosis is widely patent.

There are several clinical studies describing the preliminary experience with the MVP device. The first report concerns the first generation connector [16]: 32 patients received LIMA on LAD anastomoses constructed with the MVP. Three patients had a non hemostatic anastomosis after coupling and were converted to hand-sewn anastomoses. Patency at patient discharge was 93.5% in the MVP group compared to 91.7% in the running suture group. However because lateral leakage was observed and the amount of foreign material exposed to the blood stream was considerable, the design of the connector was modified. The same group published [17] a short series of 10 patients in which the connector was used to perform LIMA on LAD with minimal invasive direct CABGs (MIDCAB), demonstrating that the connector design is ideal for the minimal invasive approach. The 6-month angiography demonstrated 100% anastomosis patency and no stenosis (Fig. 7c). Other clinical studies demonstrated that this connector can be easily used during MIDCAB with excellent early results [18, 19].

Comments

One of the theoretical limitations of the MVP consists in the fact that it provides a non compliant anastomosis. The presence of metallic rings surrounding the anastomotic area do not allow for physiological changes of the cross sectional anastomotic area during the cardiac cycle, resulting in an anastomosis that has virtually zero compliance. Many studies in the last 20 years have underlined the correlation between myointimal hyperplasia formation and anastomotic compliance: a stiff anastomosis is more subject to stenosis than a compliant one [14].

Other potential limitations consists in the difficulty to deploy the magnets onto a calcified coronary artery wall since it is necessary to “sandwich” the vessel wall between the central intraluminal ring and both lateral pontoons. The device in its present configuration does not allow the construction of diamond-shaped side-to-side anastomoses. Therefore a sequential anastomosis can only be constructed automatically if the graft and target vessel are parallel to each other, a condition that is rarely fulfilled in daily practice.

This anastomotic device is based on an ingenious and simple method and early clinical experience is very encouraging. However, only more extensive and controlled clinical study will definitively assess the value of the magnetic connector.

7.4 The Heartflo Anastomosis Device

The Heartflo™ Anastomosis Device (Perclose Inc., Redwood City, CA) is one of the most promising surgical tools to facilitate end-to-side and side-to-side interrupted suture anastomoses for CABG [20]. Ten years of arterial closure device experience has led the Perclose’s engineers to develop the “Heartflo” device [21]. Extensive bench testing and animal studies have been performed to verify the design and functionality of the device.

Device design

The Heartflo is a multi-suture anastomotic device and consists of a hydraulically activated delivery mechanism and two branches, with each branch housing needles and the opposite ends of ten 7-0 polypropylene sutures (Fig. 8). This is a surgical instrument that automates the suture delivery process during the anastomosis procedure via the simultaneous delivery of ten standard 7-0 polypropylene sutures through the vessel wall of the graft, and then through the wall of the coronary artery. After the automatic deployment, the surgeon manually ties off the ten sutures to complete the

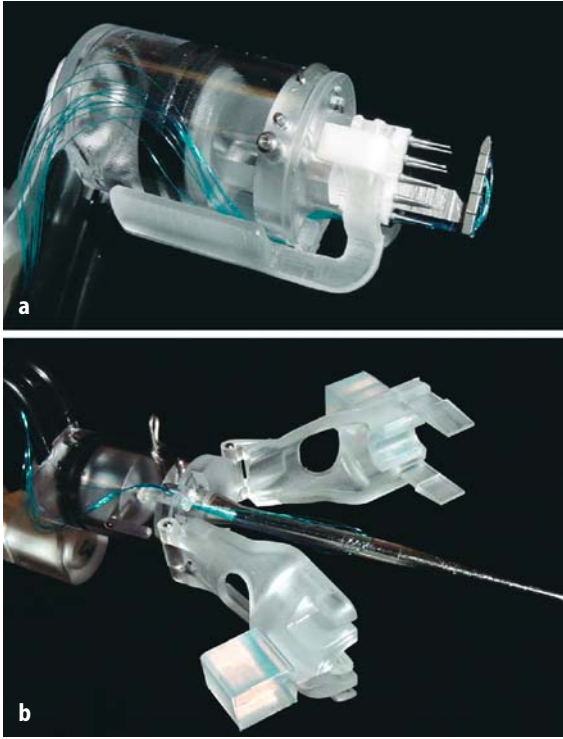


Fig. 8. Close-up view of Heartflo device. Coronary side (a) and graft side with arms open (b) for end-to-side anastomosis. c Schematic representation of Heartflo sewing machine.

anastomosis, similar to a hand-sewn interrupted anastomosis (Fig. 9). Critical for the tissue capture, is the size of the arteriotomy that is performed with dedicated scissors making a 4 mm incision in which the device fits perfectly. Animal tests showed that most of the time, tying 8 out of 10 stitches could guarantee haemostasis if the missed stitches are on the opposite side of the anastomosis.

Experimental work up and clinical results

We have designed a clinical prospective study in order to assess the consistency of the procedure, considering procedural success as a haemostatic anastomosis obtained without adding extra stitches [22]. Secondary endpoints were:

Time of anastomosis construction and ease-of-use issues (device insertion, needle deployment and suture management on a three-point scale). Major adverse cardiac events: myocardial infarction, haemorrhage or ischemia necessitating revascularization.

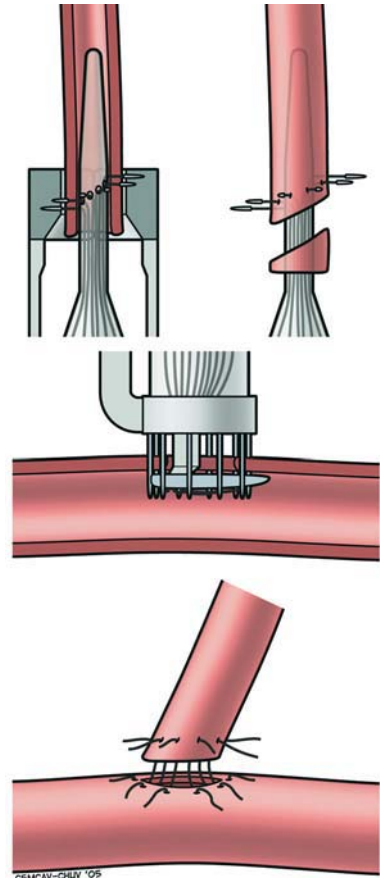


Fig. 8c

CEMCAV-CHUV '05

Eleven patients scheduled for elective on pump CABGs were enrolled and received a total of 15 anastomoses constructed with the device (12 end-to-side and 3 side-to-side) on 2 mm target vessels. 13 out of 15 anastomoses were completed with the device. 5 out of 13 required 1 additional stitch and 8 out of 13 required more stitches to assure hemostasis. Average time to perform device-supported anastomosis with interrupted sutures was 17 min. In 2 out of 15 cases the procedure was switched to a traditional hand-sewn anastomosis. All patients survived and post-operative period was uneventful. The 6 months follow-up showed no clinical or instrumental evidence of residual ischemia in all patients.

The Heartflo seems to fulfill the need for a device that can reduce the time for performing an interrupted suture anastomosis during CABG.

An automated suturing device that uses the same suturing material currently used in hand-sewn anastomoses holds great attraction. This device does not leave endovascular material behind, and hence, is not likely to induce intimal proliferation as in stent based devices. Furthermore, suturing

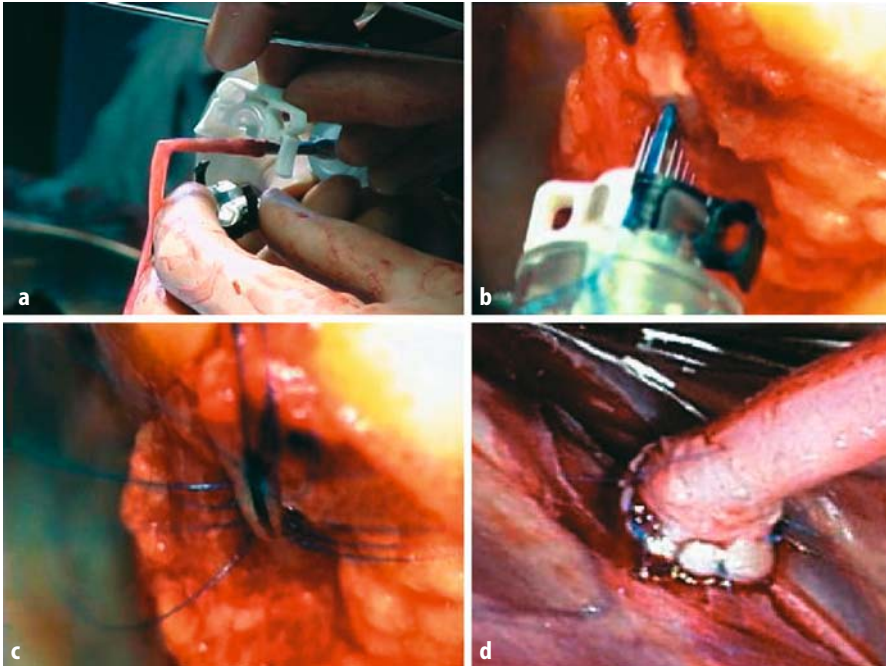


Fig. 9. The Heartflo device for end-to-side coronary anastomosis: **a** vein graft is placed on the device's foot and needles are deployed to pass the sutures through the vein. **b** The foot of the device on the coronary side is inserted in the coronary artery and needles are deployed. **c** 10 sutures of 7/0 polypropylene have been deployed through the coronary artery wall. **d** Sutures are tied and anastomosis is completed.

devices that avoid eversion of vascular edges offer additional advantages over clipping and other devices that cause edge eversion. The Heartflo does not use bonding elements that could cause excessive wall strain that has been proved to be deleterious for long term anastomoses patency [23].

The device seems to have some limitations, however. Arteriotomy must be performed with dedicated scissors in order to achieve optimal tissue capture. Bigger incisions dramatically reduce the percentage of tissue capture that is the major cause of anastomotic leak. Coronary artery must have a diameter greater than 1.6 mm and the presence of vessel calcifications can reduce the tissue capture. In our series the average time to perform the distal anastomosis was 17 min which is still high if compared to running technique and we believe the suture managing should be improved to reduce the anastomotic time.

Comments

The Heartflo concept is very attractive because of its simplicity and because it does not leave endovascular material behind. The device is a reliable instrument that provides reproducible coronary anastomoses with interrupted suture technique, but this new technology needs some changes in improving the tissue capture and in the process of handling and tying sutures, before extensive clinical application. Once tissue capture and suture management will be improved, this instrument will really help cardiac surgeons in making end-to-side coronary artery anastomoses, even on beating heart.

The production and distribution of the Heartflo Anastomotic Device is, at the present time, suspended.

7.5 Converge Coronary Anastomosis Coupler

The Converge Coronary Anastomosis Coupler has been developed by Converge Medical Inc., Sunnyvale, CA, on the base of coronary stent technology. This device consists of a two-piece implantable coupler and instruments for loading and delivery of the coupler and is intended to create an elliptical end-to-side coronary anastomosis with a take off angle of 30° , using vein graft and on beating heart.

Device design

The two-piece implantable coupler includes a series of concentric mating frames obtained with laser cutting technique from a single tube made of Nitinol, that clamp vessel tissues together to enable healing (Fig. 10). The vein graft has a minimal diameter of 3 mm and is placed over the inner frame.

The outer frame is placed over the tissue-covered inner frame securing the end of the graft in a sandwich configuration to ensure device-graft connection (Fig. 11). The frames are then deflected with a dedicated deployment tool for insertion into a coronary artery in a 30° take off angle with an end-to-side configuration. Arteriotomy has to be 5 mm in length to guarantee perfect graft-artery wall apposition with the target coronary artery having at least a 2 mm inner diameter. The coupler is then inserted into the coronary artery first with its toe, then with its heel, and the device is released. Releasing the coupler, the deflected elements return to their original shape and secure the distal part of the vein graft against the arterial wall. The anastomosis is generally completed in less than 3 min. The anastomosis has an elliptical shape and a cross-sectional area of 11.9 mm^2 .

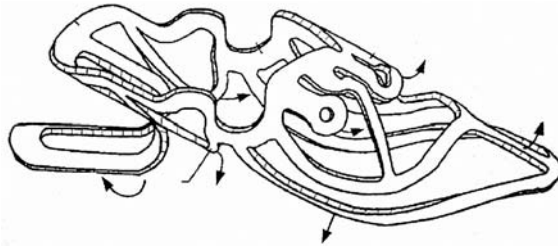


Fig. 10. Schematic draw of the saphenous vein-to-coronary, 30° end-to-side coupling device.



Fig. 11. a The connector (metallic frame) is applied to the saphenous vein graft prior to its deployment into the coronary artery. **b** How the coupler appears before its deployment into the coronary artery.

This complex design has the advantage of avoiding graft or coronary piercing and reducing the amount of metal exposed to the blood stream: the BENIS is 21.6 mm². In case of trouble, the coupler can be easily removed using a special tool without damaging the coronary artery.

Experimental work up and clinical results

Bench tests confirmed a minimally disruptive blood flow path and excellent fatigue resistance of Nitinol frames. In an animal study involving 21 sheep, the 1 year patency rate of free carotid artery graft to circumflex artery was 100% assessed with angiogram and intravascular ultrasound. Pathological examination showed a widely patent anastomosis in all cases with no intimal hyperplasia and no anastomotic stenosis. The coupler frames were covered with a thin layer of endothelium-lined neointima [24]. Those excellent results still have to be confirmed by clinical trials. Shoenich and coauthors have successfully implanted the Coupler in 3 patients scheduled for on pump CABGs. In one patient minor anastomotic bleeding was controlled by arranging the bypass graft along the axis of the coronary

vessel with fibrin glue. The average mean flow through the Coupler was 51 ml/min, compared to an average flow rate of 24 ml/min in conventionally sutured vein grafts [25]. The same group published the results of a multicenter, prospective, non-randomized, open study enrolling 33 patients scheduled for on pump and arrested heart CABGs receiving at least 1 venous bypass on the circumflex or on the right coronary arteries. All patients received 1 distal anastomosis constructed with the coupler and coronary angiogram 2 months after surgery. In 4 cases, minor anastomotic bleeding was treated by slightly changing the position of the coupler within the anastomosis or with the use of fibrin glue. The post-operative period was uneventful. After 2 months, one graft was occluded (96% coupler patency rate), and one showed 50% stenosis at the coupler level. 30 out of 37 hand sewn venous graft were patent (81% running suture patency rate), but those results cannot be compared because the coupler grafts were done on bigger coronary arteries with better runoffs.

Comments

This is one of the most promising devices because it satisfies several criteria considered fundamental for success: it provides anastomoses with optimal takeoff angle and low BENIS and the coupler can be easily removed without damaging coronary artery. However, loading the coupler onto the vein graft is a long and cumbersome procedure that requires significant graft manipulation and anastomosis leak seems to be common, but not dramatic. Another potential disadvantage might be the clip mechanism that holds vessel's ends in place: it can cause endothelial trauma in case of excessive manipulation and relocation attempts. Furthermore, the intramural stress within the coupled vessel walls could be as excessive to compromise the healing processes. The last concern is how to follow up patients having coronary anastomoses constructed with the converge device: angiography seems to be inadequate because the internal and external metallic frames give rise to artefacts. The device's shape appears distorted so that no morphological information about stenosis can be safely obtained.

7.6 Cardica C-Port

The C-Port, designed and manufactured by Cardica Inc., Redwood City, CA, can be considered a novel and more sophisticated version of the stapler proposed by Androsov in early 50's, demonstrating, once more, that new technologies make an old dream come true. The result is a device allowing the construction of end-to-side anastomosis with interrupted suture technique, the sutures being stainless steel staples (Fig. 12).

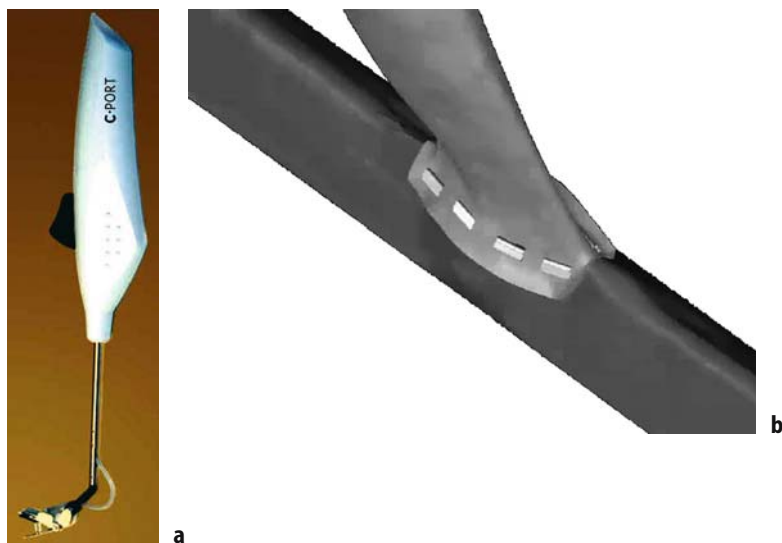


Fig. 12. **a** Cardica C-Port delivery system. **b** Schematic view of the interrupted sutureless anastomosis constructed with the Cardica C-Port.

Device description

This anastomosis device includes an expandable tube configured in such a way as to have a vein graft secured to the tube. The vein graft is pre-loaded onto the delivery system: vein is inserted through the center of the tubular delivery device and everted over the distal end. An arteriotomy of 5 mm in length is then created and the graft is inserted into the coronary artery. The delivery device has an expandable linkage positioned at its distal end and its expansion causes a first radially extended flange to fold outward. This first flange abuts the interior wall of the target coronary artery and a second flange is formed which abuts the exterior wall of the target vessel, trapping the coronary artery wall between the two flanges and securing the end of the graft vessel into the arteriotomy. The C-Port system can be used in conduits with diameters as small as 1 mm.

Experimental work up and clinical results

The C-Port has been evaluated in a European multi-center, prospective, clinical trial enrolling 110 patients scheduled for on pump CABGs. The trial compared the 6 months patency rate of venous bypasses constructed using this device to historical results achieved with traditional suture technique. Results showed a patency rate of 97% versus 85%. For the first time, these excellent results show that distal connectors may improve the outcome of vein CABGs.

Comments

Wall eversion and graft manipulation are potential drawbacks of this technique, but preliminary clinical results seem to refute this assumption.

With the current design 2–3 additional stitches are necessary to close the anvil hole at the heel and toe. The anastomosis has a perfect geometrical shape and the amount of blood exposed non-intimal surface is comparable to a sutured anastomosis, thus requiring no special anticoagulation protocol. This is the only anastomotic device able to create a side-to-end anastomosis in 1 mm diameter coronary artery. Moreover, it still works properly if small coronary plaque is present.

At the present time, this is probably the most promising device for sutureless vascular anastomoses.

7.7 The S2 Anastomotic System

The Borst group from Utrecht has always been very active in the development of new technologies applied to cardiovascular surgery, in particularly in the creation of alternative ways to construct vascular anastomosis. One of the most promising devices is the S2 Anastomotic System first presented in 2002, allowing the construction of distal coronary anastomoses. This device has been developed by taking into account all the fundamental surgical principles of minimizing vessel wall trauma, foreign material, and non-endothelialized surfaces exposed to the blood. It is an easy-to-use, one-shot anastomotic device that significantly pushes the barrier for less invasive coronary bypass surgery.

Device design

The S2 Anastomotic System (S2AS), (iiTech BV, Amsterdam, The Netherlands) is a stapler designed to create side-to-side anastomosis. It consists of a thin, expandable meandering ring (thickness 0.07 mm) and 8 marginally broader, initially straight staples made of stainless steel and mounted on a delivery system. Preloading consists of passing the device through the free distal end of the graft and out through a 5 mm arteriotomy. After expansion, the connector creates a rounded octagonal anastomotic orifice of slightly more than 2 mm diameter (Fig. 13). The staples are deformed to a circular shape of 0.5 mm diameter. The connector is suitable for target coronary arteries of 1.6 to 2.1 mm ID, with a graft size of at least 2 mm ID. The applicator securely covers all staple points until firing-off the device, allowing safe intravascular manipulation, positioning, and removal without firing-off, if necessary. One of the key points is the sequence of actions that

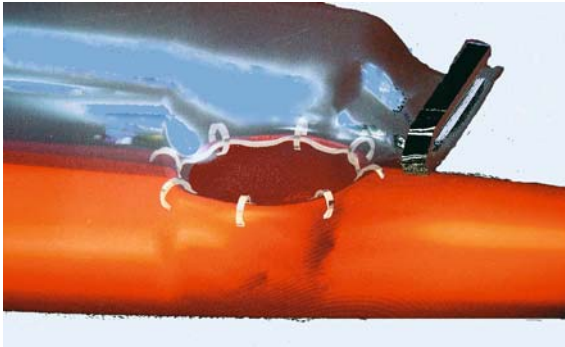


Fig. 13. Schematic view of the coronary anastomosis constructed with the S2 Anastomotic System.

control device deployment. The first is radial expansion of the “meandering ring” followed by closure of all staples. This sequence provides an unimpeded introduction of the device into the vessels and helps to reliably position the vessel walls between the anvils before stapling. Smooth introduction into the target vessel is supported by a shoe-like structure at the tip of the device. Subsequently, the device is introduced into the arteriotomy of the targeted coronary artery in a position perpendicular to the epicardium by first inserting the toe of the shoe in a way comparable to the introduction of an aortic punch. As a result, any contact between the back wall of the coronary artery and the staples is avoided. The applicator is activated by remote control using a hydraulic pressure unit connected to the applicator with flexible tubing to avoid transmitting any undue forces to the vessel tissue. When the pressure is released, the device returns to the unexpanded state for controlled withdrawal from the anastomosis site and the distal stump of the internal thoracic artery graft. The anastomosis is completed with a clip closing the distal free end of the arterial graft [27].

Experimental work up and clinical results

The S2AS was used in 10 adult pigs on an antiplatelet regimen. In each animal, the device was used to create an internal thoracic artery to left anterior descending bypass on a beating heart. A small arteriotomy of approximately 1 mm was made in the internal mammary artery using a 15° microsurgical knife followed by insertion of a conical tool to produce a standardized opening of approximately 2 mm in diameter. Next, the arterial graft was mounted onto the distal end of the S2AS applicator between the anvils of the staple-like connector. After coronary occlusion, the LAD arteriotomy was performed in a stepwise fashion. First, a small 1-mm incision was made with the 15° microsurgical knife which was extended to approximately 2 mm using standard microscissors. A conical tool was used in an upstream direction to check the size of the arteriotomy and slightly dilate it, if necessary, to ensure subsequent smooth insertion of the device. Next,

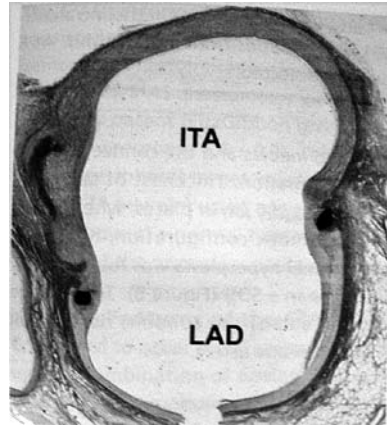


Fig. 14. Histologic transverse cross-section of a LITA-to-LAD anastomosis at 5 weeks postoperatively. Note the internal connector covered by small layer of neointimal tissue. ITA, internal thoracic artery; LAD, left anterior descending artery.

the mounted S2AS was inserted into the LAD, and after scrutinizing for proper positioning, the applicator was activated, resulting in expansion followed by closure of the staples of the vessel connector. Subsequently, the applicator was withdrawn from the distal end of the graft. After clip placement on the distal graft to convert the side-to-side anastomosis into an end-to-side configuration, perfusion through the graft was initiated, and the LAD was ligated proximal to the anastomosis.

The anastomoses were evaluated intraoperatively and at 5 weeks by functional flow measurements, postmortem angiography, and histomorphologic examination. In all pigs, the device rapidly created successful anastomoses on target vessels of 1.6 to 2 mm inner diameter, with coronary ischemia time of 3 min. There were no technical failures or anastomotic leaks requiring additional sutures. Both intraoperatively and at the time of death, angiography demonstrated widely patent bypasses, with FitzGibbon grade A in all animals.

The macroscopic examination revealed an anastomotic orifice of 2 mm. Histomorphologic evaluation showed a normal healing response with negligible neointima covering the connector and limited streamlining repair tissue formation between the staple-like elements of the connector (Fig. 14). Thickness of this layer ranged from 30 to 100 μm on the metal parts to 300 μm in places where anastomotic recesses, resulting from the anastomotic configuration, had been covered. Full-thickness medial necrosis was recorded near the penetrating staple elements of the ring frame. No medial necrosis or thinning of either the coronary or the thoracic artery was observed in between the staple elements. No extensive or full-thickness media inflammation was seen in any of the anastomoses.

Comments

This experimental study demonstrates that the S2AS consistently created automated, fast, and reliable internal thoracic to coronary artery anastomoses on the porcine beating heart with excellent graft patency and healing characteristics. When compared to other coronary anastomotic connectors the S2AS includes 4 useful features:

The delivery system guarantees by radial expansion the correct tissue positioning between the anvils before stapling takes place.

The anvils allowed the exertion of force directly on the staples.

The blood exposed non intimal surface is limited to 0.07 mm avoiding the necessity of aggressive anticoagulation or antiplatelet therapy.

With the staple ends completely covered by the anvils, perpendicular introduction of the S2AS applicator can be performed easily and without the risk of capturing the back wall of the coronary artery.

An important additional advantage of the side-to-side approach is the favourable take-off angle and complete directional freedom of the graft that prevents kinking. However, this study has a limited follow-up and these results need to be further substantiated with longer-term survival studies. In addition, the feasibility of the system in small-caliber, human, atherosclerotic coronary arteries remains to be established.

7.8 Distal Anastomotic Device

The Distal Anastomotic Device (DAD) designed and manufactured by Bypass Ltd, Hertzlia, Israel, permits the construction of elliptical sutureless coronary end-to-side anastomoses with either arterial and vein graft.

Device design

The DAD is an elliptical Nitinol ring provided with 8 pins that auto expands adapting itself to the coronary anatomy. The vein or artery graft is inserted through a side opening in the delivery system that has the DAD pre-charged at its distal end and passed through it using a special snare. The distal end of the graft is then pierced with the 8 pins in order to ensure the device-graft connection. The device is inserted into the coronary in which an arteriotomy has been done using dedicated scissors and the connector delivered. Pushing a button, the pins diverge to approximate and fix graft and coronary walls. Minimum coronary diameter is 2 mm. Proximal anastomosis can be done before or after the automatic distal one, at the surgeon's convenience.

Experimental work up and clinical results

The efficacy and long term patency of this device has been assessed in a sheep model [28]. The study design consisted of creating 20 coronary artery bypasses on beating heart, using saphenous veins or internal mammary artery as conduit and the DAD for the construction of the distal anastomosis. Bypass patency was assessed with transit time flowmeter soon after the anastomosis construction, and after 6 months. The average time required for the construction of the sutureless anastomoses was less than 30 s. Half of the anastomoses leaked and 6 required additional stitches to control the bleeding. All anastomoses were open immediately after their construction and the pulsatility index was above 3 in all cases. The 6 months follow up showed that 3 out of 20 anastomoses were occluded (15%), and 9 out of 20 had important myointimal hyperplasia, with a mean thickness of 400 μm , causing significant luminal stenosis. Almost all anastomoses were found to have mural injuries to the graft as well as to the coronary artery. However, all those results are substantially equivalent to those obtained from a control group.

Comments

The success of this device has yet to be established and even if the take off angle is optimal and the anastomosis width is favourable, this animal study has shown a few of the device's limitations in terms of achievement of optimal tissue capture which can be reduced when the incision is too large and cause bleeding. On the other hand, a smaller arteriotomy can hinder device insertion into the coronary artery. The graft loading is cumbersome and time consuming. Results in terms of graft occlusion and stenosis due to myointimal hyperplasia, are not encouraging even if they do not differ from controls. Moreover, in 8 out of 20 devices, the disconnection between the Nitinol and stainless steel components was detected, and, even if those fractures were not associated with bleeding or anastomosis disruption and are probably due to the device manipulation during the device explants and examination, their presence suggests that this device deserves additional fatigue tests.

References

1. Schaff HV, Zehr KJ, Bonilla LF et al. (2002) An experimental model of saphenous vein to coronary artery anastomosis with the St. Jude Medical Stainless Steel connector. *Ann Thorac Surg* 73:830–836
2. Eckstein FS, Bonilla LF, Meyer BJ et al. (2001) Sutureless mechanical anastomosis of a saphenous vein graft to a coronary artery with a new connector device. *Lancet* 357:931–932

3. Eckstein FS, Meyer BJ, Bonilla L et al. (2002) First clinical results with a new mechanical connector for coronary artery anastomoses in CABG. *Circulation* 106(Suppl 1):I1-4
4. Eckstein FS, Bonilla LF, Schaff HV et al. (2002) Two generations of the St. Jude Medical ATG coronary connector systems for coronary artery anastomoses in coronary artery bypass grafting. *Ann Thorac Surg* 74:S1363-1367
5. Zehr KJ, Hamner CE, Bonilla L, Berg T, Cornelius R, Hindrichs P, Scha HV (2003) Evaluation of a novel 2 mm internal diameter stainless steel saphenous vein to coronary artery connector: laboratory studies of on-pump and off-pump revascularization. *Eur J Cardio Thorac Surg* 23:925-934
6. Carrel T, Englberger L, Keller D, Windecker S, Meier B, Eckstein F (2004) Clinical and angiographic results after mechanical connection for distal anastomosis in coronary surgery. *Thorac Cardiovasc Surg* 127(6):1632-1640
7. Wiklund L, Bonilla LF, Berglin E (2005) A new mechanical connector for distal coronary anastomoses in coronary artery bypass grafting: a randomized, controlled study. *J Thor Cardiovasc Surg* 129:146-150
8. Solem JO, Boumzebra D, Al-Buraiki J, Nakeeb S, Rafeh W, Al-Halees Z (2000) Evaluation of a new device for quike sutureless coronary artery anastomosis in surviving sheep. *Euro J Cardio Thorac Surg* 17:312-318
9. Tozzi P, Solem JO, Boumzebra D, Mucciolo A, Genton CY, Chaubert P, von Segesser LK (2001) Is the GraftConnector a valid alternative to running suture in end-to-side coronary arteries anastomoses? *Ann Thorac Surg* 72(3):S999-1003
10. Bar FW, van der Veen FH, Benzina A, Habets J, Koole LH (2000) New biocompatible polymer surface coating for stents results in a low neointimal response. *J Biomed Mater Res* 52(1):193-198
11. Garasic JM, Edelman ER, Squire JC et al. (2000) Stent and artery geometry determine intimal thickening independent of arterial injury. *Circulation* 101(7):812-818
12. Marty B, Dirsch O, von Segesser LK, Schneider J, Turina M (1997) Reaction of the blood vessel wall to microporous endovascular prostheses. *Vasa* 26(1):33-38
13. Galgut P, Pitrola R, Waite I, Doyle C, Smith R (1991) Histological evaluation of biodegradable and non degradable membranes placed transcutaneously in rats. *J Clin Periodontol* 18(8):581-586
14. Loop FD (2000) Anastomotic techniques. In: Cox JL (ed) *Operative techniques in thoracic and cardiovascular surgery: a comparative atlas*. WB Saunders, Philadelphia, PA, pp 222-230
15. Filsoufi F, Farivar RS, Aklog L, Anderson CA, Chen RH, Lichtenstein S, Zhang J, Adams DH (2004) Automated distal coronary bypass with a novel magnetic coupler (MVP system). *Thorac Cardiovasc Surg* 127(1):185-192
16. Klima U, Falk V, Moritz A, Mohr FW, Haverich A, Wimmer-Greinecker G (2003) Magnetic vascular coupling in coronary artery bypass grafting: a multicenter trial. *J Thorac Cardiovasc Surg* 126(5):1568-1574
17. Klima U, Mac Vaughn H, Bagaev E, Maringka M, Kirschner S, Beilner J, Haverich A (2004) Magnetic vascular port in minimally invasive direct coronary artery bypass grafting. *Circulation* 110(11 Suppl 1):II55-60
18. Falk V, Walther T, Jacobs S, Wolf, Mohr FW (2005) Facilitated MIDCAB using a magnetic coupling device. *Ann Thorac Surg* 79(2):691-693

19. Casselman FP, Meco M, Dom H, Foubert L, Van Praet F, Vanermen H (2004) Multivessel distal sutureless off-pump coronary artery bypass grafting procedure using magnetic connectors. *Ann Thorac Surg* 78(2):38–40
20. Shennib H, Korkola SJ, Bousette N, Giaid A (2000) An automated interrupted suturing device for coronary artery bypass grafting: automated coronary anastomosis. *Ann Thor Surg* 70:1046–1048
21. Silber S (2000) Ten years of arterial closure devices: a critical analysis of their use after PTCA. *Z Kardiol* 89(5):383–389
22. Tozzi P, Stumpe F, Ruchat P, Marty B, Corno AF, von Segesser LK (2001) Preliminary clinical experience with the Hartflo anastomosis device. *Thorac Cardiovasc Surg* 49(5):279–282
23. Scheltes JS, Heikens M, Pistecky PV, van Andel C, Borst C (2000) Assessment of patented coronary end-to-side anastomotic devices using micromechanical bonding. *Ann Thorac Surg* 70(1):218–221
24. Magovern JA, Solien EE, Groth DM, Whayne JG, Fleischman SD (2003) A facilitated sutureless coronary anastomosis that is rapid, reproducible and geometrically optimized. *Heart Surg Forum* 6(Suppl 1):S34
25. Schoeneich F, Boening A, Brandt M, Lotti R, Cremer J (2003) First clinical experience with a 30 degree end-to-side coronary anastomosis coupler. *Heart Surg Forum* (Suppl 1):S19
26. Boening A, Schoeneich F, Lichtenberg A, Bagaev E, Klima U, Cremer J (2005) First clinical results with a 30° end-to-side coronary anastomosis coupler. *Eur J Cardiothorac Surg* 27:876–881
27. Suyker W, Buijsrogge MP PhD B, Suyker PTW, Verlaan C, Borst C, Gründeman PF (2004) Stapled coronary anastomosis with minimal intraluminal artifact: the S2 Anastomotic System in the off-pump porcine model. *J Thorac Cardiovasc Surg* 127(2):498–503
28. Bar-El Y, Tio FO, Shofti R (2003) An automatic sutureless coronary anastomotic device: initial results of an animal study. *Heart Surg Forum* 6(5):369–374

8

Sutureless anastomotic devices for vascular surgery

■ Introduction

Over the past ten years, vascular surgeons have witnessed very few changes in their domain, with the exception of the endovascular treatment of some vascular diseases, probably because they are traditionally conservative adopters of new technologies. However, they are now more receptive than ever to any new devices and procedures that can potentially facilitate their everyday work and increase patients' benefits. The introduction of minimally invasive techniques for major vascular reconstructions is a potential solution that could both save the vascular surgeon's core activity and reduce patient trauma. In this context, the medical industry can consistently help the surgeon in dealing with vascular reconstructions that are more and more complex due to the aging population and the increasing number of patients' comorbidity. Performing standard suture techniques for vascular anastomosis construction by endoscopic means, requires tremendous surgical ability, has a very long learning curve and it is a time consuming procedure. Furthermore, it is a matter of fact that when the surgical procedure becomes very technically demanding the surgical risk increases as well. Therefore, to make the endoscopic approach widely accepted, surgeons need an alternative way to construct vascular bypass in order to reduce the technical demand and speed up the procedure. It is mandatory that the clinical outcome remain the same if not improve.

In this chapter we review the most advanced sutureless techniques for vascular reconstruction, their secrets and potential pitfalls.

8.1 Vessel closure system

In 1985, Kirsch and associates from Loma Linda University (CA) developed an original method for the construction of both end-to-end and end-to-side microvascular anastomosis using microclips. This technique consists of arcuate-legged clips applied to everted vessel edges in an interrupted fashion forming a flange [1–12]. The Food and Drug Administration

granted vascular anastomosis and reconstruction approval to market in December 1993, and the device was designated the VCS (Vessel Closure System) clip applicator system by the United States Surgical Corporation (USSC, Norwalk, Connecticut). Despite marketing clearance, the USSC decided to withhold general distribution of the device until two prospective, randomized clinical trials were conducted [14, 15]. So far, this is the sutureless anastomotic device for which we have acquired the largest experimental and clinical experience with more than 70 peer-reviewed articles published.

■ Device design

Clips are made of titanium and are available in 4 sizes, based on the distance between the fully open jaws of the clip: small (0.9 mm) medium (1.4 mm), large (2.0 mm), and extra large (3.0 mm). The system is composed of a clip applicator that acts as an everting forceps, and a clip remover. Once the clip is fired, it produces a focal and interrupted compression of the everted vessel wall without penetration of the vessel lumen or changes in lumen diameter.

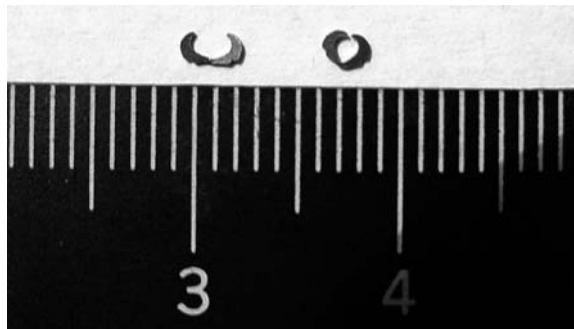


Fig. 1. VCS clip in open (left side) and closed (right side) configuration.

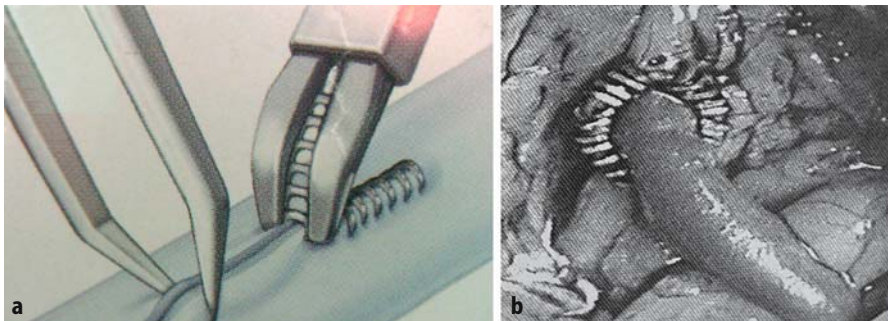


Fig. 2. **a** Schematic representation of VCS use. **b** Intraoperative view of end-to-side anastomosis constructed with VCS.

Therefore, the clip is defined extravascular or non-penetrating and this is probably the key element for the excellent long-term results in terms of anastomosis patency. This technique demands precise vessel preparation and the result is an interrupted suture anastomosis with wall eversion and intima-to-intima apposition. The arcuate legs and back span confer the property of auto regulating the final pressure between the clip tips.

VCS can be used with arteries, veins and PTFE graft as well.

■ Experimental work up and clinical results

The VCS clips have been tested in several animal models depending on the target application: from rat to calf model, the VCS was used to construct microvascular anastomoses as well as aortic repair. The parameters most frequently determined were patency, the healing pattern of the anastomosis, and the anastomotic time.

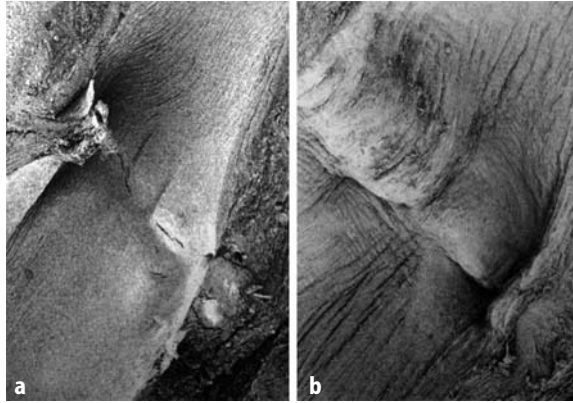
If we consider the studies in which the patency was assessed with duplex sonography or angiography and the mean follow-up is over 30 days, patency rates varied from 89% to 98%, and were, in general, similar to the sutured controls. In two experimental studies lower patency rates for clips were reported. Interposition bridge grafts performed by Gerbault and co-workers [16] in rat vessels ranging from 0.3 mm to 2 mm in diameter had patency rates approaching 75%. However, with four anastomoses, this was a small group and there were no sutured controls. Akita [17] experienced patency rates down to 43% for clipped 2-mm polytetrafluoroethylene (PTFE) grafts compared with 100% for sutured controls.

Further assessment of the experimental clipped anastomosis included tensile strength, blood flow profile measurement, intimal hyperplasia thickness, compliance measurements, and endothelial function analysis. Tensile strength of clipped anastomoses was tested in several different models. Kirsch [5] found that clipped microvascular anastomoses come apart at pressures higher than 400 mmHg, which far exceeds clinical systolic blood pressures and Pikoulis [18] substantially confirmed those results in a pig model where anastomoses on iliac arteries were performed.

Most reports demonstrated that the healing pattern with clips was similar to if not better than that with sutures. In the acute phase, the number of inflammatory and multinucleated giant cells, and the amount of fibrin and platelet aggregation is reduced with clips [19]. In addition, the exposure of the subendothelial matrix to the blood stream is more extensive in the sutured specimens. Almost all longer-term studies have shown that the degree of intimal hyperplasia is similar [19] or less [20] with clips as compared with sutures (Fig. 3).

With regard to anastomotic compliance, Baguneid [21] showed in in-vitro experiments that anastomoses performed with clips resulted in improved paraanastomotic compliance profiles and reduced intimal damage when compared with running sutures.

Fig. 3. Scanning electron microscopic view of the anastomotic line of end-to-end anastomosis of rat abdominal aorta 4 weeks postoperatively: clip closure (a) has smooth endothelial layer, while interrupted polypropylene suture (b) has some degree of myointimal hyperplasia.



The suture technique employing the VCS is considered a time sparing procedure with respect to standard interrupted suture technique. Even if the anastomotic time depends on several factors, such as the surgical exposure of the vessels, the vessel diameter, the length of the anastomosis, the surgeon's skills, and the quality of the vessels to be anastomosed, clips are associated with reduced anastomotic times mostly because the knot-tying phase is avoided.

The VCS clips have been used in the last 10 years in various clinical settings, from microvascular tissue transfer to transplantation surgery.

In an elegant study, Zeebregts and co-workers reported on the use of small- and medium-sized clips in 65 arteries and 45 veins during free tissue transfer [22]. The results were compared to those of conventional sutured anastomoses and anastomoses made with the Unilink ring system (3M Healthcare, St. Paul, Minnesota). The mean anastomotic time when either clips or rings were applied was significantly shorter than that with sutures. Early flap failure was caused by arterial anastomotic failure in 8 cases. All were sutured and represented 5% of all sutured arterial anastomoses. None of the clipped arterial anastomoses failed. Early flap failure was caused by venous anastomotic failure in 11 patients. Three of these were sutured, representing 6% of all sutured venous anastomoses; 7 were anastomosed with rings (5%); and 1 was clipped (2%). It was concluded that the patency rate of clipped vessels was at least as good as patency rates of vessels anastomosed with sutures or rings.

The largest clinical experience with clipped vascular constructs is with vascular access for hemodialysis. Papalois reported one of the largest series enrolling 50 patients in which the VCS was used to create A-V fistula [23]. The anastomotic time was approximately 5 min. In 3 cases it was necessary to apply one extra clip to stop minor anastomotic bleeding. After a follow-up of 2 months to 1 year, all fistulas were in use for dialysis.

Cook [24] conducted a prospective randomized study in which 41 clipped and 45 sutured access procedures with 6-mm PTFE loop grafts

were entered. The follow-up time ranged from 0 to 36 months with an average of 17 months. Both primary and secondary patency rates, as well as flow characteristics, were similar. Although the clipped anastomoses were safe, they had no patency advantage over sutured ones in this study. Cooper [25] retrospectively reviewed the clinical course of 48 clipped PTFE graft anastomoses and compared them with 34 sutured controls. There was no significant difference in incidence of graft infection or pseudoaneurysm formation. Although operation times were reduced with clips, primary patency rates and complication rates were similar.

A major advantage of using VCS in transplant surgery is the possibility to reduce the graft ischemic time. Jones [26] reported in his series of 21 consecutive clipped renal transplants a 51% reduction of the warm ischemia time when compared with a historical group of 31 sutured renal transplants (24.0 and 42.4 min, respectively, $P < 0.005$). Patients with severely diseased iliac vessels did not receive clips but were included in the control group. The clipped anastomoses were associated with three complications. First, there was acute thrombosis in one artery, which the author attributed to the small size of the donor and recipient artery. Second, there was a significant leak in an arterial anastomosis, since the clips were not large enough to grasp both vessel walls. And third, there was a case of venous bleeding between clips, resulting from a size discrepancy between the donor vein and the venotomy. All three complications were repaired with conventional suturing, and none caused any irreversible damage.

Kirsch [27] reported the results of 100 clipped patch angioplasties after carotid endarterectomies in 97 patients, all carried out by the same surgeon. The follow-up period ranged over 5 years. Four patients had wound hematomas requiring reexploration; 1 patient experienced a major stroke in the immediate postoperative period; and another patient had a transient ischemic attack that resolved within 24 h. None of the clipped carotid angioplasty patients developed a hemodynamically significant postoperative stenosis.

Aarnio et al. [28] described a series of 17 patients with severe claudication or incipient gangrene of the foot, who underwent bypass surgery with clipped vascular anastomoses. The arterial reconstruction included 16 femoropopliteal and 1 femorotibial bypasses using either greater saphenous vein or PTFE graft. Altogether 26 of the 34 anastomoses could be made with clips, all of which were patent with duplex examination at an average of 11 months after operation. Clips could not be applied in the remaining 8 anastomoses, because the arterial wall was too thick and calcified. Postanastomotic leakage occurred in 4 of the 26 anastomoses owing to poor apposition of anastomotic walls, necessitating the placement of additional sutures.

■ Comments

The VCS clips have proven to be versatile and provide the surgeon with the option of a successful nonsuture alternative. VCS clips have been used world-wide in approximately 30,000 vascular cases since January 1997: 20,000 vascular accesses, 5,000 femoropopliteal and aortofemoral reconstructions, 2,000 carotid reconstructions, 3,000 microvascular, transplant, arteriotomy and venotomy closures, and 3,000 miscellaneous cases [13]. The vast majority of publications pertaining to the VCS clip over the past 5 years have been positive or at least, showed results comparable to suture technique. Positive clinical outcomes seem to be correlated with the improved physical characteristics of the clipped interrupted anastomotic line as opposed to the appearance of the conventional, penetrated running suture. An asset of the clip is that it does not penetrate or disrupt endothelium, nor does it reside intraluminally. The clipped anastomotic line is interrupted, allowing for improved compliance and the anastomotic sites are promptly and completely endothelialized, whereas intraluminal suture material is associated with endothelial breakage and platelet deposition. These clip-mediated events translate clinically into a smoother laminar flow profile, and a flush interface between endothelial cells and vascular graft with reduced anastomotic intimal hyperplasia.

Clip constructs have equivalent or greater burst and tensile strength than sutured constructs.

However, this technique has a few limitations. The major pitfall is that there is the real and fundamental need for symmetrical vessel wall eversion and approximation with additional corner stitches and the use of everting forceps prior to clip placement. The learning curve is long and steep and correct deployment of VCS clip requires a surgical skill as much, if not greater, than for suture technique. Experience over the past few years has demonstrated that the necessity of symmetrical eversion prior to application of a secure clip requires skill, practice, and teaching. Training courses provide a “hands-on” environment that may be superior to learning in the operating room. Learning the VCS technique by the “see one, do one, teach one” adage in live surgery is a real pitfall, as the surgeon does not have the opportunity to explore acceptable and unacceptable limits of the clip system such as clip spacing and sizing and controlling clip security [13].

8.2 The one-shot system

The one-shot device allows the multiple firing of VCS clips and can be considered the natural evolution of the VCS concept. This technology should overcome the limitations of the VCS single apposition and fulfills the need for quicker high-quality anastomoses.



Fig. 4. One-shot stapler with a cartridge that is loaded circumferentially containing 12 equally spaced clips. Inlay shows the tip of the one-shot stapler.

■ Device design

The instrument (United States Surgical One-Shot system United States Surgical Corporation, Norwalk, CT) simultaneously applies either 10 or 12 nonpenetrating, arcuate-legged titanium clips to symmetrically everted vessel or prosthetic conduit edges, enabling the construction of compliant end-to-side and end-to-end anastomoses (Fig. 4). The anastomotic device consists of a circumferentially preloaded, disposable cartridge (10 to 12 clips) activated by one squeeze of the instrument handle. The graft is pulled through a disposable cartridge housing the 12 medium or large VCS clips, and then everted over the distal clip tips. Because symmetrical vessel wall eversion and approximation is critical to successful clip application, an optimally everted intima-to-intima configuration is attained by the contour of the disposable clip-containing cartridge within the recipient vessel.

The loading unit everts the opening in the recipient vessel and maintains approximation to the already everted donor vessel held in place by the exposed clip tips. After the clips are fired simultaneously, the cartridges separate to allow easy withdrawal of the device from the anastomotic construct. The disposable cartridge is angled at 45 degrees to accomplish an oblique end-to-side anastomosis and filled with either 10 or 12 large or medium VCS clips, depending on vessel diameter and thickness. Dimensions of disposable loading units vary in size to enable anastomosis of vessels as small as 1.8 mm outer diameter. A special configuration is being tested for synthetic polytetrafluoroethylene graft conduits, but is not yet commercially available. The device works well with expanded polytetrafluoroethylene prosthetic conduits.

■ Experimental work up and clinical results

The device has successfully created jugular vein interpositional jump grafts in the pig common carotid artery and femoral vein jump grafts in both dog and pig femoral arteries (20 animals). Fourteen consecutive porcine internal mammary (2 mm outer diameter) to left anterior descending (2 to 3 mm outer diameter) end-to-side coronary anastomoses have been performed and are currently in long term follow-up. Clipped anastomotic constructs are at least physically and functionally equivalent to control suture constructs and demonstrate augmented blood flow. Clipped anastomotic constructs are “blood-tight” in contrast to those created with sutures, and have physical properties (burst, tensile, strength) equivalent or superior to those attainable by suture.

The interrupted, nonpenetrated, flanged anastomotic line formed by clips has proven in both experimental and prospectively randomized clinical trials to be both biologically and technically superior to junctions attainable by conventional, hand-sewn vascular anastomoses [29, 30].

■ Comments

The one-shot device represents a technical advance over the standard clip applicator because the entire anastomotic circumference is formed simultaneously, thus facilitating the reconstruction and reducing the risk of clip misplacement. However, even if FDA approval was obtained in 1997 and results are promising, this device has not been widely accepted. The reasons could reside in the fact that wall eversion causes the loss of 3 to 4 mm of vessel length and the vessel wall has to be soft enough to allow the eversion which is rarely the case with diseased arteries.

8.3 The Vascular Join

The sutureless anastomotic device presented in this chapter fulfils all the above described needs and represents a breakthrough product that will probably establish the new gold standard for vascular anastomosis.

The Vascular Join (Idee & Sviluppo LLC, Bologna, Italy) is a breakthrough surgical instrument enabling the restoration of any severed vessel's continuity and integrity without using any of the suture or non-suture techniques ever described. Vessel edges are joined layer by layer and no foreign material is exposed to the bloodstream resulting in an almost complete “*restitutio ad integrum*”, as Romans used to define a complete recovery.

■ Device design

The Vascular Join consists of two metallic rings each of which is fixed to the extremity of the two conduits being joined together. A third Teflon based element keeps the two rings together with a snap-on system and guarantees the continuity of the severed conduit in an end-to-end configuration. No limitation of use exists with respect to vessel size.

A schematic representation of the procedure is reported in Figure 5.

In the end-to-side, having 45° takeoff angle configuration, a saddle element is attached outside the target vessel by means of hooks that penetrate the vessel wall without going through it. An oval arteriotomy is created using a dedicated rotary blade. The graft, with a pre-mounted 45° ring, is then inserted to complete the anastomosis (Fig. 6).

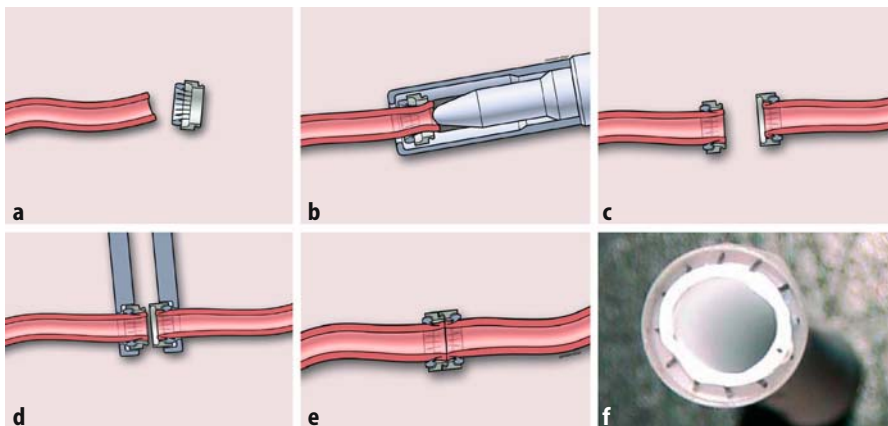


Fig. 5. **a** and **b**: One connecting element is inserted onto the vessel end using the delivery device. **c** The same procedure is repeated on the other end of the severed vessel. **d** The 2 elements are snapped on. **e** The anastomosis is completed. **f** Vascular Join mounted on 6 mm e-PTFE graft.

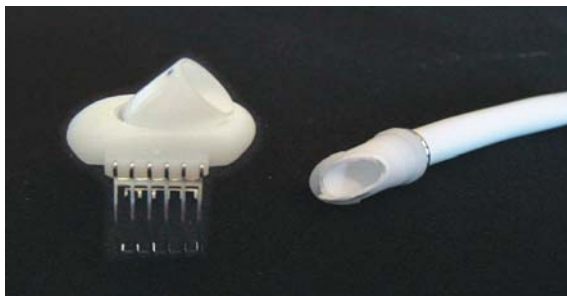


Fig. 6. Vascular Join end-to-side anastomotic device. The saddle element is positioned onto the vessel (side part) vessel-device connection is ensured by extravascular hooks. The end side has been loaded on e-PTFE prosthesis.

■ Experimental work up

After extensive bench tests, an animal study has been designed to address the following endpoints:

- Consistency and reproducibility of restoring vessel continuity avoiding bleeding and/or flow turbulence;
- assessment of the “layer by layer” vessel apposition;
- assessment of the absence of foreign material in the vessel lumen;
- consistency and reproducibility of the sutureless anastomosis when an artificial conduit (ePTFE graft) is used;
- occurrence of thrombosis and stenosis due to myointimal hyperplasia compared to running suture technique;
- early and long term patency rate with respect to running suture technique.

In 20 adult sheep both carotid arteries were isolated, severed and anastomosed in end-to-end fashion using the connector on one side (Fig. 7). The same procedure was repeated on the other side, but the anastomosis was

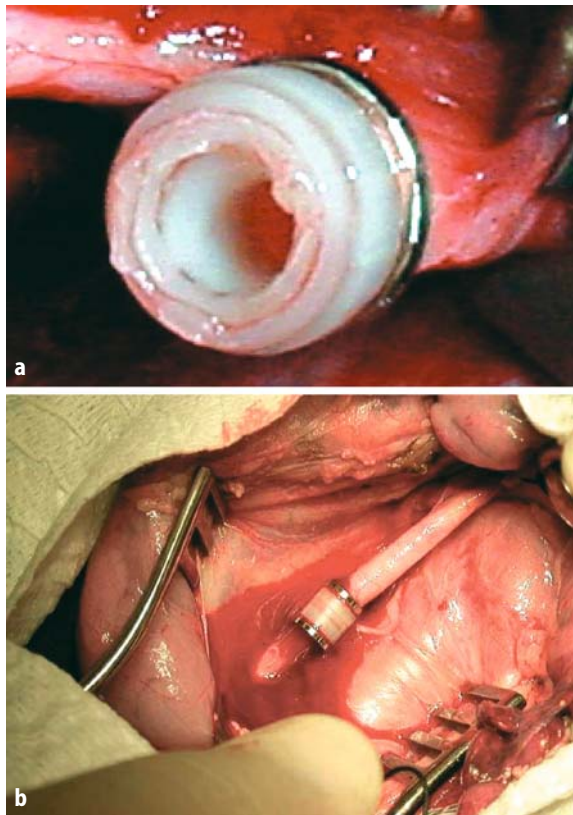


Fig. 7. Animal 3 (adult sheep). A 6 mm \varnothing connecting element has been deployed at the distal part of a severed carotid artery. The device guarantees the perfect opening of the vessel lumen: anastomosis shape and diameter are determined by the connector diameter. **a** Note the absence of metallic or plastic material in the vessel lumen. **b** The end-to-end anastomosis is completed.

constructed using the running suture technique (6/0 polypropylene) as control.

In 5 animals, a 4 mm \varnothing , 30 mm in length, ePTFE graft is interposed in between the severed carotid artery. On one side the anastomoses were constructed with the sutureless device (Fig. 8), on the other side with the running suture technique.

Animals received Aspirine 100 mg per day and all anastomoses were followed up with echo-color doppler control at 1, and 3 and 6 months. In 5 animals carotid angiogram (Fig. 9) and intravascular ultrasound (Fig. 10) were obtained at 3 months. Animals were sacrificed after 6 months and histopathology examination was carried out.

All sutureless anastomoses were successfully completed. The device delivery system was extremely easy to use and no technical failure occurred. In 2 cases a small leak occurred, but it was controlled with a few minutes of sponge compression. It took less than one minute to perform each sutureless anastomosis versus 6 ± 3 min for running suture.

Doppler ultrasound has been used to assess the long term patency rate. All sutureless anastomoses were wide open with maximal flow velocity of 100 cm/s (Fig. 11), meaning that there were no stenosis.

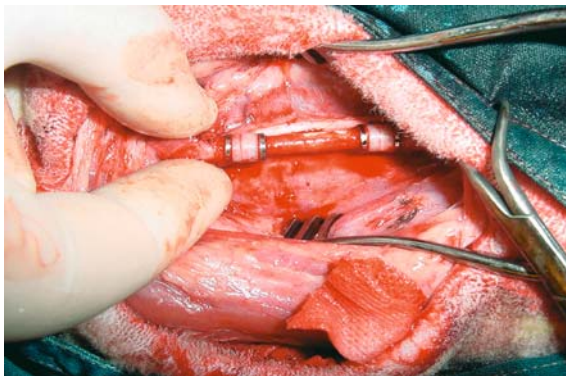


Fig. 8. Figure 3: Animal 3. A 4 mm \varnothing ePTFE graft (IMPRA), 30 mm in length has been used to create a carotid-to-carotid bypass. Both anastomoses, proximal and distal, are performed using two connectors. Carotid flow distal to the anastomosis is 400 ml/min.

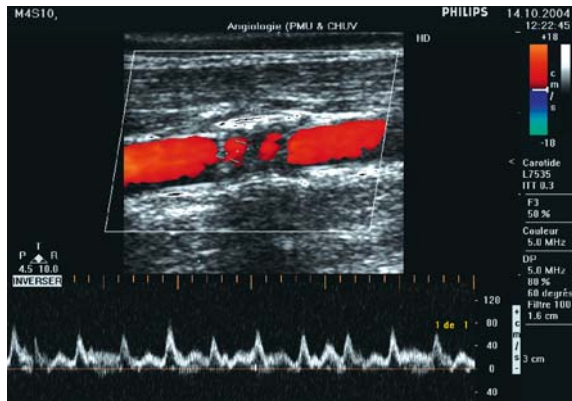


Fig. 9. Three months carotid artery angiography. A 4 mm e-PTFE graft (IMPRA) has been used to perform a carotid-to-carotid artery bypass. Anastomoses are wide open without signs of stenosis. Carotid artery is 6 mm in diameter, while the graft is 4 mm: this justifies the diameter discrepancy seen in the picture. Connectors are clearly visible on X-ray.

Fig. 10. Three-month follow up. IVUS demonstrated the perfect junction between the two severed parts of the vessel. No intimal flap or dissection was detected.



Fig. 11. Three months follow-up. Flow is laminar, without acceleration or turbulence. The mean flow velocity at the anastomotic site is 50 cm/s.



Histology work up showed that metallic connector parts were within the vessel wall (Fig. 12). No foreign material was detected in the vessel lumen, and therefore, there was no contact between the blood stream and device components. The “layer by layer” vessel apposition was confirmed. Vessel width was respected. There wasn’t any sign of myointimal hyperplasia nor inflammation.

■ Comments

The Vascular Join is a reliable instrument that provides reproducible vascular anastomoses even with synthetic grafts. The 6-month follow-up shows excellent results since the luminal width is comparable to that of the native

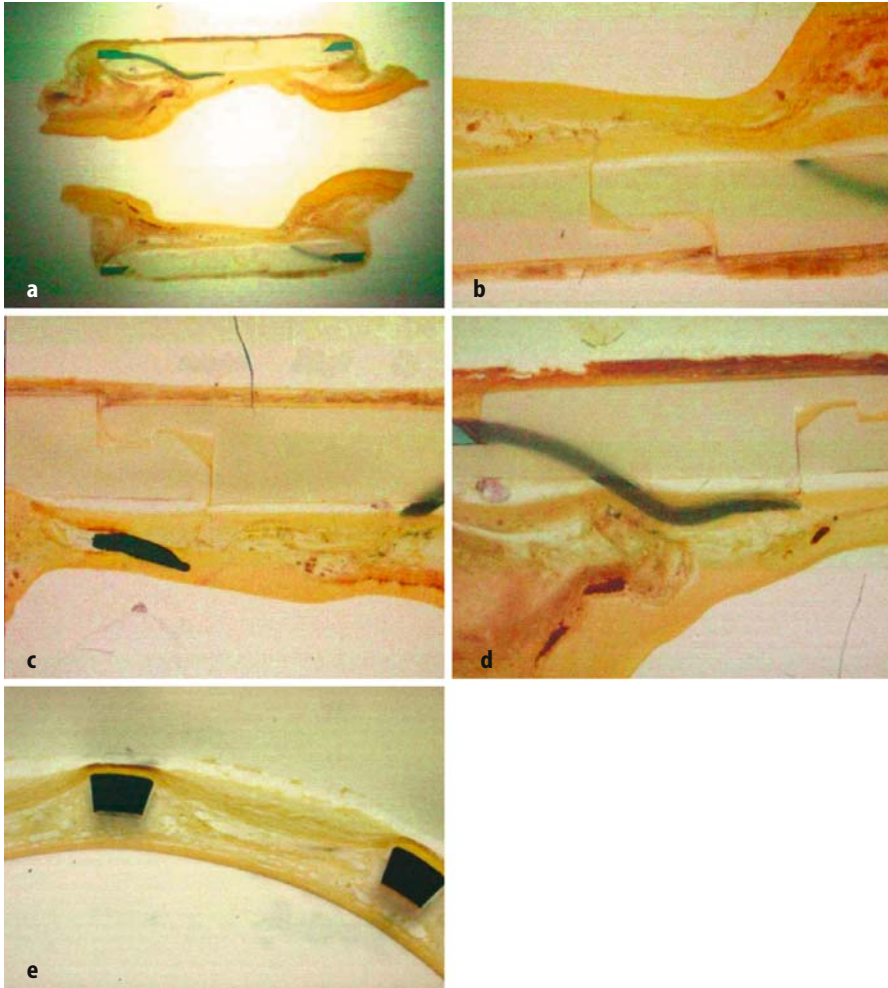


Fig. 12. **a** 4× magnification of axial section. Six months after sutureless end-to-end anastomosis of the carotid artery. Vessel edges were properly aligned without signs of overlapping or stenosis. **b**, **c** and **d** 10× magnification of axial section. The metallic component of the connector was within the vessel wall and no foreign material was in the vessel lumen. There was any myointimal hyperplasia and integrity of the vessel wall was completely restored. **e** 10× magnification. Circumferential section. Metallic pins were within the vessel wall. No myointimal hyperplasia was detected. No signs of chronic inflammation were visible.

vessel and the flow is laminar. Neither myointimal hyperplasias nor chronic inflammatory reaction were seen.

One of the key elements that make this device totally different from all other sutureless devices, is that there is no foreign material (metal or polymers) inside the vessel. The ring stays outside the vessel and the connec-

tion between the ring and the vessel is made in such a way that there is no contact between the device and the blood stream. These unique technical characteristics dramatically reduce the risk of thrombosis and myointimal hyperplasia at the anastomotic site, definitely improving the anastomosis long-term patency rate. Moreover, there is no need for anti-platelet drug administration.

Another key element consists in the fact that intima, media and adventitia of the severed vessel, are joined in a physiological way, avoiding the vessel wall eversion. The 3 layers are faced “layer by layer” so that intima is in contact with intima, media with media and adventitia with adventitia. This is the first time a surgical technique for vascular anastomosis provides such a natural physiologic vascular reconstruction.

The third unique key element consists in the fact that this connector also works with synthetic grafts (ePTFE and Dacron), either thick or thin wall, of any diameter. This characteristic expands the clinical applications of the vascular join to include even the most complex vascular reconstructions.

The Vascular Join is extremely easy to use and the anastomosis construction takes less than 60 s. This surgical technique is simple and intuitive and, therefore, requires at most a one-day learning curve. The anastomoses are consistent and reproducible in almost all surgical conditions, with vein and with synthetic grafts.

■ References

1. Zhu YH, Kirsch WM, Cushman R et al. (1985) Comparison of suture and clip for microvascular anastomoses. *Surg Forum* 36:492–495
2. Kirsch WM, Zhu YH, Hardesty RA et al. (1993) Nonpenetrating clips successfully replacing sutures in base of skull surgery. *Skull Base Surg* 3:171–181
3. Zhu YH, Steckel R, Kirsch WM (1994) Comparative evaluation of suture and nonpenetrating metal clips for vascular reconstruction. *Surg Forum* 45:593–597
4. Kirsch WM, Zhu YH, Gaskill D et al. (1992) Tissue reconstruction with nonpenetrating arcuate-legged clips: potential endoscopic applications. *J Repr Med* 37:581–586
5. Kirsch WM, Zhu YH, Hardesty RA, Chapolini R (1992) A new method for microvascular anastomosis: report of experimental and clinical research. *Am Surg* 58:722–727
6. Zhu YH, Kirsch WM (1992) A new surgical technique for venous reconstruction: the nonpenetrating clip. In: Chang JB (ed) *Modern vascular surgery*, vol 5. Springer, New York, pp 425–463
7. Kirsch WM, Zhu YH, Boukouvalas Z, Cushman R (1993) Instrumentation. In: Lee S (ed) *Color atlas of microsurgery*. IEA Publishers, St. Louis, pp 63–71
8. Kirsch WM, Zhu YH, Boukouvalas Z, Hardesty RA (1993) Microvascular anastomoses: surgical technique. In: Lee S (ed) *Color atlas of microsurgery*. IEA Publishers, St. Louis, pp 73–78

9. Kirsch WM, Zhu YH, Boukouvalas Z et al. (1993) Morphologic events during healing of microvascular anastomoses. In: Lee S (ed) *Color atlas of microsurgery*. IEA Publishers, St. Louis, pp 79–88
10. Kirsch WM, Zhu YH, Hardesty RA et al. (1993) The non-penetrating arcuate-legged clip: clinical applications. In: Lee S (ed) *Color atlas of microsurgery*. IEA Publishers, St. Louis, pp 89–101
11. Kirsch WM, Zhu YH, Boukouvalas Z et al. (1993) The anastomoses of small arteries and veins by clips: a description of instruments. In: Wang Z-G (ed) *Vascular surgery*. International Academic Publishers, Beijing, pp 41–46
12. Kirsch WM, Zhu YH, Boukouvalas Z et al. (1993) Microvenous anastomoses and arterial grafting: comparison of clip suture. In: Wang Z-G (ed) *Vascular surgery*. International Academic Publishers, Beijing
13. Zeebregts CJ, Kirsch WM, van den Dungen JJ, Zhu YH, van Schilfgaarde R (2004) Five years' world experience with nonpenetrating clips for vascular anastomoses. *Am J Surg* 187(6):751–760
14. Hammond SJ, Kirsch WM, Wahlstrom PGE et al. (1995) A multi-centered controlled clinical trial comparing clips to suture for construction of vascular access sites for hemodialysis. *Cardiovasc Surg* 3(1):136
15. Schild AF (1997) Use of a vascular staple device for creation of AV fistulas and bridge grafts for hemodialysis. In: Henry ML, Ferguson RM (eds) *Vascular access for hemodialysis-V*. WL Gore & Assoc and Precept Press, Chicago, pp 95–102
16. Gerbault O, Arrouvel C, Servant J-M (1998) Anastomoses par microagrafes VCS sur des vaisseaux de diamètre inférieur à 2 millimètres: étude expérimentale préliminaire chez le rat. *Ann Chir Plast Esthét* 43:27–39
17. Akita M, Takenaka H, Harada M (2002) Can nonpenetrating vascular closure staples and hepatocyte growth factor prevent intimal hyperplasia following ePTFE grafting of the carotid artery in rabbits. *Surg Today* 32:618–622
18. Leppäniemi A, Wherry D, Pikoulis E (1997) Arterial and venous repair with vascular clips: comparison with suture closure. *J Vasc Surg* 26:24–28
19. Zeebregts C, van den Dungen J, Buikema H (2001) Preservation of endothelial integrity and function in experimental vascular anastomosis with non-penetrating clips. *Br J Surg* 88:1201–1208
20. Komori K, Shoji T, Furuyama T (2001) Non-penetrating vascular clips anastomosis inhibited intimal thickening under poor runoff conditions in canine autogenous vein grafts. *Eur J Vasc Endovasc Surg* 21:241–247
21. Baguneid MS, Goldner S, Fulford PE (2001) A comparison of para-anastomotic compliance profiles after vascular anastomosis: nonpenetrating clips versus standard sutures. *J Vasc Surg* 33:812–820
22. Zeebregts C, Acosta R, Böländer L (2002) Clinical experience with nonpenetrating vascular clips in free flap reconstructions. *Br J Plast Surg* 55:105–110
23. Papalois VE, Romagnoli J, Hakim NS (1998) Use of vascular closure staples in vascular access for dialysis, kidney and pancreas transplantation. *Int Surg* 83:177–180
24. Cook JW, Schuman ES, Standage BA, Heintz P (2001) Patency and flow characteristics using stapled vascular anastomoses in dialysis grafts. *Am J Surg* 181:24–27
25. Cooper BZ, Flores L, Ramirez JA (2001) Analysis of nonpenetrating clips versus sutures for arterial venous graft anastomosis. *Ann Vasc Surg* 15:7–12

26. Jones JW (1998) A new anastomotic technique in renal transplants reduces warm ischemia time. *Clin Transplant* 12:70–72
27. Kirsch WM, Cavallo C, Anton T (2001) An alternative system for cerebrovascular reconstructions: non-penetrating arcuate-legged clips. *Cardiovasc Surg* 9:531–539
28. Aarnio P, Järvinen O, Varjo P (2000) Vascular clips in anastomoses of femoropopliteal arterial reconstruction. *Int J Angiol* 9:62–64
29. Nataf P, Hinchliffe P, Manzo S, Simpson J, Kirsch WM, Yong Hua Zhu, Anton Th (1998) Facilitated vascular anastomoses: the one-shot device. *Ann Thorac Surg* 66:1041–1044
30. Nataf P, Kirsch WM, Hill A et al. (1997) Nonpenetrating clips for coronary anastomoses: initial clinical experience. *Ann Thorac Surg* 63:S135–S137

9

Human body and metal alloys: the never ending fight

■ Introduction

The most remarkable targets achieved in the last two decades by scientific progress in the domain of the cardiovascular diseases share at least one technical element: the use of metal alloys. Coronary and peripheral stents, endoprostheses and vascular connectors are all made of different metal alloys that are more than biocompatible: these devices are all permanently exposed to the bloodstream and should last for a lifetime.

It is generally thought that almost all metals do not interact with the human immune system and do not affect biological functions. This is not precisely true and could represent the unpredictable factor eventually leading to implant failure. In this chapter we review the most recent studies concerning metal-body interaction, showing that this interaction is more important than it seems because the human body attacks metal implants resulting in a slow and progressive reduction of the metal's physical properties.

■ Characteristics of metals used in implants

The performance of any material in the human body is controlled by two sets of characteristics: biofunctionality and biocompatibility. With the wide range of materials available in the 21st century, it is relatively easy to satisfy the requirements for mechanical and physical functionality of implantable devices. Therefore, the selection of materials for medical application is usually based on considerations of biocompatibility. Superior fracture and fatigue resistance have made metals the materials of choice for traditional load-bearing applications. When metals and alloys are considered, the susceptibility of the material to corrosion and the effect the corrosion has on the tissue are the central aspects of biocompatibility. Corrosion resistance of the currently used 316L stainless steel, cobalt-chromium, and titanium-based implant alloys relies on their passivation by a thin surface layer of oxide. Stainless steel is the least corrosion resistant and should be used for temporary implants only. The titanium and Co-Cr alloys do not corrode in the body; however, metal ions slowly diffuse through the oxide layer and

accumulate in the tissue. When a metal implant is placed in the human body, it generally becomes surrounded by a layer of fibrous tissue with a thickness proportional to the amount and the toxicity of the dissolution products and to the amount of motion between the implant and the adjacent tissues. Pure titanium may elicit minimal of fibrous encapsulation under certain conditions, whereas the proliferation of a fibrous layer as much as 2 mm thick is often encountered with the use of stainless steel implants.

■ Fatigue-crack propagation in Nitinol

Nitinol is a titanium based thermoelastic material composed of approximately 50% atomic nickel which originally gained fame during the 1960s for its shape-memory behavior. Nitinol has become an attractive replacement for the currently used stainless steel based implantable medical devices, because of its improved resistance to corrosion in the biological environment, its interesting nonlinear mechanical behavior, and its thermoelasticity.

While the absence of corrosion fatigue, at least when a 10 Hz cycle is applied, and the persistence of the superelastic effect after cyclic loading are excellent, the fatigue-crack limit below which the Nitinol is presumed inactive, is found to be very low when compared to other metallic structural

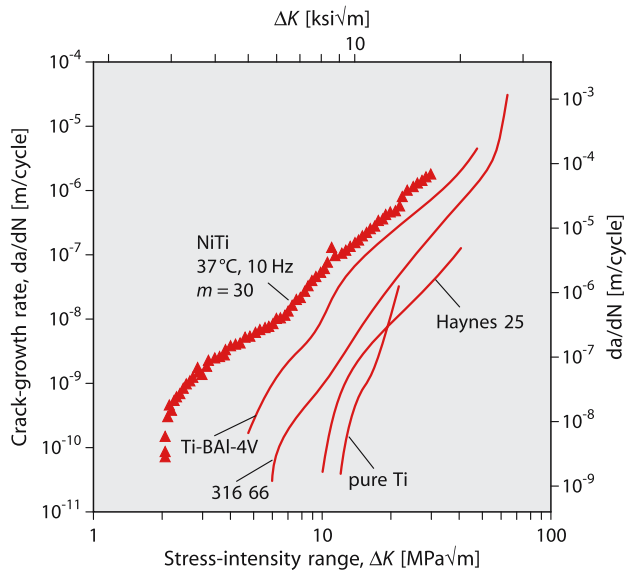


Fig. 1. Comparison of fatigue-crack growth rates for various biomedical metallic alloys. All tests were conducted in air. Nitinol (NiTi) shows fatigue-crack growth rate significantly lower than stainless steel (316L SS) and pure titanium.

materials used for biomedical implants. Figure 1 is a plot of the fatigue-crack grow rates for Nitinol compared with other biomedical metallic alloys such as stainless steel, pure titanium, Ti₆Al-4V and Cobalt-Chrome alloy (generally used for cardiac valve prostheses). Although these data are for moist air environments rather than for simulated body fluid, the fatigue limit is the lowest and the crack-grow rates are the fastest in Nitinol. Specifically, Nitinol is 6 times less resistant than stainless steel. However, it should be noted that several of these alloys show a reduction in their thresholds in corrosive environments whereas Nitinol appears to be far less susceptible to such effects [2].

This comparison may be quite relevant for the architecture of endovascular devices (connector included) having a very fine structure. Devices have to be designed in such a way as to prevent any crack propagation since the component size is so small that a crack, once initiated, would quickly spread through the entire stent cross section with unfavorable consequences.

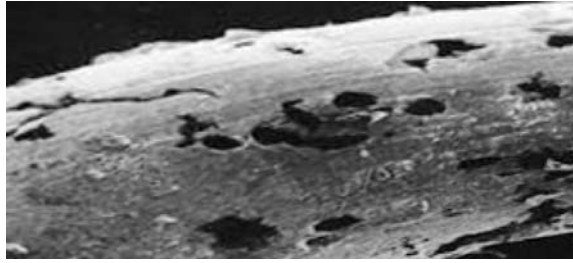
■ Clinical findings

Corrosion of any metallic implant is undesirable for two reasons. First, the corrosion or degradation of the metal may make it structurally weaker or diminishing proper function. Second, the resulting corrosion products may react unfavorably with the tissue immediately adjacent to the metal implant or even at distant sites in the body. In most cases, the corrosion rate against the safe dose threshold and the potential subclinical effects of corrosion products are perhaps of greater importance than the effects of corrosion on the structural function of the metallic implants in biological systems.

The analysis of 6 Nitinol based endoprostheses retrieved 13 to 53 months after their implantation in patients, exhibited similar healing and structural modifications. The woven polyester sleeve showed evidence of fiber damage and breakage leading to the formation of openings. The luminal surface endografts showed incomplete healing characterized by a poorly organized, nonadherent thrombotic matrix of variable thickness. Multiple fractures of metallic wire were detected with conduit kinking. Scanned electron microscopy of the cleaned Nitinol wires from all areas of the explanted endoprostheses revealed corrosion on the surface of the wires. Corrosion marks were distributed in a homogeneous fashion all over the Nitinol wires (Fig. 2). In one specimen, highly corroded areas were observed mostly near the platinum coil markers.

Ionic bombardment tests revealed signals for oxygen, nickel and titanium increase, suggesting an oxidation process of the alloy. The chemical analysis confirmed that the concentration of titanium and nickel on the surface of the wires was not homogenous. The nickel concentration was 2 to 5 times less than that of titanium, regardless of the duration of the implanta-

Fig. 2. Scanning electron photomicrographs of Nitinol endoprosthesis retrieved 15 months after implantation in patient's abdominal aorta. The wires are severely corroded all over the metallic frame.



tion. The first layer was composed of carbon resulting from residual traces of organic elements remaining on the surface after cleaning, followed by a layer of highly oxidized titanium with low nickel concentration [3].

Galvanic corrosion may occur from differences within the metal itself. For example, the distribution of the oxide coat may not be uniform, resulting in areas of relative oxygen depletion that are made relatively anodic.

The corrosion marks that were observed support the consensus that Nitinol is not inert, so the biocompatibility of this material needs reappraisal. Other studies have shown that a stable oxide layer at the surface of the alloy increases resistance to corrosion under physiological conditions [4, 5]. The uniformity, rather than thickness of this layer is the predominant factor in this improved resistance to corrosion. This layer also prevents the diffusion of elements, cations or anions into the physiological environment. The consequence of the release of Ni and Ti elements in the blood have not been clearly established.

Some investigators have suggested that stent grafts used for the treatment of aortic aneurysms may trigger a systemic inflammatory response syndrome characterized by low-grade fever and elevated C-protein levels probably induced by cytokines released from the mural thrombus in the aneurysm [6].

A closer collaboration between clinicians, engineers and industry is mandatory to validate the materials and structures used in current and future bioprotheses and to obtain the best possible long-term outcome for patients.

■ References

1. Gotman I (1997) Characteristics of metals used in implants. *J Endourol* 11(6): 383–389
2. McKelvey AL, Ritchie RO (1999) Fatigue-crack propagation in Nitinol, a shape memory and superelastic endovascular stent material. *J Biomed Mater Res* 47:301–308
3. Guidion R, Marois Y, Douville Y, King MW, Castonguay M, Traoré A, Formichi M, Staxrud LE, Norgren L, Bergeron P, Becquemin J-P, Egana JM, Harris PL (2000) First generation aortic endografts: analysis of explanted stentor devices from the EUROSTAR Registry. *J Endovasc Ther* 7(2):105–122

4. Trépanier C, Tabrizian M, Yahia LY (1998) Effect of modification of oxide layer of NiTi stent corrosion resistance. *J Biomed Mater Res* 43:433–440
5. Wever DJ, Veldhuizen AG, deVries J (1998) Electrochemical and surface characterization of a nickel-titanium alloy. *Biomaterials* 19:761–769
6. Norgen L, Swartbol P (1997) Biological responses to endovascular treatment of abdominal aortic aneurysms. *J Endovasc Surg* 4:169–173

■ Introduction

As it has been illustrated in the previous chapters, there is a great variety of sutureless anastomosis devices and each of these is based on original principles and has its *pros and cons*. All have been judged safe and consistent and all show excellent experimental long-term results. For those being the object of clinical studies, preliminary results are very promising. In other words, all the presented devices can potentially succeed and replace the standard suture technique. However, new generations of connectors have introduced new issues to be evaluated including overloading, double loading, skiving of aortic punch, variations in operative techniques and graft movement. Therefore, it is not that easy to establish whether a sutureless device is a valid and safe alternative to suture technique and if it can be widely used.

The experience with the first Nitinol connector has shown that if it had been evaluated at 6 months by angiography, stenoses and occlusions would have been discovered.

Anastomotic devices eliminate factors which contribute to poor patient outcome but their benefits with new procedures are unresolved: the device may contribute to graft failure for reasons that include compliance mismatch, materials that promote local thrombus and inflammation, vessel trauma caused by device deployment, design of anastomosis prejudicial to laminar flow and difficulty with revision.

New anastomotic technologies are probably developing faster than the profession's ability to provide evidence-based data to support their application. In 1994, The American College of Surgeons statement on emerging technologies and the evaluation of credentials affirmed: "It is equally essential that the value and safety of a new procedure be established before it is widely used on patients" [1]. Behind this statement there is the need to protect patients while promoting scientific progress.

Unfortunately, when we look at the history of cardiovascular surgery, conclusive statements on long-term effectiveness and safety have not preceded the majority of vascular anastomosis devices being introduced in clinical trials or directly marketed. Nowadays, new procedures and any significant changes in conventional techniques should be adopted after they

have been tested under controlled conditions and proved to be safe and effective. Moreover, if adverse event rates were high, the device would not be acceptable, even if patency rate were good. Minimal safety and effectiveness requirements for in vitro and in vivo animal studies, as well as what is acceptable when device withdrawing is necessary due to technical failure, must be defined. A standard animal model with each device subjected to similar follow-up periods is needed to offer reliable comparisons between devices before they are accepted for clinical use.

On the other hand, exceptionally demanding directives can jeopardize the development of new technologies by intimidating potential innovators as well as investors with evident consequences on the economical asset of many medical industries.

To answer these complex ethical and economical issues, on March 2004, the Food and Drug Administration had organised a meeting of experts. The panel was asked to address 7 questions concerning:

- 1) the choice of control in the clinical trial required to evaluate vascular anastomosis devices for CABG;
- 2) the study design characteristics (differences in proximal and distal sutureless devices) and criteria to determine whether a failure is device related;
- 3) the necessity of adopting different evaluation criteria for an arterial conduit and a venous conduit;
- 4) whether the primary endpoint of the study should be the graft patency, the myocardial perfusion or both;
- 5) the criteria applied to the evaluation of the device safety, as distinguished from device effectiveness;
- 6) the duration of the follow up for premarket evaluation and the opportunity for a post market follow up to assess long-term device effectiveness;
- 7) the right tool to assess graft patency (angiography versus CT scan or MRI) and the timing.

■ FDA criteria for anastomotic technologies approval

There are two pathways by which a new medical device can come to the United States marketplace. One looks very much like the process by which a new prescription drug gains FDA approval. Approval requires a finding that the device is safe and effective, or, more accurately, provides benefits that outweigh its risks. FDA approval is based on the results of clinical trials in randomized human subjects, whose data are submitted to, and closely evaluated by the FDA. For example, a new implant of almost any sort is likely to have gone through this premarket approval (PMA) process.

But the United States' laws require another pathway to the market for devices that represent modest advances on the existing technology. For such devices the US law affords a less rigorous path to the market, known

as the 510 K or premarket notification process. To follow this pathway, the maker must give the FDA advance notice of its plan to market the product and demonstrate, not that the product is safe and effective based on clinical studies, but it is substantially equivalent to an existing device or technique. This is a significantly less rigorous burden than required by the PMA process.

On March 2004, FDA stated that sutureless anastomosis devices may follow the 510 K pathway to be approved. Criteria for clinical study design concerning connectors to be used in CABGs are:

- The primary endpoint should be patency.
- A randomised clinical trial is not necessary. However, some sort of control or comparison group is necessary. The type of control (inpatient, matched control or historical data) has to be determined on the basis of statistical analysis. Propensity score may not be appropriate.
- Six month results are considered as long-term follow-up. Follow-up longer than 12 months is too late because atherosclerosis could affect the results.
- Anastomosis patency has to be assessed with angiogram. A post market follow up is necessary for a minimum of 1 year and this could take place by phone once patency is determined
- Results have to be compared to historical results of hand sewn anastomosis at 6 months.

FDA mandated a study having as benchmarks the cut off values of historical 6-month patency rate of arterial (IMA) and vein (SVG) conduits routinely used to construct coronary artery bypasses (Fig. 1). The handsewn suture has a well documented history over the past 30 years [2]. From 1979 to 2001, 30 studies were published and results of a meta-analysis involving 6 275 LIMA on LAD grafts demonstrate a historical patency rate of 99% at

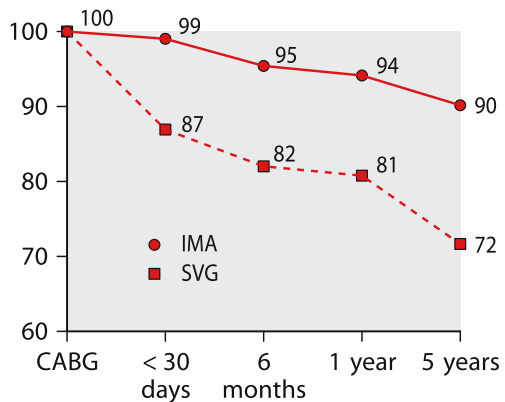


Fig. 1. Historical patency rate of IMA over and SVG.

1 month, 95% at 6 months and 94.5% at 12 months. A meta-analysis involving 28 083 SVG demonstrates a historical patency rate of 87.9% at 1 month, 84% at 6 months and 82.7% at 12 months.

It is clear that attrition occurs in the first 30 days and reasonably good science suggests that anastomoses heal at about 2 months. After that point, failures are due to patient factors, ongoing atherosclerosis, and improper medication. Six-month follow-up is considered reasonable for clinical studies; follow-up longer than 12 months is too late because atherosclerosis dominates the outcome.

However, it should be considered that data on handsewn anastomoses are 30 years old: back then, patients were younger, vessels were better and diabetes was less common. Today, we face different patients and we should assess today's patency rates including the rates for off and on pump procedures.

Study size calculation: in order to reach statistic significance (80% power to have 90% confidence of a 5% interval), any clinical study aiming to compare the 6 month patency rate of a new sutureless anastomosis device should include a minimum of 160 patients for IMA (90% patency) and a minimum of 258 patients for SVG (80% patency).

Although CT-scan, MRI, and electron beam angiography are helpful, conventional angiography still represents the gold standard for demonstrating graft patency and to detect possible stenosis and it also offers the additional possibility of percutaneous interventions if required. Qualitative and quantitative methods should be used to evaluate each anastomosis. Whereas qualitative methods would include estimates of TIMI flow grade and general assessment of patency, quantitative evaluation includes assignment of a FitzGibbon score. Finally, precise assessment of the luminal diameter of the target coronary artery and of the graft proximal and distal to the anastomosis as well as the diameter of the anastomosis itself would allow the calculation of the ratio of the anastomosis to the coronary artery and also the average percent of diameter stenosis.

In the last 50 years we have learned a lot about sutureless cardiovascular anastomosis and all this experience is the starting point for the next generation of devices that will eventually enable the construction of the *ever-patent* anastomosis.

■ References

1. American College of Surgeons statement on emerging technologies and the evaluation of credentials (1994) *Am Coll Surg Bull* 79:40–41
2. Tatoulis J, Buxton BF, Fuller JA (2004) Patencies of 2127 arterial to coronary conduits over 15 years. *Ann Thorac Surg* 77:93–101

Subject index

A

Abbe 1
absorbable anastomotic coupler 6
albumin solder 61
anastomosis inflow 48
anastomosis take off angle 76
anastomotic compliance 44
anastomotic inflow 40
anastomotic shear stress 45
anastomotic stapler 4
anastomotic technologies 136
Androsov 4, 105
anvil 56, 92
Aortic Anastomotic Device (AAD) 79
arterial compliance 20, 22
axial and circumferential wall shear stress 31
axial deformation 18
axial strain 20
axial stress 40

B

BENIS 75, 90, 104
Berggren 6
Bernoulli's Law 14
biological glue 9
Blakemore 3
Blood Exposed Non Intimal Surface (BENIS) 60
blood/metal interface 93
breaking strain 55

C

Carrel 1, 53, 58
circumferential stress σ_θ 17
circumferential strain 20
Co-Cr 130
Converge Coronary Anastomosis Coupler 103
C-Port 105

CorLink 55, 79
cross-circumferential stress 46
Cross Sectional Anastomotic Compliance (CSAC) 43
cross sectional compliance 21, 22, 40, 41
cyanoacrylate glues 61, 64

D

Distal Anastomotic Device (DAD) 110

E

Enclose 67
echo-tracking system 21
end-to-end anastomosis 40, 42
end-to-end carotid artery anastomosis 42
end-to-side anastomosis 43, 44, 122
end-to-side coronary anastomosis 87, 103, 120
equation of blood-flow 28

F

fibrin glues 61
flow dynamics 12

G

Goetz 5
Gorisch 8
Graft Connector 91
Gudov 4

H

Haller 6
heat-shrink tubing 7
Heartflo 99
Heartstring 66
historical patency rate 137

I

Inokuchi 4
interrupted suture 40
interrupted vs. running suture 40
intimal hyperplasia 15, 25, 26, 33, 40
intimal thickening 26
ivory cuffs 1

J

Jain 8

K

Kirsch 7, 114, 116, 118

L

Landon 3
lasers 8, 61
layer by layer 123, 125, 127
LeConte 1

M

magnesium rings 2
Magnetic Vascular Positioner (MVP) 95
Miller-cuff technique 33, 44, 45
myointimal hyperplasia 12, 34, 35, 46, 49, 57, 59, 93, 123

N

Nakayama 5
Navier-Stokes equations 27, 29, 30
Nitinol 55, 59, 70, 84, 91, 103, 104, 110, 131, 135
Nitinol wire 63

O

Obora 6
One-Shot System 120
Ostrup 6
ox shin bones 1

P

PAS-Port 82
Payr 1
Poiseuille 25, 48
Poisson ratio 32

Q

Q-CAB 55, 58

R

Reynolds numbers 15
running suture 40

S

S2 Anastomotic System 107
shear stress 15, 44, 45, 59
side-to-side anastomosis 70
silver tubes 1
Spyder 84
stainless steel, 316, L 130
St. Jude Medical Coronary Connector 87
sutureless anastomosis 54
sutureless anatomic compliance 59
sutureless end-to-end vascular anastomosis 62
Symmetry Aortic Connector 70

T

tantalum ring 6
transfer sheet 58
take off angle 59, 78, 103, 122
– anastomosis 76
Titanium 130

U

U-Clip 63
Unilink 6, 7, 117

V

Vascular Join 55, 61, 121
vein cuff 44
Vessel Closure System 115
vitallium tubes 3
volumetric compliance 21

W

Wall eversion 56
wall-shear stress 26, 32, 40, 45, 48
– axial 31
– circumferential 31
Womersley flow 25
Womersley Parameter 15

Y

Young's moduli 31